Wrocław University of Technology

Civil Engineering

Dariusz Łydżba

EFFECTIVE PROPERTIES OF COMPOSITES
Introduction to Micromechanics

Wrocław 2011

Wrocław University of Technology

Civil Engineering

Dariusz Łydżba

EFFECTIVE PROPERTIES OF COMPOSITES
Introduction to Micromechanics

Wrocław 2011

Reviewer: Tomasz Strzelecki

Contents

Preface

A common feature in mathematical formulations of mechanical behavior of solid material is an explicit assumption of that the material is homogeneous within itself. Apparently, in real materials, given their discrete structure, the presence of heterogeneities and discontinuities is evident at the level of grain clusters and/or microcracks. In this context, the postulate of homogeneity must be understood in a broader, more abstract sense and should be applied only with respect to the natural scale of observation.

The homogeneity of material is understood in a statistical sense; i.e., in a homogeneous system the local arrangement of grains/microcracks is said to be invariant with respect to translation. In other words, the mechanical as well as geometric properties of grain clusters/microcrkracks, are independent of position relative to the chosen frame of reference.

For materials that in the actual scale of observation may be considered as statistically homogeneous, it seems natural to employ smoothing techniques to develop descriptions that are similar to those used for homogeneous continua. Indeed, the existing experimental data indicates that for a material containing a large number of heterogeneities, the response at the macro-level is virtually the same, in an average sense, as that of a homogeneous body. Thus, in order to solve a boundary value problem formulated for a material with a sufficiently large number of inhomogeneities, the notion of 'equivalent' continuum is introduced whose average macroscopic response is synonymous with that of the original material. In other words, from an engineering perspective, the material is considered to be homogeneous on the macro-scale. In civil engineering, this approximation forms the basis of vast majority of numerical approaches employed in engineering practice.

The primary objective of the homogenization method is to define for a given heterogeneous medium, which possesses the property of statistical homogeneity, an

'equivalent' homogeneous material that has the same 'average' properties. In other words, the homogenization approach is aimed at establishing an equivalent macroscopic description of a given physical process based on the description of the same phenomenon at the level of micro-inhomegeneities.

There are two distinct approaches in formulating the homogenization problem (e.g. Refs. [1,2]). The first methodology incorporates the notion of representative volume element (RVE) and is based on volume averaging of the basic field variables. As a result, the fields that are strongly discontinuous at the level of inhomogeneities undergo 'smoothing' through the process of volume averaging. Thus, this approach is often referred to as a smoothing method or a micromechanics. The other methodology is known as the mathematical theory of homogenization. In this case, the mathematical transition from micro- to macro-level is accomplished by introducing a scale parameter $\varepsilon > 0$, which is associated with a characteristic dimension of inhomogeneity (i.e. average pore size), and imposing the requirement of $\varepsilon \to 0$. The formulation that is obtained in the limit corresponds to the macroscopic description for an equivalent homogeneous continuum.

In this book, the basic principles of homogenization technique are reviewed with emphasis on application to problems related to civil engineering. In order to distinguish between different scales employed, the description developed at the level of inhomogeneities is referred to as *microscopic*, while that corresponding to equivalent continuum is termed as *macroscopic*. Similarly, the physical field variables employed at the micro-level are referred to as *micro*-fields, while those at the equivalent continuum level as *macro*-fields (e.g. micro-stress/strain vs. macro-stress/strain tensors, etc.). Special attention is paid on the methods of effective properties estimation. Two different approaches are presented, i.e. methods based on a single inclusion solution called as analytical methods and numerical estimation of effective properties from a digital image of microstructure.

Throughout the book an index notation with Einstein convention is used that the repeated indices indicates summation from 1 to 3. An example of the notation used is presented below:

$$x_i e_i = x_1 e_1 + x_2 e_2 + x_3 e_3$$
$$\sigma_{ij}\varepsilon_{ij} = \sigma_{1j}\varepsilon_{1j} + \sigma_{2j}\varepsilon_{2j} + \sigma_{3j}\varepsilon_{3j} =$$
$$= \sigma_{11}\varepsilon_{11} + \sigma_{12}\varepsilon_{12} + \sigma_{13}\varepsilon_{13} +$$
$$+ \sigma_{21}\varepsilon_{21} + \sigma_{22}\varepsilon_{22} + \sigma_{23}\varepsilon_{23} +$$
$$+ \sigma_{31}\varepsilon_{31} + \sigma_{32}\varepsilon_{32} + \sigma_{33}\varepsilon_{33}$$

CHAPTER 1

_____

Micro-Macro Passage

The basic assumption in the homogenization approach that is perceived as a smoothing method, is the postulate of the existence of a representative volume element (RVE). The latter is defined as the smallest volume that contains all the essential information required to describe the structure and properties of the material on the macro-scale [3].

In order to take into account the statistical nature of the microstructure of random heterogeneous media, RVE must be large enough to be statistically representative, i.e. it must include all elements of a microstuctural arrangement. This implies that RVE should contain a sufficiently large number of inhomogeneities, such as grains, inclusions, voids, microcracks, etc. [4]. At the same time, RVE must be small compared to entire volume of the considered material so that the equivalent medium may be defined as macroscopically homogeneous.

The transition from micro to macro-scale is based on the averaging operation. If $u(Y)$ is the considered physical field in micro-description, then the associated macro-field is represented by its average over RVE, i.e.

$$\langle u \rangle (X) = \int_{V_{RVE}} u(Y) m(Y - X) dV \qquad (1.1)$$

In eq. (1.1) two sets of coordinates are engaged; $X = (x_1, x_2, x_3)$ - defining the location of the centroid of RVE and $Y = (y_1, y_2, y_3)$ specifying the position of a material point within RVE. Clearly, both these spatial coordinates X and Y describe the same

geometric domain (Fig.1.1). Furthermore, $m(Y)$ is a weight function and integration is carried over the elementary volume V_{RVE}.
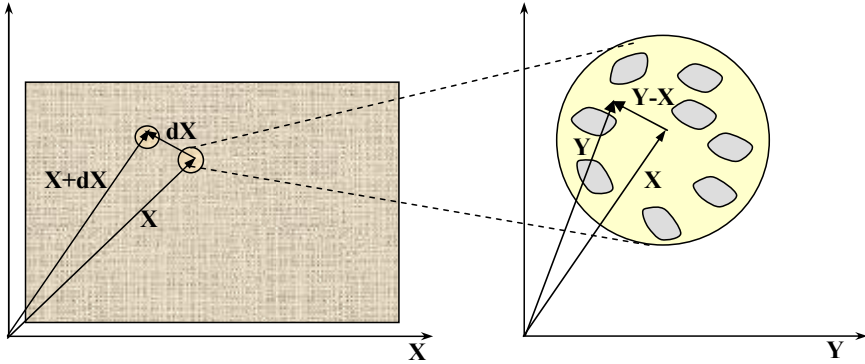

Fig.1.1. Schematic view at averaging process

In physical terms, the averaging (1.1) implies that to each material point X (i.e. centroid of RVE) a physical field is attributed that represents the average, with weight $m(Y)$, of the original micro-field. If the material contains a number of phases, e.g. solid skeleton with voids filled with a fluid, as a result of averaging a hypothetical equivalent continuum is created that has a homogeneous structure, i.e. each point contains all phases simultaneously (Fig. 1.2). Furthermore, it is clear from (1.1) that in the smoothing process two families of variables are employed, i.e. macroscopic variables $\langle u \rangle$ describing the equivalent continuum and the microscopic variables $u(Y)$ that define the state within RVE.

The weight function $m(Y)$ must be selected in such a way that all macroscopic variables have a clear physical significance, i.e. they are measurable from experiments conducted at the macro-scale. Note that if the weight function is a constant and has the value equal to $1/V_{RVE}$, then the macro-variable is identified with the volume average of the corresponding micro-field. In case of density, for example, such an average is physically justified. However, when the stress field is concerned, the macroscopic variable should represent the force per unit area, so that it should be taken as the average of microstress per unit area. Similar situation arises in case of fluid flow through porous media. Here, the macroscopic variable should represent the flux, i.e. the averaging should be conducted over the area.
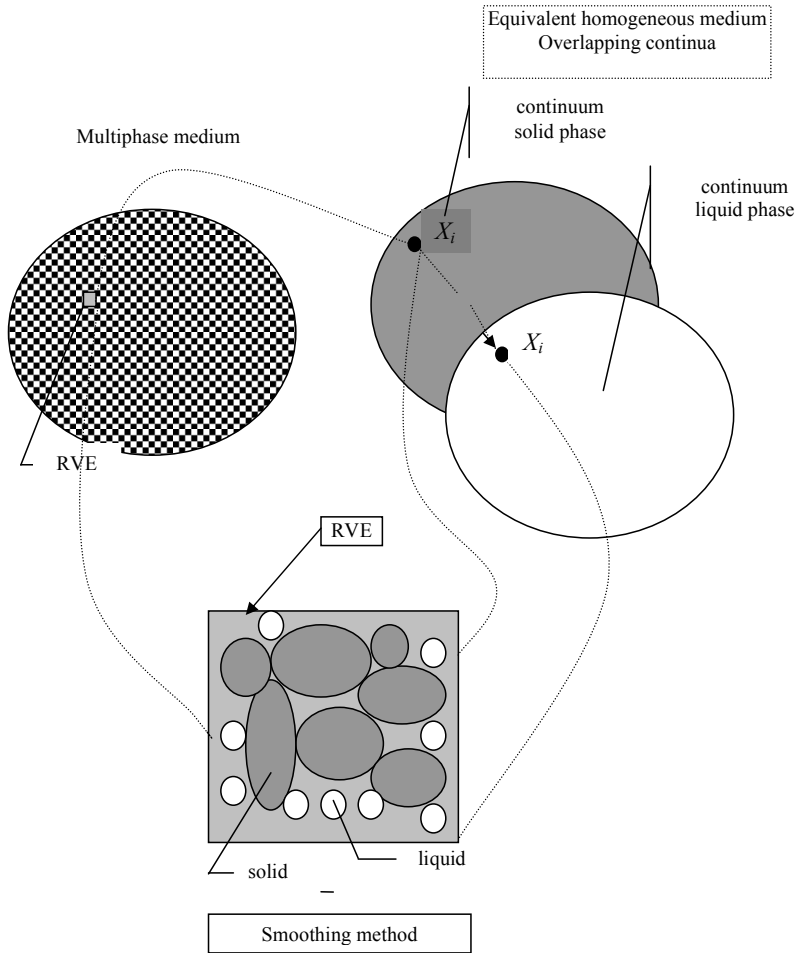
Fig.1.2. Schematic of a smoothing method

The micro-macro transition, i.e. development of a macroscopic description from that at the micro-level, consists of transforming the latter, through appropriate averaging procedure, into a framework in which only the macroscopic variables are employed. In what follows, two basic smoothing techniques are reviewed. The first one is typically applied to analysis of flow in porous media, while the second one is representative of

problems involving specification of equivalent mechanical properties of heterogeneous media.

1.1   Methods of weight and volume averaging

In mechanics of multiphase media, the most commonly used smoothing techniques are the weight and volume averaging (see Refs. [5-8]). Let us examine first the weight averaging approach, as the other one is a particular case of it.
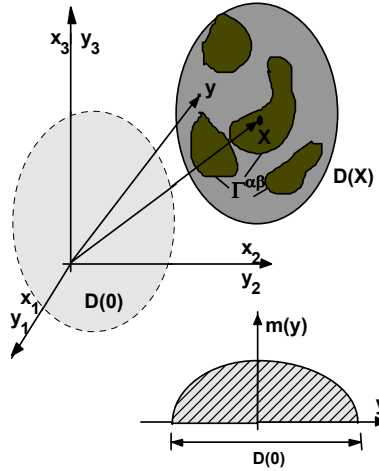
Fig.1.3. Change of the observation scale by the spatial convolution with a weight function $m(y)$

Let $m(Y)$ be a positive even function, with compact support in $D(0)$, such that (Fig. 1.3)

$$\int_{D(0)} m(Y)dV = 1 \qquad (1.2)$$

By definition, the macroscopic quantity $\left\langle g^{\alpha} \right\rangle$ associated with a given microscopic field $g^{\alpha}(Y)$ is the convolution with respect to the spatial variable

$$m*\left(g^{\alpha}\right) = \left\langle g^{\alpha} \right\rangle = \int_{D(X)} h^{\alpha}(Y)\, g^{\alpha}(Y)\, m(Y-X)dV \qquad (1.3)$$

where $h^\alpha(Y)$ is a characteristic function for the phase α, occupying the volume $V_\alpha \subset V_{REV}$, defined as

$$h^\alpha(Y) = \begin{cases} 1 & \text{for} \quad Y \in V_\alpha \\ 0 & \text{for} \quad Y \notin V_\alpha \end{cases} \tag{1.4}$$

The transformation laws governing the 'micro-macro' transition are the consequence of definition (1.2) and the standard rules of differentiation. The derivation, in case of a two-phase medium, is provided below.

Consider a medium containing two distinct phases α and β, whose distribution is defined by the characteristic functions $h^\alpha(Y)$, $h^\beta(Y)$. Denote by $\psi(Y)$ the microscopic variable to be transformed to macro-level and assume that

$$\psi(Y) = \begin{cases} h^\alpha \, \psi(Y) = \psi^\alpha \\ h^\beta \, \psi(Y) = \psi^\beta \end{cases} \tag{1.5}$$

According to definition (1.3)

$$m * \left(\frac{\partial \psi}{\partial y_i} \right) = \int\limits_{D(X)} \left\{ h^\alpha \frac{\partial \psi^\alpha}{\partial y_i} + h^\beta \frac{\partial \psi^\beta}{\partial y_i} \right\} m(Y - X) \, dV \tag{1.6}$$

The right-hand side of eq.(1.6) may be expressed as

$$\begin{aligned}
&\int\limits_{D(X)} \left\{ h^\alpha \frac{\partial \psi^\alpha}{\partial y_i} + h^\beta \frac{\partial \psi^\beta}{\partial y_i} \right\} m(Y - X) \, dV \\
&= \int\limits_{D(X)} \left\{ h^\alpha \frac{\partial \psi^\alpha \, m(Y - X)}{\partial y_i} + h^\beta \frac{\partial \psi^\beta \, m(Y - X)}{\partial y_i} \right\} \\
&\quad - \int\limits_{D(X)} \left\{ h^\alpha \, \psi^\alpha + h^\beta \, \psi^\beta \right\} \frac{\partial m(Y - X)}{\partial y_i} \, dV
\end{aligned} \tag{1.7}$$

Applying now Green's theorem to the first of the integrals on the right-hand side of (1.7) leads to

$$\int_{D(X)} \left\{ h^\alpha \frac{\partial \psi^\alpha}{\partial y_i} + h^\beta \frac{\partial \psi^\beta}{\partial y_i} \right\} m(Y-X) \ dV$$

$$= \int_{A^\alpha} \psi^\alpha \, m(Y-X) n_i^\alpha dS + \int_{A^\beta} \psi^\beta \, m(Y-X) n_i^\beta dS +$$

$$+ \int_{\Gamma^{\alpha\beta}} \left[\psi^\alpha - \psi^\beta \right] m(Y-X) n_i^{\alpha\beta} dS -$$

$$- \int_{D(X)} \left\{ h^\alpha \ \psi^\alpha + h^\beta \ \psi^\beta \right\} \frac{\partial m(Y-X)}{\partial y_i} \ dV$$

(1.8)

The geometric parameters employed in (1.8) above, are schematically shown in Fig. 1.4a. In particular: A^α, A^β are the boundaries of the region $D(X)$ that belong to individual phases α and β, respectively; $\Gamma^{\alpha\beta}$ is the interphase boundary; n_i^α, n_i^β are the unit vectors normal to A^α, A^β, respectively, and $n_i^{\alpha\beta}$ is the unit normal to the interphase boundary. Note that the latter, i.e. $n_i^{\alpha\beta}$, is directed towards the phase β.

The integrals over A^α, A^β are both identically zero. This is because the weight function $m(Y-X)$ has compact support in $D(0)$, so that $m(Y-X) = 0$ for all points that belong to A^α and A^β. Thus, in view of (1.6) and (1.8), the following rule applies

$$m * \left(\frac{\partial \psi}{\partial y_i} \right) = \int_{\Gamma^{\alpha\beta}} \left[\psi^\alpha - \psi^\beta \right] m(Y-X) \, n_i^{\alpha\beta} dS$$

$$- \int_{D(X)} \left\{ h^\alpha \ \psi^\alpha + h^\beta \ \psi^\beta \right\} \frac{\partial m(Y-X)}{\partial y_i} \ dV$$

(1.9)

Let us define now the partial derivative of $m * \psi$ with respect to the macroscopic spatial variable x_i. Again, according to the definition (1.3), there is

$$\frac{\partial}{\partial x_i} (m * \psi) = \frac{\partial}{\partial x_i} \int_{D(X)} \left\{ h^\alpha \ \psi^\alpha + h^\beta \ \psi^\beta \right\} m(Y-X) dV$$

(1.10)

In this case, the partial derivative of volume integral over a variable domain needs to be evaluated; i.e. as $X \to X + dX$ the domain $D(X)$ moves to a neighboring $D(X + dX)$, Fig. 1.4b. Such a derivative is defined as (see Ref.[9])
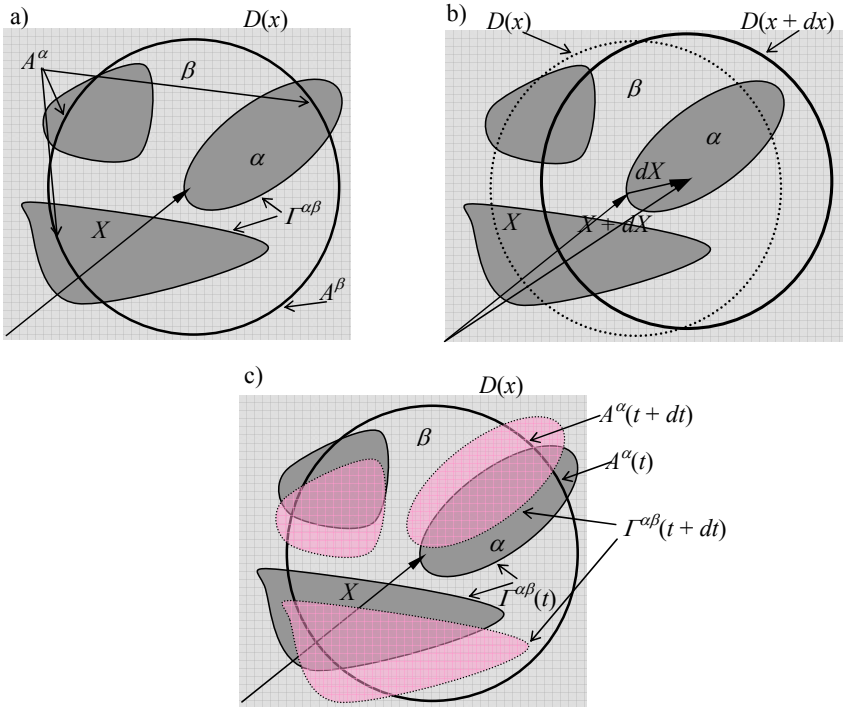
Fig.1.4. Representative elementary volume of two-phase medium considered (a),
geometrical interpretation of partial macroscopic space derivative (b),
geometrical interpretation of partial time derivative (c)

$$
\frac{\partial}{\partial x_i}\left(m * \psi\right) = \lim_{dx_i \to 0}\ \frac{1}{dx_i}\left\{ \int\limits_{D(X+dX)} \left\{ h^\alpha\ \psi^\alpha + h^\beta\ \psi^\beta \right\}\ m\left(Y-X\right)\ dV \right.
$$

$$
\left. - \int\limits_{D(X)} \left\{ h^\alpha\ \psi^\alpha + h^\beta\ \psi^\beta \right\}\ m\left(Y-X\right) dV \right\}
\tag{1.11}
$$

In general, there are two distinct contributions to the difference on the right-hand side of eq.(1.11); one over the region that is common to both $D(X)$ and $D(X+dX)$ and one where they differ [9]. The former contribution is

$$\int_{D(X)} \left\{ h^\alpha \, \psi^\alpha + h^\beta \, \psi^\beta \right\} \frac{\partial m(Y-X)}{\partial x_i} dV \tag{1.12}$$

The latter contribution comes from the value of $\psi(Y)m(Y-X)$ on the boundary multiplied by the volume swept by boundary particles during the translation dX. The displacement of a point on the boundary of $D(X)$ is dX; thus, the volume swept by particles of a surface element dS is $dV = dx_i \, n_i \, dS$. The contribution from the region $D(X) \cup D(X+dX) - D(X) \cap D(X+dX)$ is therefore equal to

$$\int_{A^\alpha} \psi^\alpha \, m(Y-X) \, n_i^\alpha dS + \int_{A^\beta} \psi^\beta \, m(Y-X) \, n_i^\beta dS \tag{1.13}$$

so that eq.(1.11) becomes

$$\begin{aligned}
\frac{\partial}{\partial x_1}(m*\psi) = &\int_{D(X)} \left\{ h^\alpha \, \psi^\alpha + h^\beta \, \psi^\beta \right\} \frac{\partial m(Y-X)}{\partial x_i} dV + \\
&+ \int_{A^\alpha} \psi^\alpha \, m(Y-X) \, n_i^\alpha dS + \int_{A^\beta} \psi^\beta \, m(Y-X) \, n_i^\beta dS
\end{aligned} \tag{1.14}$$

Again, the integrals over A^α, A^β are both identically zero as the weight function $m(Y-X)$ has compact support in $D(0)$. In addition, there is

$$\frac{\partial m(Y-X)}{\partial x_i} = -\frac{\partial m(Y-X)}{\partial y_i} \tag{1.15}$$

which allows to express the relation (1.14) in an equivalent form

$$\frac{\partial}{\partial x_i}(m*\psi) = -\int_{D(X)} \left\{ h^\alpha \, \psi^\alpha + h^\beta \, \psi^\beta \right\} \frac{\partial m(Y-X)}{\partial y_i} dV \tag{1.16}$$

Comparing now eqs. (1.16) and (1.9), the first 'micro-macro' transformation rule is obtained for the weight averaging scheme, i.e.

$$m*\left(\frac{\partial \psi}{\partial y_i}\right) = \frac{\partial}{\partial x_i}(m*\psi) + \int_{\Gamma^{\alpha\beta}} \left[\psi^\alpha - \psi^\beta \right] n_i^{\alpha\beta} \, m(y_i - x_i) dS \tag{1.17}$$

The second transformation rule is the relation between the averaged value of the time derivative of ψ and the partial derivative with respect to time of the average value of ψ. Note that

$$m * \left(\frac{\partial \psi}{\partial t} \right) = \int\limits_{D(X)} \left\{ h^\alpha \frac{\partial \psi^\alpha}{\partial t} + h^\beta \frac{\partial \psi^\beta}{\partial t} \right\} m(Y - X) dV \qquad (1.18)$$

while

$$\frac{\partial}{\partial t} (m * \psi) = \frac{\partial}{\partial t} \int\limits_{D(X)} \left\{ h^\alpha \psi^\alpha + h^\beta \psi^\beta \right\} m(Y - X) dV \qquad (1.19)$$

In this case, in contrast to (1.10), the integration domain remains fixed, while the phase distribution in $D(x_i)$, described by characteristic functions h^α and h^β, undergoes the evolution, Fig.1.4c. By analogy to the former case involving representation (1.11), two distinct contributions can be identified to the derivative (1.19). The first is the contribution from the region that is common to both phases, i.e.

$$\int\limits_{D(X)} \left\{ h^\alpha \frac{\partial}{\partial t} \left[\psi^\alpha m(Y - X) \right] + h^\beta \frac{\partial}{\partial t} \left[\psi^\beta m(Y - X) \right] \right\} dV \qquad (1.20)$$

while the second is the contribution from moving boundaries, i.e.

$$\begin{aligned}
\int\limits_{A^\alpha} \psi^\alpha m(Y - X) v_i^\alpha n_i^\alpha dS &+ \int\limits_{A^\beta} \psi^\beta m(Y - X) v_i^\beta n_i^\beta dS \\
&+ \int\limits_{\Gamma^{\alpha\beta}} \left[\psi^\alpha - \psi^\beta \right] m(Y - X) v_i^{\alpha\beta} n_i^{\alpha\beta} dS
\end{aligned} \qquad (1.21)$$

Here, v_i^α, v_i^β are the velocities of A^α, A^β and $v_i^{\alpha\beta}$ refers to the velocity of the interphase boundary.

Since the boundary of $D(X) = A^\alpha(t) \cup A^\beta(t) = A^\alpha(t + dt) \cup A^\beta(t + dt)$ is now fixed, Fig.1.4c, the volume swept by boundary particles over dt is equal to zero, so that $v_i^\alpha n_i^\alpha dS = v_i^\beta n_i^\beta dS = 0$. Thus,

$$\begin{aligned}
\frac{\partial}{\partial t}(m * \psi) &= \int\limits_{D(X)} \left\{ h^\alpha \frac{\partial}{\partial t} \left[\psi^\alpha m(Y - X) \right] + h^\beta \frac{\partial}{\partial t} \left[\psi^\beta m(Y - X) \right] \right\} dV \\
&+ \int\limits_{\Gamma^{\alpha\beta}} \left[\psi^\alpha - \psi^\beta \right] m(Y - X) v_i^{\alpha\beta} n_i^{\alpha\beta} dS
\end{aligned} \qquad (1.22)$$

Furthermore, the weight function $m(Y - X)$ is independent of time, so that eq.(1.22) can be expressed in the form

$$\frac{\partial}{\partial t}(m * \psi) = \int_{D(X)} \left\{ h^\alpha \frac{\partial}{\partial t} \psi^\alpha + h^\beta \frac{\partial}{\partial t} \psi^\beta \right\} m(Y - X) dV$$
$$+ \int_{\Gamma^{\alpha\beta}} \left[\psi^\alpha - \psi^\beta \right] m(Y - X) v_i^{\alpha\beta} n_i^{\alpha\beta} dS \tag{1.23}$$

Comparing now eqs. (1.23) and (1.18), the second 'micro-macro' transformation rule is obtained for the weight averaging scheme, i.e.

$$m * \left(\frac{\partial \psi}{\partial t} \right) = \frac{\partial}{\partial t} (m * \psi) - \int_{\Gamma^{\alpha\beta}} \left(\psi^\alpha - \psi^\beta \right) n_i^{\alpha\beta} v_i^{\alpha\beta} m(Y - X) dS \tag{1.24}$$

For a special case, when the weight function is constant and equal $1/V_{REV}$ within a sphere of volume V_{RVE} while it vanishes outside this sphere, the transformation rules (1.17) and (1.24) reduce to a form that is representative of spatial averaging (see Ref. [10])

$$\left\langle \frac{\partial \psi}{\partial y_i} \right\rangle = \frac{\partial}{\partial x_i} \langle \psi \rangle + \frac{1}{V_{REV}} \int_{\Gamma^{\alpha\beta}} (\psi^\alpha - \psi^\beta) \, n_i^{\alpha\beta} dS$$
$$\left\langle \frac{\partial \psi}{\partial t} \right\rangle = \frac{\partial}{\partial t} \langle \psi \rangle - \frac{1}{V_{REV}} \int_{\Gamma^{\alpha\beta}} (\psi^\alpha - \psi^\beta) \, n_i^{\alpha\beta} \, v_i^{\alpha\beta} dS \tag{1.25}$$

Note that in this case the weight function is said to be discontinuous at the boundary of $D(X)$. This, however, has no implications on the spatial averaging rules. Indeed, the transformation rule for the time derivative (1.24) was obtained without imposing any restrictions on the value of the weight function along the boundary. At the same time, the derivation of the spatial derivative (1.17) employed the condition of vanishing of the weight function at the boundary of $D(X)$, viz. eqs. (1.9) and (1.16). Comparing, however, the earlier representation (1.8) with the corresponding form (1.14), it is evident that the transformation rule (1.17) holds good without invoking the constraint of vanishing of the respective surface integrals. Thus, the discontinuity of the weight function does not affect the structure of the micro-macro transformation in the spatial averaging approach.

Summarizing, eqs. (1.17) and (1.24) are the basic transformation rules for a transition from micro- to macro-scale that employs the weight averaging approach, i.e.

$$m*\left(\frac{\partial \psi}{\partial y_i}\right) = \frac{\partial}{\partial x_i}(m*\psi) + \int\limits_{\Gamma^{\alpha\beta}} \left(\psi^\alpha - \psi^\beta\right) n_i^{\alpha\beta}\, m(y_i - x_i)dS$$

$$m*\left(\frac{\partial \psi}{\partial t}\right) = \frac{\partial}{\partial t}\,(m*\psi) - \int\limits_{\Gamma^{\alpha\beta}} \left(\psi^\alpha - \psi^\beta\right) n_i^{\alpha\beta}\, v_i^{\alpha\beta}\, m\left(y_i - x_i\right)dS$$

At the same time, eqs.(1.25) give the rules corresponding to the volume averaging scheme, i.e.

$$\left\langle \frac{\partial \psi}{\partial y_i}\right\rangle = \frac{\partial}{\partial x_i}\langle\psi\rangle + \frac{1}{V_{\text{REV}}} \int\limits_{\Gamma^{\alpha\beta}} (\psi^\alpha - \psi^\beta)\, n_i^{\alpha\beta}dS$$

$$\left\langle \frac{\partial \psi}{\partial t}\right\rangle = \frac{\partial}{\partial t}\langle\psi\rangle - \frac{1}{V_{\text{REV}}} \int\limits_{\Gamma^{\alpha\beta}} (\psi^\alpha - \psi^\beta)\, n_i^{\alpha\beta}\, v_i^{\alpha\beta}dS$$

The transformation rules specified above define the averaging procedure only; i.e. they do not incorporate any information on the interaction between RVE and the rest of the body. As a consequence, the micro-macro transition cannot, in general, be fully described by employing these relations alone. This is illustrated below by an example in which an attempt is made to transform the local microscopic description of a flow of an incompressible viscous fluid in a rigid porous medium using the transformation rules (1.25).

The microscopic description incorporates the following governing equations:
- incompressibility condition

$$\frac{\partial v_i}{\partial y_i} = 0 \quad \text{in } V_f \tag{1.26}$$

- kinematic constraint along the solid-fluid interface

$$v_i = 0 \quad \text{on } \Gamma \tag{1.27}$$

- equilibrium requirement

$$\frac{\partial \sigma_{ij}}{\partial y_i} = 0 \quad \text{in } V_f \tag{1.28}$$

16

- constitutive relation

$$\sigma_{ij} = -p\delta_{ij} + \mu \left(\frac{\partial v_i}{\partial y_j} + \frac{\partial v_j}{\partial y_i} \right) \quad \text{in } V_f \tag{1.29}$$

In the equations above, V_f is the volume of fluid in RVE, v_i is the fluid velocity, p is the fluid pressure and μ is the viscosity coefficient. Employing now the averaging scheme (1.25) in relation (1.26), together with (1.27), gives the macroscopic form of incompressibility condition, i.e.

$$\frac{\partial \langle v_i \rangle}{\partial x_i} = 0 \tag{1.30}$$

Apparently, eq.(1.30) is a standard constraint for an incompressible continuum. Applying the averaging procedure to equations of static equilibrium yields

$$\frac{\partial \langle \sigma_{ij} \rangle}{\partial x_i} + \frac{1}{V_{REV}} \int_{\Gamma} \sigma_{ij} \, n_i \, dS = 0 \tag{1.31}$$

while the averaging of the constitutive relation (1.29) gives

$$\langle \sigma_{ij} \rangle = -\langle p \rangle \delta_{ij} + \mu \left(\frac{\partial \langle v_i \rangle}{\partial x_j} + \frac{\partial \langle v_j \rangle}{\partial x_i} \right) \tag{1.32}$$

Finally, substituting eq.(1.32) as well as (1.29) in eq.(1.31), and employing the incompressibility condition (1.30), yields

$$0 = -\frac{\partial \langle p \rangle}{\partial x_j} + \mu \nabla_x^2 \langle v_j \rangle + \frac{1}{V_{REV}} \int_{\Gamma} \left[-p\delta_{ij} + \mu \left(\frac{\partial v_i}{\partial y_j} + \frac{\partial v_j}{\partial y_i} \right) \right] n_i \, d\Gamma \tag{1.33}$$

It is apparent that eq.(1.33) contains not only macro- but also micro-variables. Thus, without additional assumptions, the averaged form (1.33) cannot be perceived as a macroscopic description. The reason behind it is the lack of hypothesis that would define the response along boundaries between RVE and the rest of the medium. Therefore, the averaging scheme alone leads to a macroscopic equilibrium statement that incorporates unidentified terms responsible for the interaction between constituents; such as the last term in representation (1.33).

In order to complete a transformation between different observation scales, the microscopic description needs, in general, to be supplemented by suitable boundary conditions at the peripheries of RVE. These conditions should reflect, as closely as possible, the actual state of RVE within the considered medium (cf. [11]).

Incorporation of specific boundary conditions in the local description is often referred to as a 'closing hypothesis'. It allows isolating RVE from its environment and, thus, narrowing the scope of analysis to the examination of mechanical characteristics of RVE alone. Furthermore, the specification of boundary conditions for RVE allows to define appropriate 'localization laws', i.e. relations between macroscopic variables and their micro-counterparts, for a given microstructure of the material.

For composite solids, the simplest and most frequently employed closing hypothesis is the assumption of uniform stress/strain state. However, such a hypothesis is justified only when the size of individual inhomegeneities is small compared to dimensions of RVE. In case of periodic media, i.e. when the material structure can be reconstructed based on a single RVE cell, the boundary conditions incorporate the local periodicity of the considered physical fields.

1.2. Continuum micromechanics

As mentioned earlier, the applicability of weight/volume averaging alone is limited due to the absence of boundary conditions between RVE and the rest of the body. The specification of these conditions supplements the micro-description and leads to a boundary value problem which, in turn, allows for transition from micro to macro-level. This is illustrated by an example that is provided below.

Consider diffusion process in a micro-heterogeneous solid material. Assume that the solid matrix contains several constituents that have different coefficients of diffusion. Let the distribution of constituents be random and the medium be statistically homogeneous on the macro-scale. The micro-description of the diffusion process is based on:
- Fick's law, which assumes a linear relation between the mass flux of the diffusing substance and the concentration gradient, i.e.

$$q_i^\alpha = -D^\alpha \frac{\partial C^\alpha}{\partial y_i} \quad \text{in} \quad V^\alpha \tag{1.34}$$

- the conservation of mass

$$\frac{\partial C^\alpha}{\partial t} + \frac{\partial q_i^\alpha}{\partial y_i} = 0 \quad \text{in} \quad V^\alpha \tag{1.35}$$

In the equations above, the index α refers to a given constituent. Thus, V^α is the volume occupied by this constituent in RVE, so that $V_{RVE} = \sum_{\alpha=1}^{N} V^\alpha$ and $\alpha = 1, 2, ... N$. Furthermore, q_i^α is the mass flux of the diffusing substance, C^α is the concentration and D^α is the coefficient of diffusion in constituent α. The flux is said to be continuous at the interfaces between the constituents.

Applying the spatial averaging rules, described in the preceding section, eq.(1.35) can be written as

$$\frac{\partial \langle C \rangle}{\partial t} + \frac{\partial \langle q_i \rangle}{\partial x_i} = 0 \tag{1.36}$$

where

$$\langle q_i \rangle = -\left\langle D^\alpha \frac{\partial C^\alpha}{\partial y_i} \right\rangle \tag{1.37}$$

Note that without specifying the boundary conditions at the peripheries of RVE, the average flux $\langle q_i \rangle$ cannot be expressed as an explicit function of macroscopic variables $\langle C \rangle$ and x_i.

In order to formulate the boundary conditions, note that since $\langle C^\alpha \rangle = \langle C \rangle$ and $\left\langle \dfrac{\partial C^\alpha}{\partial y_i} \right\rangle = \dfrac{\partial \langle C \rangle}{\partial x_i}$, the concentration of the considered substance at any point within RVE can be defined as

$$C = \frac{\partial \langle C \rangle}{\partial x_i}(y_i - x_i) + \langle C \rangle + \overline{C} \tag{1.38}$$

Here, the index α has been omitted as the concentration is defined as a function of position within RVE, i.e. $C = C(Y - X)$. The coordinates x_i specify, once again, the location of the centroid of RVE, while $\overline{C} = \overline{C}(Y - X)$ is referred to as corrector. The presence of corrector function in (1.38) is the result of the heterogeneity of solid matrix; for a homogeneous medium $\overline{C}(Y - X) = 0$, while for an inhomogeneous one there is $\langle \overline{C}(Y - X) \rangle = 0$. The latter constraint can be formally obtained by averaging (1.38) and noting that $\langle y_i - x_i \rangle = 0$.

Now, the boundary conditions for RVE are typically formulated by assigning specific values to corrector or its gradient. For a periodic structure, the periodicity of corrector function is postulated; whereas for random media, the vanishing of the corrector or its gradient is assumed.

In order to express the average flux $\langle q_i \rangle$ in terms of macroscopic variables, consider a stationary diffusion process within RVE

$$\frac{\partial q_i}{\partial y_i} = 0 \quad \text{in} \quad V_{RVE} \tag{1.39}$$

Assigning a zero value to the corrector along boundaries of RVE and substituting the Fick's law (1.34) together with (1.38) in (1.39), one obtains

$$\begin{cases} -\dfrac{\partial}{\partial y_i}\left\{D\left[\dfrac{\partial \langle C\rangle}{\partial x_i} + \dfrac{\partial \bar{C}}{\partial y_i}\right]\right\} = 0 & \text{in} \quad V_{RVE} \\[4mm] \bar{C} = 0 & \text{on} \quad \partial V_{RVE} \end{cases} \tag{1.40}$$

where $D = D^\alpha$ for $Y \in V^\alpha$. Note that the variables x_i, $\langle C\rangle$ and $\dfrac{\partial \langle C\rangle}{\partial x_i}$ are associated with the centroid of RVE and are thus independent of the spatial coordinates y_i.

The boundary value problem (1.40) has a linear form, so that $\bar{C}$ is linearly dependent on the macroscopic gradient $\dfrac{\partial \langle C\rangle}{\partial x_i}$, i.e.

$$\bar{C} = A_i \dfrac{\partial \langle C\rangle}{\partial x_i} \tag{1.41}$$

where $A_j = A_j(Y - X)$ is the solution of (1.40) corresponding to macroscopic gradient with its *j*-component equal to one and the remaining ones equal to zero.

By introducing now a tensor field $B_{ij} = B_{ij}(Y - X)$ defined as

$$B_{ij} = \dfrac{\partial A_i}{\partial y_j} \tag{1.42}$$

the gradient of the corrector can be expressed as

$$\dfrac{\partial \bar{C}}{\partial y_i} = B_{ij}\dfrac{\partial \langle C\rangle}{\partial x_j} \tag{1.43}$$

Finally, utilizing eqs.(1.38) and (1.43), the so-called 'localization law' can be established that relates the local value of the concentration gradient, at an arbitrary point within RVE, to its macroscopic counterpart, i.e.

$$\dfrac{\partial C}{\partial y_i} = \dfrac{\partial \langle C\rangle}{\partial x_i} + \dfrac{\partial \bar{C}}{\partial y_i} = P_{ij}\dfrac{\partial \langle C\rangle}{\partial x_j} \tag{1.44}$$

where $P_{ij} = \left(\delta_{ij} + B_{ij}(Y - X)\right)$ is referred to as the localization operator. The relation (1.44) allows now to express the macroscopic flux of the diffusing substance as a function of the concentration gradient, i.e.

$$\langle q_i\rangle = -\left\langle DP_{ij}\right\rangle\dfrac{\partial \langle C\rangle}{\partial x_j} = -D_{ij}^{\text{hom}}\dfrac{\partial \langle C\rangle}{\partial x_j} \tag{1.45}$$

The equation above represents the macroscopic constitutive relation which describes the diffusion process in a medium that is homogeneous at the macro-scale. The tensor D_{ij}^{hom} is the effective (homogenized) diffusion tensor.

It should be noted that by introducing the volume average of P_{ij} for constituent α, i.e.

$$\left\langle P_{ij} \right\rangle^{\alpha} = \frac{1}{V^{\alpha}} \int_{V^{\alpha}} P_{ij} \, dV \qquad (1.46)$$

the effective diffusion tensor can be expressed in the equivalent form

$$D_{ij}^{\text{hom}} = \sum_{\alpha=1}^{N} c^{\alpha} D^{\alpha} \left\langle P_{ij} \right\rangle^{\alpha} \qquad (1.47)$$

where $c^{\alpha} = V^{\alpha} / V_{RVE}$ is the volume fraction of constituent α.

In special cases that involve simple microstructures, a straightforward assessment of D_{ij}^{hom} can be made. Assume, for example, that the constituents are distributed in such a way that in each of them the average value of the concentration gradient is the same as the value representative of the macroscale. In this case $\left\langle P_{ij} \right\rangle^{\alpha} = \delta_{ij}$, so that

$$D_{ij}^{\text{hom}} = \sum_{\alpha=1}^{N} c^{\alpha} D^{\alpha} \delta_{ij} \qquad (1.48)$$

The distribution of constituents and the average direction of diffusion corresponding to this scenario are shown schematically in Fig.1.5a.
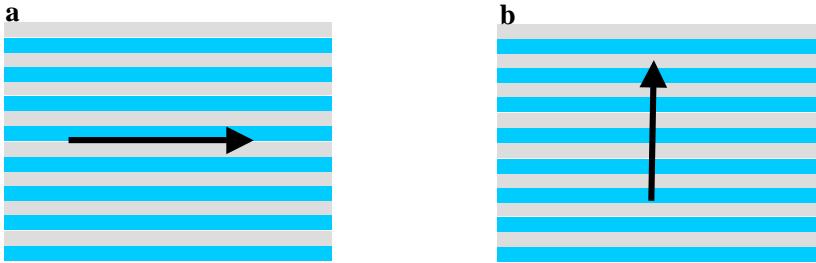

Fig.1.5. Composite with a layered microstructure

On the other hand, if the distribution of constituents is such that in each of them the average mass flux is the same as that at the macro-scale, then

$$D_{ij}^{\text{hom}} = D^{\alpha} \left\langle P_{ij} \right\rangle^{\alpha} \tag{1.49}$$

Note that the averaging of eq.(1.44) results in $\left\langle P_{ij} \right\rangle = \delta_{ij}$, therefore

$$\sum_{\alpha=1}^{N} c^{\alpha} \left\langle P_{ij} \right\rangle^{\alpha} = \delta_{ij} \tag{1.50}$$

Taking now into account eqs.(1.49) and (1.50), the following relation is obtained

$$\sum_{\alpha=1}^{N} c^{\alpha} \left\langle P_{ij} \right\rangle^{\alpha} = \sum_{\alpha=1}^{N} c^{\alpha} \frac{D_{ij}^{\text{hom}}}{D^{\alpha}} = \delta_{ij} \quad \Rightarrow \quad D_{ij}^{\text{hom}} = \frac{\delta_{ij}}{\sum_{\alpha=1}^{N} \dfrac{c^{\alpha}}{D^{\alpha}}} \tag{1.51}$$

The values of components of the effective diffusion tensor are again representative of a layered structure; this time, however, the direction of diffusion is along the layering.

It is evident from the discussion above that by supplementing the micro-description with suitable boundary conditions a macroscopic form of the diffusion law is obtained. In addition, in case when the geometry of microstructure is specified, the components of the effective diffusion tensor can be defined as an explicit function of diffusion coefficients of constituents. The later requires, in a general case, the solution of the boundary value problem (1.40) and the specification of the localization operator $P_{ij} = P_{ij}(Y - X)$.

It is noted that if the boundary conditions invoke periodicity of corrector, or if the gradient of the corrector is said to be zero along the boundary of RVE, then the general form of the constitutive relation remains the same as that of (1.45). Moreover, if RVE is large enough then the effective diffusion tensor is independent of the type of boundary condition employed.

Diffusion process consists of random molecular motions. At the same time, in formulating the response at the micro-level, viz. eqs.(1.34) and (1.35), a classical approach of continuum mechanics has been employed. Thus, the framework does not take into account the existence of substructures at a lower level of magnification. In general, the application of the tools of continuum mechanics at the micro-level for the

description of physical processes (such as heat transfer, mass transport, deformation, etc.) is referred to as *continuum micromechanics*. This approach is aimed primarily at assessing the macroscopic 'effective' response for a given microstructure under a prescribed change in external agencies. Clearly, the framework allows for examining the influence of micro-structural parameters on the characteristics at the macro-level.

Apparently, the specific mathematical description and its solution at the micro-level both depend on properties of constituents and the type of physical phenomena that occurs; viz. diffusion, filtration, chemical dissolution, brittle fracture, plastic deformation, etc. The class of problems is clearly quite broad. In what follows, the discussion is limited to fundamental definitions and description of procedures employed in continuum micromechanics in relation to quasi-static deformation in composite solid bodies.

To begin with, consider a composite medium in which all constituents are linearly elastic. In this case, the formulation at the micro-level is based on:

- equations of static equilibrium

$$\frac{\partial \sigma_{ij}}{\partial y_i} = 0 \tag{1.52}$$

- constitutive relations that govern the response of constituents

$$\sigma_{ij} = D_{ijkl}\varepsilon_{kl}(U) \tag{1.53}$$

where $U = (u_1, u_2, u_3)$ is a displacement vector and D_{ijkl} is the elastic stiffness tensor,

- kinematic strain-displacement relations (small deformation regime)

$$\varepsilon_{ij}(U) = \frac{1}{2}\left(\frac{\partial u_i}{\partial y_j} + \frac{\partial u_j}{\partial y_i}\right) \tag{1.54}$$

- continuity requirements for displacement and traction vectors at the interfaces between the constituents.

The macroscopic measure of strain, associated with the micro-strain tensor $\varepsilon_{ij}(U)$, is defined as the average over the volume of RVE, i.e.

$$\left\langle \varepsilon_{ij} \right\rangle = \frac{1}{V_{\text{RVE}}} \int_{V_{\text{RVE}}} \varepsilon_{ij}(U) \ dV \tag{1.55}$$

Similarly, the macroscopic variable associated with given micro-stress field σ_{ij} is defined as

$$\left\langle \sigma_{ij} \right\rangle = \frac{1}{V_{\text{RVE}}} \int\limits_{V_{\text{RVE}}} \sigma_{ij} dV = \frac{1}{V_{\text{RVE}}} \int\limits_{\partial V_{\text{RVE}}} \sigma_{ik} n_k \left(y_j - x_j \right) dS \qquad (1.56)$$

The relations above indicate that the macro-strain tensor is implicitly defined through the kinematic boundary conditions, while the macro-stress is defined by the traction acting at the boundaries of RVE. Furthermore, if RVE is perceived as a parallelepiped, then the volume average of the stress tensor is the same as the average taken over the corresponding surface area. The 'effective' response of the composite, regarded as an equivalent homogeneous medium, is defined by the relation between $\left\langle \varepsilon_{ij} \right\rangle$ and $\left\langle \sigma_{ij} \right\rangle$. It should also be noted that since the displacement is continuous at the interface between constituents then, according to the spatial averaging rules,

$$\left\langle \varepsilon_{ij}(U) \right\rangle = \frac{1}{2} \left(\frac{\partial \left\langle u_i \right\rangle}{\partial x_j} + \frac{\partial \left\langle u_j \right\rangle}{\partial x_i} \right) \qquad (1.57)$$

The microscopic displacement field can be expressed in the form analogous to that employed in the context of diffusion problem, eq.(1.38), i.e.

$$u_i = \left\langle \varepsilon_{ij} \right\rangle \left(y_j - x_j \right) + \left\langle u_i \right\rangle + \bar{u}_i \qquad (1.58)$$

Here, $\bar{u}_i = \bar{u}_i (Y - X)$ are components of vector $\bar{U}$ which is again viewed as a corrector that accounts for heterogeneity of the microstructure of RVE. For random media, the boundary conditions are normally defined by assuming a zero value for the corrector $\bar{u}_i$ or by imposing a uniform traction $\sigma_{ij} n_j = T_i$ on ∂V_{RVE}, where n_i is the unit normal to the boundary. For periodic media, the periodicity of corrector and its derivative is assumed.

The functional form (1.58) implies that

$$\varepsilon_{ij}(U) = \left\langle \varepsilon_{ij} \right\rangle + \varepsilon_{ij} \left(\bar{U} \right) \qquad (1.59)$$

Substituting the above equation in the constitutive relation (1.53) and utilizing the equilibrium constraints (1.52), the following relation is obtained

25

$$\frac{\partial}{\partial y_i}\left[D_{ijkl}\left\langle\varepsilon_{kl}\right\rangle + D_{ijkl}\varepsilon_{kl}\left(\bar{U}\right)\right] = 0 \tag{1.60}$$

Adopting now one of the boundary conditions, i.e. vanishing of the corrector, its periodicity or uniformity of traction along the boundary, the general solution to the boundary value problem for RVE can be expressed in the form

$$\bar{u}_i\left(Y - X\right) = A_{ijk}\left\langle\varepsilon_{jk}\right\rangle \tag{1.61}$$

where the tensorial field $A_{ijk} = A_{ijk}\left(Y - X\right)$ is the solution to eq.(1.60), for a specific boundary condition, under $\left\langle\varepsilon_{lm}\right\rangle = \frac{1}{2}\left(\delta_{lj}\delta_{mk} + \delta_{lk}\delta_{mj}\right)$.

Following the same procedure as that outlined for the diffusion problem, the 'localization law' can be established as

$$\varepsilon_{ij}\left(U\right) = P_{ijkl}\left\langle\varepsilon_{kl}\right\rangle \tag{1.62}$$

The tensorial field $P_{ijkl} = P_{ijkl}\left(Y - X\right)$ is the localization operator that defines the micro-strain in terms of the macroscopic effective strain measure. The averaging of eq.(1.62) leads to the following constraint

$$\left\langle P_{ijkl}\right\rangle = \frac{1}{2}\left(\delta_{ik}\delta_{jl} + \delta_{il}\delta_{jk}\right) \tag{1.63}$$

The constitutive relation at the macro-level has the form

$$\left\langle\sigma_{ij}\right\rangle = \left\langle D_{ijkl}\varepsilon_{kl}\left(U\right)\right\rangle = \left\langle D_{ijkl}P_{klmn}\right\rangle\left\langle\varepsilon_{mn}\right\rangle \tag{1.64}$$

so that the effective elastic stiffness tensor is defined as

$$D_{ijmn}^{\text{hom}} = \left\langle D_{ijkl}P_{klmn}\right\rangle \tag{1.65}$$

If the composite medium within RVE contains N distinct constituents $\alpha = 1, 2, ..., N$, then by employing the averaging over the respective volumes V^{α}, the relation (1.65) can be expressed in the equivalent form

$$D_{ijkl}^{\text{hom}} = \sum_{\alpha=1}^{N} c^{\alpha} D_{ijmn}^{\alpha}\left\langle P_{mnkl}\right\rangle^{\alpha} \tag{1.66}$$

where c^{α} are the volume fractions.

26

Furthermore, by analogy to relation (1.62), a similar localization law can be formulated for the stress tensor, i.e.

$$\sigma_{ij} = S_{ijkl} (Y - X) \langle \sigma_{kl} \rangle \qquad (1.67)$$

where the localization operator is defined as

$$S_{ijkl} = D_{ijmn} P_{mnpq} \left[D_{pqkl}^{\text{hom}} \right]^{-1} \qquad (1.68)$$

Here, $\left[D_{pqkl}^{\text{hom}} \right]^{-1}$ represents the effective compliance operator, which is defined as the inverse of the elastic stiffness.

Quite often, when formulating the macroscopic relations the closing hypothesis employs, instead of boundary conditions, the so-called Hill's macro-homogeneity condition. The latter is expressed as

$$\langle \sigma_{ij} \varepsilon_{ij} \rangle = \langle \sigma_{ij} \rangle \langle \varepsilon_{ij} \rangle \qquad (1.69)$$

In this case, the basic hypothesis defining the equivalent medium is that of equivalence in energy. It needs to be emphasized that the equality (1.69) needs to be satisfied for arbitrary ε_{ij} and σ_{ij}, even when these quantities are not explicitly related through a constitutive law. The only requirement is that the microscopic stress field must be a self-equilibrated one, it must satisfy the equilibrium conditions (1.52). It should also be noted that Hill's macro-homogeneity condition is identically satisfied in case when the boundary conditions described earlier are employed (cf. Ref.[11]).

As an equivalent approach, the problem can be formulated by invoking the principle of minimum potential energy. Among all virtual displacement fields $u_i(y_i)$ satisfying the kinematic boundary conditions, the actual one is characterized by the minimum value of the potential energy. For composite comprising N constituents, the actual displacement field within RVE is the one that minimizes the average strain energy density, i.e.

$$\inf_{U \in K(\langle \varepsilon_{ij} \rangle)} \langle w(Y, \varepsilon_{ij}(U)) \rangle = \inf_{U \in K(\langle \varepsilon_{ij} \rangle)} \left\langle \sum_{\alpha=1}^{N} h^{\alpha} w^{\alpha} \left(\varepsilon_{ij}(U) \right) \right\rangle \qquad (1.70)$$

where *inf* stands for infimum and

$$w^{\alpha}(\varepsilon_{ij}(U)) = \frac{1}{2} D_{ijkl}^{\alpha} \varepsilon_{ij}(U) \varepsilon_{kl}(U) \qquad (1.71)$$

is the strain energy in constituent α. Invoking, as the closing hypothesis, the uniformity of the strain field, the kinematically admissible displacement field is represented by the set

$$K(\langle \varepsilon_{ij} \rangle) = \left\{ U \mid u_i = \langle \varepsilon_{ij} \rangle (y_j - x_j) \quad \text{on} \quad \partial V_{REV} \right\} \tag{1.72}$$

The expression (1.70) defines the macroscopic (equivalent) strain energy potential

$$W\left(\langle \varepsilon_{ij} \rangle\right) = \inf_{U \in K(\langle \varepsilon_{ij} \rangle)} \left\langle w\left(Y, \varepsilon_{ij}(U)\right) \right\rangle \tag{1.73}$$

which, in turn, defines implicitly the form of the macroscopic constitutive relation.

Note that

$$\frac{\partial W\left(\langle \varepsilon_{ij} \rangle\right)}{\partial \langle \varepsilon_{kh} \rangle} = \left\langle \frac{\partial w}{\partial \varepsilon_{ij}} \varepsilon_{ij}\left(\frac{\partial U}{\partial \langle \varepsilon_{kh} \rangle}\right) \right\rangle = \left\langle \sigma_{ij} \varepsilon_{ij}\left(\frac{\partial U}{\partial \langle \varepsilon_{kh} \rangle}\right) \right\rangle \tag{1.74}$$

where the last transformation makes use of the property that the micro-stress tensor is a derivative of the strain energy with respect to micro-strain.

Components of $\dfrac{\partial U}{\partial \langle \varepsilon_{kl} \rangle}$, in view of eq. (1.72), verify the following relation, i.e.:

$$\frac{\partial u_i}{\partial \langle \varepsilon_{kl} \rangle} = \frac{1}{2}\left(\delta_{ik}\delta_{ml} + \delta_{il}\delta_{mk}\right)\left(y_m - x_m\right) \quad \text{on} \quad \partial V_{REV} \tag{1.75}$$

It means that $\dfrac{\partial U}{\partial \langle \varepsilon_{kl} \rangle}$ is a kinematically admissible field corresponding to a unit macro-strain. According now to Hill's macro-homogeneity condition (1.69), one can write

$$\left\langle \sigma_{ij} \varepsilon_{ij}\left(\frac{\partial U}{\partial \langle \varepsilon_{kh} \rangle}\right) \right\rangle = \left\langle \sigma_{ij} \right\rangle \frac{1}{2}\left(\delta_{ik}\delta_{jh} + \delta_{ih}\delta_{jk}\right) = \left\langle \sigma_{kh} \right\rangle \tag{1.76}$$

Thus, the macroscopic constitutive relation is defined by

$$\left\langle \sigma_{ij} \right\rangle = \frac{\partial W\left(\langle \varepsilon_{kl} \rangle\right)}{\partial \langle \varepsilon_{ij} \rangle} \tag{1.77}$$

Following an analogous procedure, the macroscopic complimentary energy potential can be defined as

$$W^*\left(\left\langle \sigma_{ij} \right\rangle\right) = \inf_{\tau_{ij} \in S(\langle \sigma \rangle)} \left\langle w^*\left(Y, \tau_{ij}\right) \right\rangle = \inf_{\tau_{ij} \in S(\langle \sigma \rangle)} \left\langle \sum_{\alpha=1}^{N} h^\alpha(y)\, u^\alpha(\tau_{ij}) \right\rangle \qquad (1.78)$$

where $w^*(\tau_{ij})$ is the complimentary energy in constituent α and the statically admissible stress field is defined by the set

$$S(\langle \sigma_{ij} \rangle) = \left\{ \tau_{ij} \; \Big| \frac{\partial \tau_{ij}}{\partial y_i} = 0 \;\; \text{in} \;\; V_{\text{REV}}, \left\langle \tau_{ij} \right\rangle = \left\langle \sigma_{ij} \right\rangle \right\} \qquad (1.79)$$

In this case, the complimentary form of representation (1.77) becomes

$$\left\langle \varepsilon_{ij} \right\rangle = \frac{\partial W^*\left(\left\langle \sigma_{kl} \right\rangle\right)}{\partial \left\langle \sigma_{ij} \right\rangle} \qquad (1.80)$$

It is noted that if the stress-strain relations for constituents (defined at the micro-level by means of derivatives of strain or complimentary strain energy) are non-linear and, at the same time, the strain energy function is strictly convex, then the macroscopic representation remains the same as that in eqs.(1.77) or (1.80). Thus, the formulation of the constitutive law at the macro-scale reduces to specification of macroscopic strain or complementary strain energy potentials.

In case when the constituents are rigid perfectly-plastic, the dissipation function is convex, but not strictly convex. As a result, such composite media should be treated differently (cf. Bouchitte [12], Suquet [13, 14]). For random media, the closing hypothesis is then the condition of uniformity of plastic strain rate; while for periodic media, the condition of periodicity. The macroscopic form of the yield function becomes

$$F\left(\left\langle \sigma_{ij} \right\rangle\right) \leq 0 \Leftrightarrow \left\langle \sigma_{ij} \right\rangle \in P^h =$$
$$= \left\{ \left\langle \tau_{ij} \right\rangle \Big| \exists \tau_{ij}(y) \;, \frac{\partial \tau_{ij}}{\partial y_i} = 0, \left\langle \tau_{ij} \right\rangle = \left\langle \sigma_{ij} \right\rangle, f^\alpha\left(\tau_{ij}\right) \leq 0 \;\; \forall y \in V_\alpha \; \wedge \; \forall \alpha \right\} \qquad (1.81)$$

while the flow rule takes the form

$$\left\langle \dot{\varepsilon}_{ij}^p \right\rangle = \lambda \frac{\partial F\left(\left\langle \sigma_{kl} \right\rangle\right)}{\partial \left\langle \sigma_{ij} \right\rangle} \qquad (1.82)$$

In summary, the specification of the effective response of a composite medium requires the solution of an appropriately formulated boundary value problem and the averaging of the primary variables. In case of deterministic heterogeneous media, such as periodic composites, the continuum micromechanics approach allows to uniquely define the effective response at the macro-scale. In case of random composites though, the statistical information on the microstructure is only partial, so that the precise evaluation of effective properties is not possible. In this case, the micromechanical considerations are used to establish the bounds for the effective properties, based on given statistical information, and/or to provide estimates corresponding to specific types of composites (Refs. [15,16,17,18]). The particular methods used for assessment of effective properties are discussed in the next section.

CHAPTER 2

_____

Analytical Methods Of Estimating
The Effective Properties

In case of micro-heterogeneous media with a periodic structure, the problem of assessment of effective properties reduces to solution of a boundary value problem that is formulated for a periodic cell. If the geometry, the distribution and physical properties of constituents are known, then the effective properties can be determined in a unique manner. For random composites the distribution of constituents and their geometry are not strictly defined, i.e. only limited statistical information is available. Typically, the primary information which can be obtained is that on volume fractions of individual constituents. Furthermore, if there is no preferred arrangement of constituents, i.e. the structure is not ordered, the other statistical information available is that stipulating the isotropy of the medium at the macro-scale.

Apparently, for random materials that are statistically homogeneous, one can invoke the hypothesis of periodicity in order to formulate the macroscopic description. It is noted, however, that methodologies for the assessment of effective properties in periodic and random media are different. In particular, in the former case, since the statistical information is incomplete, only the estimates of effective properties and the range of their admissible values can be provided. Clearly, the most established and rigorous approaches are those for estimating the effective parameters of random media in the linear range, e.g. the effective linear-elastic constants. The problem of the assessment of the response in non-linear range is still wide-open, although in the last decade some significant advances have been made (cf. Suquet & Ponte Castaneda [19]). The most common approach is the concept of a homogeneous linear comparison medium. In this case, the effective non-

linear response is estimated from the classical approach for linear media through an appropriate selection of properties of the comparison material [19].

For random media, it is important to establish the range of admissible values of effective properties. For a macroscopically isotropic medium, the narrowest range of estimates, expressed in terms of volume fractions, can be obtained using the Hashin-Shtrikman bounds (cf. Torquato [20]). For example, for a composite medium comprising N homogeneous constituents with different diffusion properties, the primary information available is that on the values of diffusion coefficients D^α, volume fractions c^α, as well as that on the isotropy of the medium at the macroscale. In this case, the Hashin-Shtrikman bounds take the form (see Ref.[20])

$$\frac{1}{\displaystyle\sum_{\alpha=1}^{N}\frac{c^\alpha}{2D_{\min}+D^\alpha}} - 2D_{\min} \leq D^{\text{hom}} \leq \frac{1}{\displaystyle\sum_{\alpha=1}^{N}\frac{c^\alpha}{2D_{\max}+D^\alpha}} - 2D_{\max} \tag{2.1}$$

where

$$D_{\min} = \min_{\alpha}\left(D^\alpha\right) \qquad D_{\max} = \max_{\alpha}\left(D^\alpha\right) \tag{2.2}$$

A similar structure of the Hashin-Shtrikman bounds is obtained for estimates of effective mechanical properties for a macroscopically isotropic linear-elastic composite comprising N constituents (see Ref.[20]), i.e.

$$\frac{1}{\displaystyle\sum_{\alpha=1}^{N}\frac{c^\alpha}{\frac{4}{3}G_{\min}+K^\alpha}} - \frac{4}{3}G_{\min} \leq K^{\text{hom}} \leq \frac{1}{\displaystyle\sum_{\alpha=1}^{N}\frac{c^\alpha}{\frac{4}{3}G_{\max}+K^\alpha}} - \frac{4}{3}G_{\max} \tag{2.3}$$

$$\frac{1}{\displaystyle\sum_{\alpha=1}^{N}\frac{c^\alpha}{H_{\min}+G^\alpha}} - H_{\min} \leq G^{\text{hom}} \leq \frac{1}{\displaystyle\sum_{\alpha=1}^{N}\frac{c^\alpha}{H_{\max}+G^\alpha}} - H_{\max} \tag{2.4}$$

$$H_{\min} = \min_{\alpha}\left(G^\alpha\frac{\frac{3}{2}K^\alpha+2G^\alpha}{K^\alpha+2G^\alpha}\right) \qquad H_{\max} = \max_{\alpha}\left(G^\alpha\frac{\frac{3}{2}K^\alpha+2G^\alpha}{K^\alpha+2G^\alpha}\right) \tag{2.5}$$

where K^α and G^α are the bulk and shear moduli, respectively, of the constituent α.

The inequalities given above define the range of acceptable values of effective properties. Apart from volume fractions and the isotropy of properties at the macroscale, no other information about the microstructure is incorporated. In general, the estimates of effective properties are typically established by using approximate schemes that employ more information about the material structure, e.g. that on the geometry of constituents. Most of the existing schemes are based on a solution of a *single inclusion problem*. Examples include approximations of Maxwell, Mori-Tanaka as well as the self-consistent scheme [41].

2.1. Diffusion problem

2.1.1. Single inclusion solution

The considerations here start with a discussion related to a diffusion problem in an infinite domain that contains a single spherical inclusion. For ellipsoidal inclusions only the final form of the solution is provided.

Consider a diffusion process in an infinite homogeneous medium that contains a single spherical inclusion of radius R (Fig.2.1). Assume that both the matrix and the inclusion are isotropic and have diffusion coefficients D^m and D^α, respectively. In order to define the geometry, introduce a spherical coordinate system with the origin fixed at the centroid of the sphere (Fig.2.1). As a boundary condition, assume that at infinity the x_3-component of the concentration gradient has a specified constant value, while the remaining components are equal to zero.
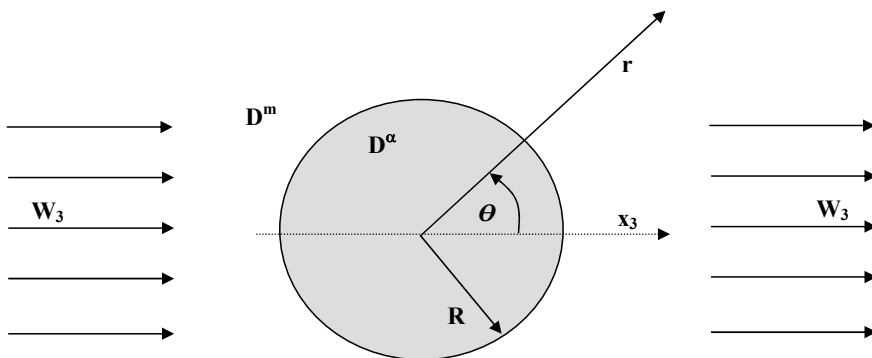

Fig.2.1. Coordinate system for sphere of radius R embedded within an infinite matrix

33

The concentration of the diffusing substance, C, satisfies the Laplace equation

$$\frac{1}{r^2}\frac{\partial}{\partial r}\left(r^2\frac{\partial C}{\partial r}\right)+\frac{1}{r^2\sin\theta}\frac{\partial}{\partial\theta}\left(\sin\theta\frac{\partial C}{\partial\theta}\right)=0 \tag{2.6}$$

where θ is an angle between the x_3-axis and the radial direction r.

Along the surface of the inclusion, both the concentration as well as the radial component of the flux vector must remain continuous. Thus,

$$C\big|_{R_-}-C\big|_{R_+}=0 \tag{2.7}$$

$$D^\alpha\frac{\partial C}{\partial r}\bigg|_{R_-}-D^m\frac{\partial C}{\partial r}\bigg|_{R_+}=0 \tag{2.8}$$

where $C\big|_{R_-}$ and $C\big|_{R_+}$ are the values of C at the surface ($r=R$) taken from the inside and outside, respectively. A similar notation is used for the flux vector as well, viz. eq.(2.8).

The boundary condition for the radial component of concentration gradient requires

$$r\to\infty \;\Rightarrow\; C\to W_3 r\cos\theta \tag{2.9}$$

where W_3 is the assumed constant value at $x_3\to\infty$.

The general solution of eq.(2.6) takes the form

$$C(r,\theta)=A_1 W_3 r\cos\theta+B_1 W_3\frac{\cos\theta}{r^2} \tag{2.10}$$

where A_1 and B_1 are constants that can be determined from the boundary condition and the continuity requirement. Since outside the sphere, the boundary condition (2.9) must be satisfied; the solution in this region takes the form

$$C(r,\theta)=W_3 r\cos\theta+B_1 W_3\frac{\cos\theta}{r^2}\qquad r\geq R \tag{2.11}$$

For the domain enclosed within the sphere, the concentration C must assume a finite value at $r=0$, so that

$$C(r,\theta)=A_1 W_3 r\cos\theta\qquad r\leq R \tag{2.12}$$

Imposing now the continuity requirements (2.7)-(2.8) in eqs.(2.11) and (2.12), a set of two simultaneous linear equations is obtained for A_1 and B_1, from which

$$A_1 = \frac{3D^m}{2D^m + D^\alpha}, \qquad B_1 = R^3 \frac{D^m - D^\alpha}{2D^m + D^\alpha} \tag{2.13}$$

Substituting the above values in the expressions (2.10) and (2.11) leads to the following representation

$$C(r,\theta) = \begin{cases} W_3 r \cos\theta + \beta_\alpha^m W_3 r \left(\dfrac{R}{r}\right)^3 \cos\theta & r \geq R \\ W_3 r \cos\theta + \beta_\alpha^m W_3 r \cos\theta & r \leq R \end{cases} \tag{2.14}$$

where

$$\beta_\alpha^m = \frac{D^m - D^\alpha}{2D^m + D^\alpha} \tag{2.15}$$

The coefficient β_α^m is commonly referred to as 'polarizability coefficient' through an analogy to electric/magnetic polarizabilities.

The value of the x_3-component of the concentration gradient inside the sphere ($r \leq R$) is defined by the relation

$$\frac{\partial C}{\partial x_3} = \frac{\partial C}{\partial r} \cos\theta - \frac{1}{r}\frac{\partial C}{\partial \theta}\sin\theta \tag{2.16}$$

which, after substitution of the second equation in (2.13), reduces to

$$\frac{\partial C}{\partial x_3} = \left(1 + \beta_\alpha^m\right)W_3 \tag{2.17}$$

The remaining components of the concentration gradient inside the inclusion, i.e. those in x_1 and x_2-directions, are equal to zero.

Note that by invoking now the notion of a localization tensor, as introduced in Section 1.2, the relation between the concentration gradient within the sphere and its value at infinity can be established, viz.

$$\frac{\partial C}{\partial x_i} = P_{ij}^{\alpha,m} W_j \qquad P_{ij}^{\alpha,m} = \left(1 + \beta_\alpha^m\right)\delta_{ij} \tag{2.18}$$

The localization tensor $P_{ij}^{\alpha,m}$ is an isotropic second-order tensor whose value depends on the diffusion coefficients of both the inclusion and the matrix.

A similar methodology can be employed to analyze the case of an ellipsoidal inclusion embedded in an infinite matrix. In this case, the solution is more complex so that only the final results, which are later employed in various approximation schemes, are provided here. If the axes of the ellipse are aligned with the coordinate axes x_i, then the latter also define the principal directions of the localization tensor $P_{ij}^{\alpha,m}$. The principal values $P_{(i)}^{\alpha,m}$ (i=1,2,3) are identified as

$$P_{(i)}^{\alpha,m} = \frac{1}{1 + A_{(i)} \dfrac{D^\alpha - D^m}{D^m}} \tag{2.19}$$

where the coefficients $A_{(i)}$ are defined by an elliptic integral

$$A_{(i)} = \frac{1}{2} R_1 R_2 R_3 \int_0^\infty \frac{dz}{\left(z + R_i^2\right)\sqrt{\left(z + R_1^2\right)\left(z + R_2^2\right)\left(z + R_3^2\right)}} \tag{2.20}$$

and the symbol R_i denotes the length of the semi-axis of the ellipse in the direction x_i. The orientation average of the localization tensor represents an isotropic tensor $P_{ij}^{\alpha,m} = P^{\alpha,m}\delta_{ij}$, whose eigenvalues are equal to

$$P^{\alpha,m} = \frac{1}{3}\sum_{i=1}^{3} \frac{1}{1 + A_{(i)} \dfrac{D^\alpha - D^m}{D^m}} \tag{2.21}$$

Particular cases of an ellipsoidal inclusion include a sphere (R_1=R_2=R_3), a needle-shaped inclusion (R_1= R_2, R_3/ R_1→∞) and a disk-shaped inclusion (R_1= R_2, R_3/ R_1→0). Apparently, for a spherical inclusion there is $A_1 = A_2 = A_3 = 1/3$, so that the relation (2.20) reduces to that obtained earlier. For a disk-shaped inclusion, the eigenvalues of the localization tensor become

$$P^{\alpha,m} = \frac{D^m + 2D^\alpha}{3D^\alpha} \tag{2.22}$$

while for a needle-shaped inclusion there is

$$P^{\alpha,m} = \frac{5D^m + D^\alpha}{3\left(D^m + D^\alpha\right)} \tag{2.23}$$

36

Before moving on to the single inclusion problem in elasticity, let us examine first different approximation schemes for dealing with assessment of effective properties within the context of a diffusion problem.

For this purpose, consider composite medium comprising N homogeneous constituents that have different diffusion properties. Assume that all constituents are isotropic within themselves and that their distribution is random. Once again, the statistical information given is that pertaining to volume fractions of constituents and the lack of preferred orientation, i.e. the isotropy of the structure at the macroscale. The problem to be solved is the assessment of the components of the effective diffusion tensor.

In what follows, all the basic approximation schemes are illustrated by considering an abstract auxiliary problem. In this problem, the analyzed composite material is perceived as a sphere of radius R that is embedded in an infinite continuum with known diffusion properties. The sphere is said to be large enough and its constituents small enough, so that the analyzed problem can be conceptually reduced to that of a single spherical inclusion contained in an infinite homogeneous domain. In this case, one can again assume that at infinity the concentration gradient is constant.

2.1.2. Maxwell approximation scheme

This scheme is typically applied to composites in which one of the constituents forms the matrix, while the remaining ones represent the spherical inclusions. Let n^α be the number of inclusions made of constituent α and contained within the primary sphere of radius R. If the radius of the inclusion is R^α, then the volume fraction of a given constituent α becomes

$$c^\alpha = n^\alpha \left(\frac{R^\alpha}{R} \right)^3 \tag{2.24}$$

A similar expression holds for the remaining constituents $\alpha = 1, 2, \ldots, N-1$; except, of course, the constituent $\alpha = N$ which forms the matrix material.

In the Maxwell's scheme it is assumed that the continuum which contains the primary sphere of radius R has the properties of the constituent that forms the matrix of this sphere. Furthermore, it is assumed that volume fraction of inclusions is small (i.e. the distribution is dilute), so that the interaction between them is neglected. In other words, far from the primary sphere, the variation in concentration field is approximated by

superimposing the variations triggered by each individual inclusion that is contained within this sphere. Thus, according to eq.(2.14), the value of the concentration sufficiently far from the sphere is determined as

$$C(r,\theta) = W_3 r \cos\theta + \sum_{\alpha=1}^{N-1} n^\alpha \beta_\alpha^m W_3 r \left(\frac{R^\alpha}{r}\right)^3 \cos\theta \qquad (2.25)$$

Taking now into account the definition (2.24) and noting that

$$\sum_{\alpha=1}^{N-1} n^\alpha \left(\frac{R^\alpha}{R}\right)^3 \beta_\alpha^m \left(\frac{R}{r}\right)^3 = \sum_{\alpha=1}^{N-1} c^\alpha \beta_\alpha^m \left(\frac{R}{r}\right)^3 \qquad (2.26)$$

the relation (2.25) can be expressed as

$$C(r,\theta) = W_3 r \cos\theta \left(1 + \sum_{\alpha=1}^{N-1} c^\alpha \beta_\alpha^m \left(\frac{R}{r}\right)^3\right) \qquad (2.27)$$

The primary sphere may be considered as a homogeneous medium with an equivalent diffusion coefficient D^{hom}. Thus, the concentration away from the sphere may also be defined as

$$C(r,\theta) = W_3 r \cos\theta \left(1 + \beta_{hom}^m \left(\frac{R}{r}\right)^3\right) \qquad (2.28)$$

where

$$\beta_{hom}^m = \frac{D^m - D^{hom}}{2D^m + D^{hom}} \qquad (2.29)$$

Thus, comparing eqs.(2.28) and (2.29), there is

$$\beta_{hom}^m = \sum_{\alpha=1}^{N-1} c^\alpha \beta_\alpha^m \qquad (2.30)$$

Employing now the definition of 'polarizability' coefficient, viz. eq.(2.15), one finally obtains

$$\frac{D^m - D^{hom}}{2D^m + D^{hom}} = \sum_{\alpha=1}^{N-1} c^\alpha \frac{D^m - D^\alpha}{2D^m + D^\alpha} \qquad (2.31)$$

Maxwell's approximation is an explicit approach, in the sense that the effective diffusion coefficient is obtained directly from parameters that define the properties of constituents. In fact, eq.(2.31) can be expressed as

$$D^{\text{hom}} = D^m \frac{3\sum\limits_{\alpha=1}^{N} c^\alpha \dfrac{D^\alpha}{2D^m + D^\alpha}}{1 + \sum\limits_{\alpha=1}^{N} c^\alpha \dfrac{D^m - D^\alpha}{2D^m + D^\alpha}} \qquad (2.32)$$

which, after some further transformations leads to

$$D^{\text{hom}} = \frac{1}{\sum\limits_{\alpha=1}^{N} \dfrac{c^\alpha}{2D^m + D^\alpha}} - 2D^m \qquad (2.33)$$

The general form of the equation above is analogous to the representation (2.1) that defines Hashin-Shtrikman bounds. It is noted that if the diffusion coefficients of inclusions, D^α, are smaller/larger than the value corresponding to the matrix, D^m, then the estimate from Maxwell's scheme is identical to upper/lower bounds of Hashin-Shtrikman.

2.1.3. Mori-Tanaka approximation scheme

Like the Maxwell's approach, this scheme has been formulated for composite media in which one of the constituents forms the matrix, while the remaining ones are the inclusions. The composite is, once again, said to be embedded within an infinite continuum whose diffusive properties are the same as those of the matrix. The distribution of inclusions is assumed to be dilute, so that the value of the concentration gradient in constituent α is assessed based on the solution for a single inclusion in an infinite matrix. Furthermore, the localization operator for the matrix is assumed to be a unit tensor. Unlike Maxwell's approach though, the Mori-Tanaka's scheme makes no a priori assumptions regarding the geometry of the inclusions; shapes other than sphere can be employed. The effective diffusion tensor is estimated based on the analysis of the flux of the substance diffusing within the composite.

The value of the flux vector in constituent α is equal to

$$\langle q_i \rangle^\alpha = -D^\alpha P_{ij}^{\alpha,m} W_j \qquad (2.34)$$

while for the whole composite medium

$$\langle q_i \rangle = \sum_{\alpha=1}^{N} c^\alpha \langle q_i \rangle^\alpha = -\sum_{\alpha=1}^{N} c^\alpha D^\alpha P_{ij}^{\alpha,m} W_j \qquad (2.35)$$

where W_{x_j} is the value of the concentration gradient at infinity.

On the other hand, the flux vector can also be defined in terms of effective diffusion tensor, i.e.

$$\langle q_i \rangle = -D_{ik}^{\text{hom}} \sum_{\alpha=1}^{N} c^{\alpha} P_{kj}^{\alpha,m} W_j \tag{2.36}$$

Thus, comparing the above representations, there is

$$\sum_{\alpha=1}^{N} c^{\alpha} \left(D^{\alpha} \delta_{ik} - D_{ik}^{\text{hom}} \right) P_{kj}^{\alpha,m} W_j = 0 \tag{2.37}$$

Eq.(2.37) must be satisfied for arbitrary values of the components of W_{x_j}, which implies that

$$\sum_{\alpha=1}^{N} c^{\alpha} \left(D^{\alpha} \delta_{ik} - D_{ik}^{\text{hom}} \right) P_{kj}^{\alpha,m} = 0 \tag{2.38}$$

Furthermore, if the distribution of constituents is random, then both tensors D_{ij}^{hom} and $P_{ij}^{\alpha,m}$ are isotropic, i.e. $D_{ij}^{\text{hom}} = D^{\text{hom}} \delta_{ij}$ and $P_{ij}^{\alpha,m} = P^{\alpha,m} \delta_{ij}$. In view of this, eq.(2.38) can be simplified to

$$D^{\text{hom}} = \frac{\displaystyle\sum_{\alpha=1}^{N} c^{\alpha} D^{\alpha} P^{\alpha,m}}{\displaystyle\sum_{\alpha=1}^{N} c^{\alpha} P^{\alpha,m}} \tag{2.39}$$

Note that if the inclusions are spherical then the above estimate is identical to that obtained from Maxwell's scheme. This can be shown by substituting eq.(2.18), together with (2.15), into eq.(2.39). Thus, the framework outlined here is often referred to as generalized Maxwell's approximation scheme. This approach covers a broad spectrum of geometrical arrangements. It applies, for examples, to composites that are anisotropic at the macroscale, e.g. those containing aligned elliptical inclusions.

It is evident from the considerations above that, for spherical inclusions, both Mori-Tanaka and Maxwell schemes are identical, in the sense that they yield the same estimate of effective properties. Within both schemes, however, the formulation of the problem is different. A common feature in these approaches is the notion of the composite medium being embedded in an infinite homogeneous domain that has the same properties as those of the matrix material. As a result, the localization tensor is determined based on the solution to the problem involving a single inclusion in an infinite continuum.

Originally, the Mori-Tanaka scheme was developed within the context of assessment of effective elastic properties of composite media with multiple constituents (Mori-Tanaka [21]). The approach outlined above gives an analogous scheme in relation to assessment of diffusive properties of composite materials. Note that for spherical inclusions, the estimate obtained here satisfies the Hashin-Shtrikman bounds. However, for macroscopically isotropic composites with elliptical inclusions the relation (2.39) may yield values that do not fall within those bounds (see, e.g. Ref.[22]). In general, the Mori-Tanaka's scheme is not *realizable*, in the sense that one cannot always construct a microstructure that will poses the effective properties predicted by this approach.

Figures 2.2 - 2.5 present the estimates of a homogenized diffusion coefficient of two-phase composite corresponding to the generalized Maxwell (Mori-Tanaka) approximation scheme. The estimates have been obtained as functions of volume fraction of inclusions embedded in the matrix. The inclusions are assumed to be of a spheroid type with semiaxes: $R_1=R_2$ and $R_3=\omega*R_1$. The contrast in the diffusion coefficients of composite components is assumed as $D^1/D^2=0.01$.
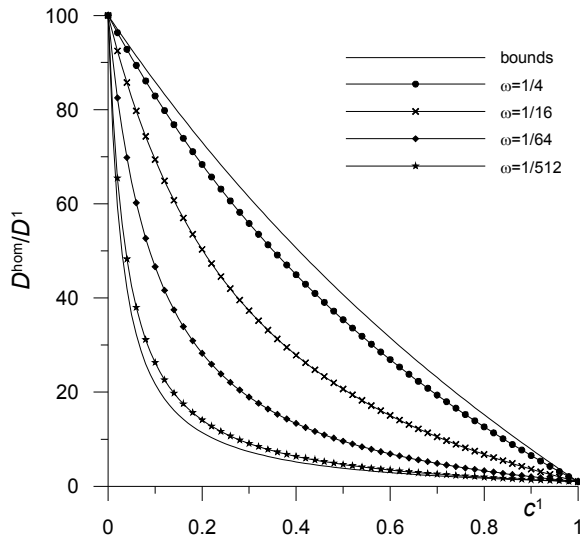

Fig.2.2. Maxwell approximation –oblate spheroids $\alpha=1$ immersed in a matrix $\alpha=2$
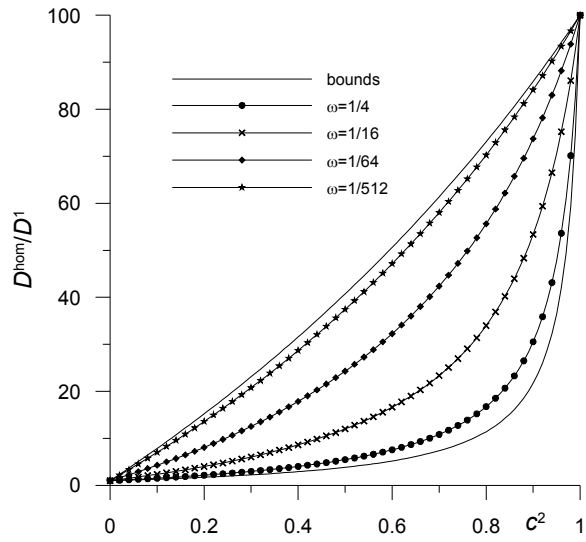
Fig.2.3. Maxwell approximation - oblate spheroids $\alpha=2$ immersed in a matrix $\alpha=1$
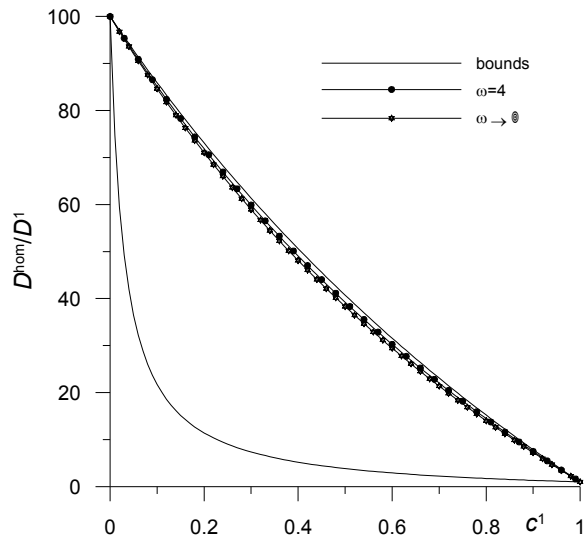

Fig.2.4. Maxwell approximation - prolate spheroids $\alpha=1$ immersed in matrix $\alpha=2$
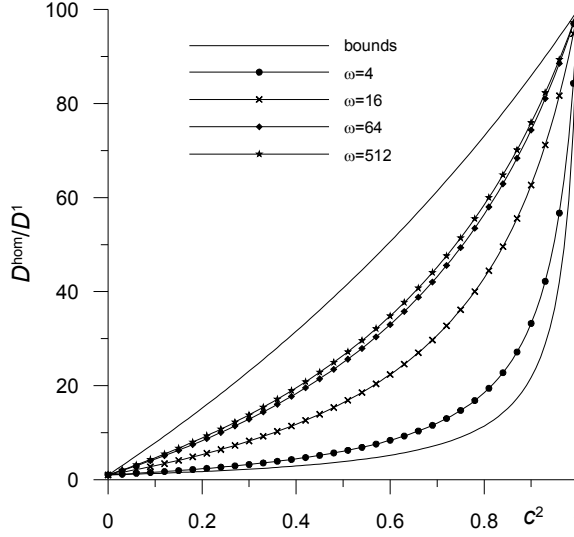
Fig.2.5. Maxwell approximation - prolate spheroids α=2 immersed in matrix α=1

2.1.4. Self-consistent approximation scheme

If the composite medium is embedded in an infinite homogeneous domain whose diffusion properties are the same as the effective properties of the composite itself, then the average value of the concentration gradient remains uniform and equal to that at infinity. In other words, the sum of perturbations triggered by individual inclusions contained within the composite is equal to zero. In the self-consistent scheme, the effective properties are assessed by approximating complex interactions among constituents by those between the constituent and the homogenized composite. Thus, a perturbation in the concentration field caused by a single inclusion within the composite is approximated by solving a problem of an inclusion embedded in a uniform matrix whose effective diffusion coefficient is the same as that of the composite. If the composite contains only spherical inclusions then, according to the solution presented earlier

$$\sum_{\alpha=1}^{N} c^{\alpha} \beta_{\alpha}^{\text{hom}} = 0 \quad \text{with} \quad \beta_{\alpha}^{\text{hom}} = \frac{D^{\text{hom}} - D^{\alpha}}{2D^{\text{hom}} + D^{\alpha}} \tag{2.40}$$

which leads to

$$\sum_{\alpha=1}^{N} c^{\alpha} \frac{D^{\text{hom}} - D^{\alpha}}{2D^{\text{hom}} + D^{\alpha}} = 0 \qquad (2.41)$$

The expression above indicates that the self-consistent scheme is an *implicit* scheme, i.e. the assessment of D^{hom} requires a solution to an implicit equation. Furthermore, in contrast to Maxwell's scheme, the self-consistent scheme treats all constituents as equivalent, in the sense that an exchange of constituents $D^{\alpha} \leftrightarrow D^{\beta}$ and $c^{\alpha} \leftrightarrow c^{\beta}$ has no impact on the macroscopic response of the composite. This means that the self-consistent scheme is particularly suited for assessing the properties of composites with polycrystalline morphology.

Note that the same estimate of effective diffusion coefficient may be obtained if the problem is formulated in terms of the flux of diffusing substance. Following the procedure analogous to that employed earlier in Mori-Tanaka's scheme, one can write

$$\sum_{\alpha=1}^{N} c^{\alpha} \left(D^{\alpha} \delta_{ik} - D_{ik}^{\text{hom}} \right) P_{kj}^{\alpha,\text{hom}} = 0 \qquad (2.42)$$

which for a macroscopically isotropic medium simplifies to

$$\sum_{\alpha=1}^{N} c^{\alpha} \left(D^{\alpha} - D^{\text{hom}} \right) P^{\alpha,\text{hom}} = 0 \qquad (2.43)$$

Substituting in (2.43) the value of $P^{\alpha,\text{hom}}$ that corresponds to spherical inclusions leads to representation (2.41). If the composite contains randomly distributed inclusions of different shapes then eq.(2.43) leads to a different estimate than that corresponding to (2.40). The relation (2.43), which is valid for isotropic composites, and (2.42) which includes composites that are anisotropic at macroscale, are considered as generalized expressions of the self-consistent scheme. It is noted that this scheme is realizable (Ref.[23]), in the sense that one can always construct a microstructure that will poses the estimated properties.

The estimate corresponding to the self-consistent scheme in comparison to that resulting from the Maxwell approximation is presented in Fig.2.6. The two-phase composite with spherical inclusions is considered. The two Maxwell estimates presented in Fig.2.6 are obtained by analyzing two different composite morphology. The first one corresponds to the case in which the component $\alpha=1$ is the inclusion whereas in the

44

second one – the component α=1 is the matrix. The contrast in the diffusion coefficients is assumed as D^1/D^2=0.01, similarly as in the cases considered before.
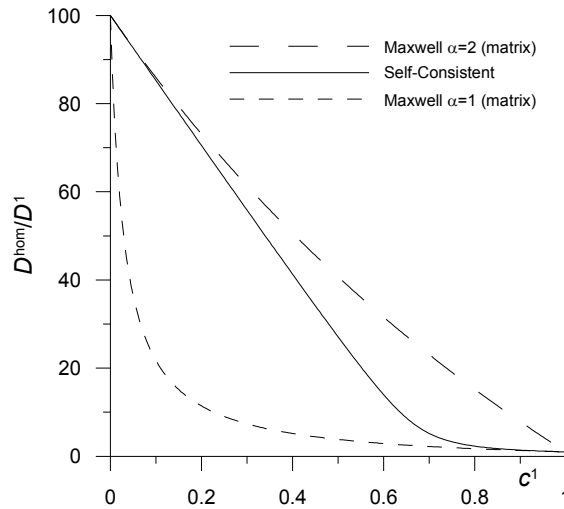

Fig.2.6. Comparison of the Maxwell and Self-consistent estimates

The estimates of the self-consistent scheme obtained for the composite with spheroidal inclusions are presented in figures 2.7-2.10.
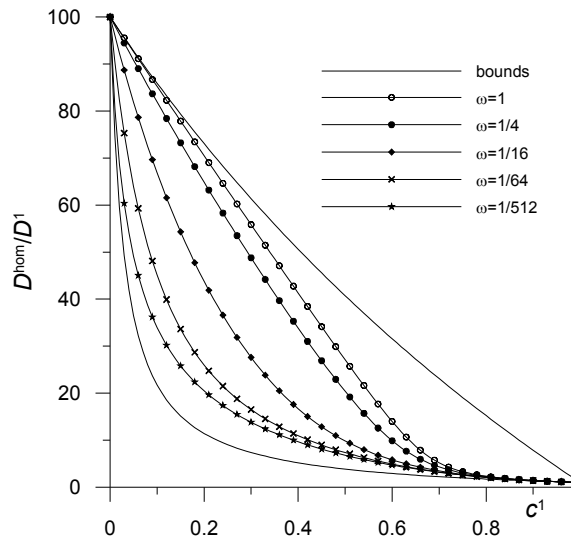

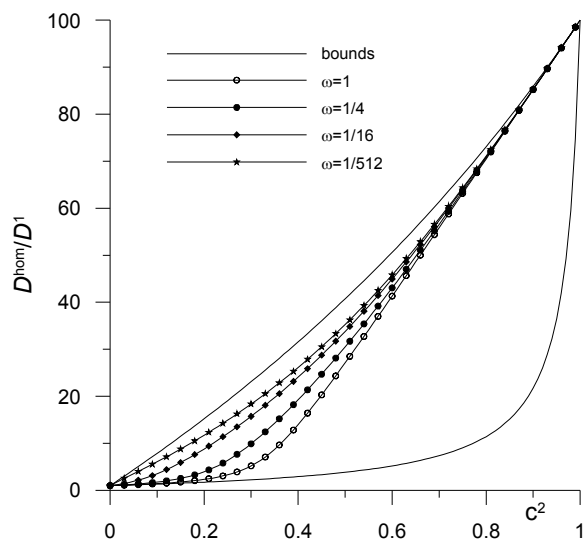Fig.2.7. Self-Consistent approximation - oblate spheroids α=1 immersed in matrix α=2

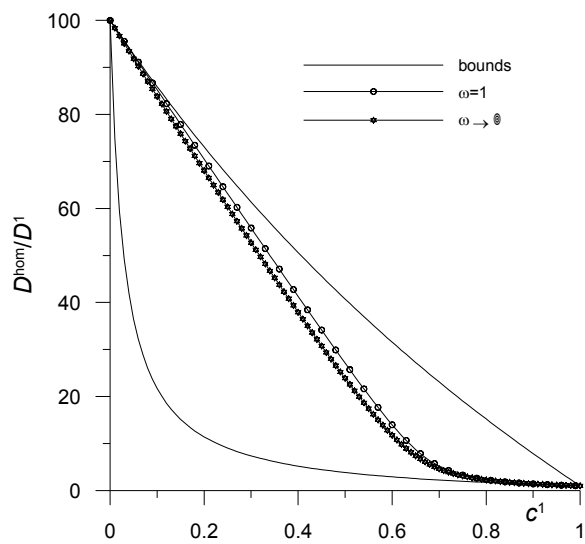Fig.2.8. Self-Consistent approximation - oblate spheroids $\alpha=2$ immersed in matrix $\alpha=1$

Fig.2.9. Self-Consistent approximation - prolate spheroids $\alpha=1$ immersed in matrix $\alpha=2$
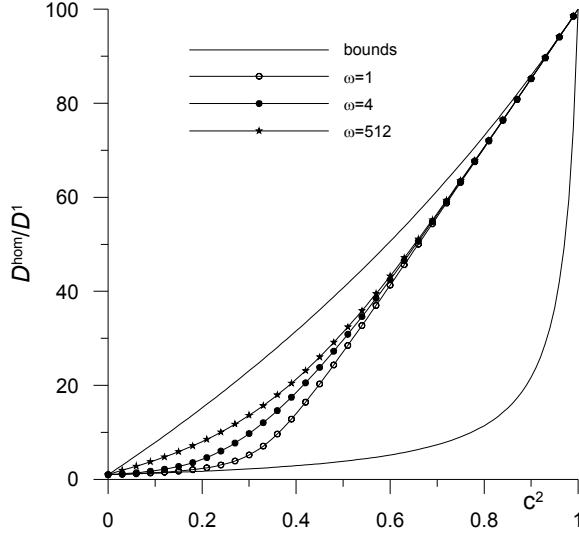
Fig.2.10. Self-Consistent approximation - prolate spheroids α=2 immersed in matrix α=1

2.2. Elasticity problem

2.2.1. Single inclusion solution

Consider an infinitely extended material with the elastic moduli D_{ijkh} containing a single ellipsoidal inclusion Ω with the elastic moduli D_{ijkh}^{Ω} subjected to a constant strain field ε_{ij}^{o} at infinity (Fig.2.11). We investigate the disturbance in the stress and strain fields caused by this ellipsoidal inclusion.

The total strain and stress fields in the material can be described by a sum of an uniform field and a corrector one, i.e.: $\varepsilon_{ij} = \varepsilon_{ij}^{o} + \varepsilon_{ij}^{d}$ and $\sigma_{ij} = \sigma_{ij}^{o} + \sigma_{ij}^{d}$. The fields ε_{ij}^{o} and σ_{ij}^{o} correspond to the case when the material is homogeneous, i.e. having no inclusion, and are induced by the constant uniform strain applied at infinity. The fields ε_{ij}^{d} and σ_{ij}^{d} represent therefore the disturbance in the strain and stress fields caused by the ellipsoidal inclusion. Using the representations introduced above, the constitutive equations of elasticity (Hooke's law) can be presented as

$$\sigma_{ij}^{o} + \sigma_{ij}^{d} = D_{ijkh}\left(\varepsilon_{kh}^{o} + \varepsilon_{kh}^{d}\right) \quad \text{in} \quad V - \Omega \tag{2.44}$$

47

$$\sigma_{ij}^o + \sigma_{ij}^d = D_{ijkh}^\Omega \left(\varepsilon_{kh}^o + \varepsilon_{kh}^d \right) \quad \text{in} \quad \Omega \qquad (2.45)$$

where $\sigma_{ij}^o = D_{ijkh}\varepsilon_{kh}^o$.

$$\left(x_1, x_2, x_3 \right) \in \Omega \Leftrightarrow \frac{x_1^2}{R_1^2} + \frac{x_2^2}{R_2^2} + \frac{x_3^2}{R_3^2} \le 1$$
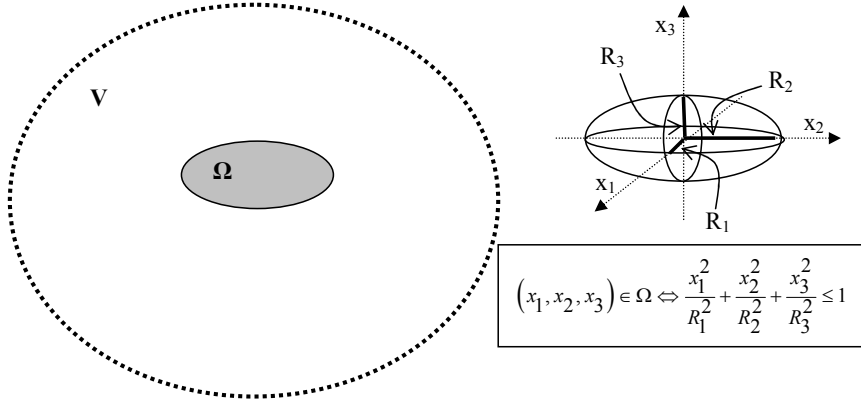
Fig.2.11. Ellipsoidal inclusion Ω with semi-axes (R_1, R_2, R_3) embedded in an infinite homogeneous medium V

The total stress field has to satisfy an equilibrium equation

$$\frac{\partial \sigma_{ij}}{\partial x_i} = 0 \qquad (2.46)$$

therefore

$$\frac{\partial \sigma_{ij}^D}{\partial x_i} = 0 \qquad (2.47)$$

is also an self-equilibrated field, since σ_{ij}^o is the uniform one. Furthermore $\sigma_{ij}^d = 0$, at infinity.

To solve the problem stated above, i.e. to determine of the strain and stress corrector fields, the Eshelby-Mura's equivalent eigenstrain principle ([24],[25]) is used in a following. This principle states that any strain field generated by an ellipsoidal inhomogeneity has a one-to-one correspondence to a fictitious eigenstrain field imposed in a domain of the inhomogeneity. In other words, instead to consider the problem of an inclusion embedded in an infinite medium one can consider the infinite homogeneous

48

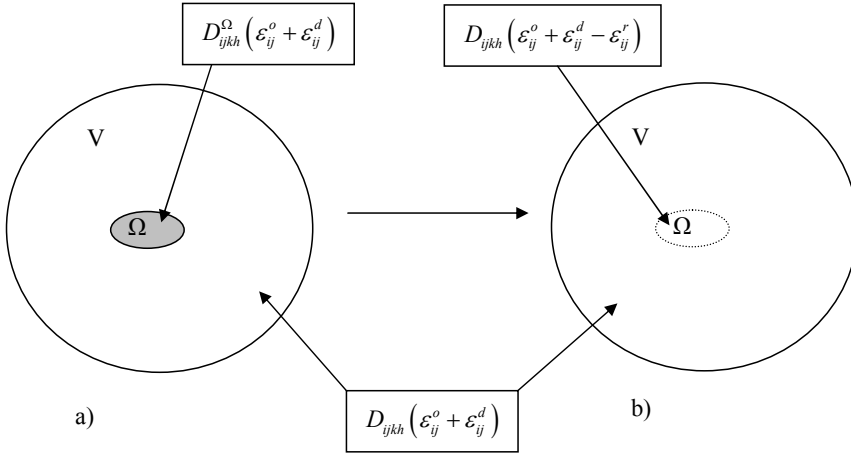medium in which the proper eigenstrain field is prescribed in a domain of the inclusion (Fig. 2.12).

Fig.2.12. Illustration of Eshelby-Mura's equivalent principle; a) initial heterogeneous body b) equivalent homogeneous body

"Eigenstrain" is a generic name to describe a transformation field that can equivalently represent induced strain due to misfit of inhomogeneities, thermal expansion, plastic strain, residual strain, etc. ; "Eigenstress" is a generic name given to a self-equilibrated transformation stress filed that can generate equivalent perturbed stress and strain distributions caused by one or several of eigenstrains in bodies which are free from any other external forces and surface constraints [24].

Consider the infinitely extended homogeneous material with the elastic moduli D_{ijkh} everywhere, containing domain Ω with an eigenstrain ε_{ij}^r (Fig.2.12b). Then, Hooke's law yields:

$$
\begin{aligned}
\sigma_{ij}^o + \sigma_{ij}^d &= D_{ijkh}\left(\varepsilon_{kh}^o + \varepsilon_{kh}^d\right) & \text{in} & \quad V - \Omega \\
\sigma_{ij}^o + \sigma_{ij}^d &= D_{ijkh}\left(\varepsilon_{kh}^o + \varepsilon_{kh}^d - \varepsilon_{kh}^r\right) & \text{in} & \quad \Omega
\end{aligned}
\tag{2.48}
$$

The necessary and sufficient condition for the equivalency of stresses and strains is

$$
D_{ijkh}^{\Omega}\left(\varepsilon_{kh}^o + \varepsilon_{kh}^d\right) = D_{ijkh}\left(\varepsilon_{kh}^o + \varepsilon_{kh}^d - \varepsilon_{kh}^r\right) \quad \text{in} \quad \Omega
\tag{2.49}
$$

The relations (2.48) imply also:

$$\sigma_{ij}^d = D_{ijkh}\varepsilon_{kh}^d \quad \text{in} \quad V - \Omega$$
$$\sigma_{ij}^d = D_{ijkh}\left(\varepsilon_{kh}^d - \varepsilon_{kh}^r\right) \quad \text{in} \quad \Omega \tag{2.50}$$

The equilibrium equation (2.47) together with the constitutive equations (2.50) create so-called eigenstrain boundary value problem:

$$D_{ijkh}\frac{\partial \varepsilon_{kh}^d}{\partial x_i} = D_{ijkh}\frac{\partial \varepsilon_{kh}^r}{\partial x_i} \quad \text{in} \quad \Omega$$

$$D_{ijkh}\frac{\partial \varepsilon_{kh}^d}{\partial x_i} = 0 \quad \text{in} \quad V - \Omega \tag{2.51}$$

$$D_{ijkh}\varepsilon_{kh}^d = 0 \quad \text{at} \quad \text{infinity}$$

It can be seen that the contribution of eigenstrain ε_{ij}^r to the equations of equilibrium is similar to that of a body force since the equations of equilibrium under body force X_j with zero ε_{ij}^r are:

$$D_{ijkh}\frac{\partial \varepsilon_{kh}^d}{\partial x_i} = -X_j \quad \text{in} \quad \Omega$$

$$D_{ijkh}\frac{\partial \varepsilon_{kh}^d}{\partial x_i} = 0 \quad \text{in} \quad V - \Omega \tag{2.52}$$

$$D_{ijkh}\varepsilon_{kh}^d = 0 \quad \text{at} \quad \text{infinity}$$

The simplest way to get the solution of (2.52) is by an application of Green's function, i.e.:

$$\varepsilon_{kh}^d(x) = \frac{1}{2}\int_\Omega X_j \left\{G_{kj,h}(x-y) + G_{hj,k}(x-y)\right\}dy \tag{2.53}$$

where $G_{kj,h}(x-y) = \partial G_{kj}(x-y)/\partial x_h$, $G_{mk}(x-y)$ is the Green's function representing the displacement component in the x_m- direction at point x when a unit body force in the x_k- direction is applied at point y in infinitely extended material . For an infinite linear elastic medium, the Green's function is a solution of the following equation

$$D_{ijkl}\frac{\partial^2 G_{mk}}{\partial y_l \partial y_j} + \delta(x-y)\delta_{mi} = 0 \tag{2.54}$$

and its analytical form can be presented as [24]:

$$G_{ij}(x) = \frac{1}{16\pi G(1-v)|x|}\left[(3-4v)\delta_{ij} + \frac{x_i x_j}{|x|^2}\right] \quad \text{where} \quad |x| = \sqrt{x_i x_i} \quad (2.55)$$

Constants G and v are shear modulus and Poisson's ratio, respectively.

Using the Green's function, the solution of eigenstrain boundary value problem (2.51) can be written as:

$$\varepsilon_{kh}^d(x) = -\frac{1}{2}\int_\Omega D_{ijlm}\frac{\partial \varepsilon_{lm}^r}{\partial y_i}\left\{G_{kj,h}(x-y) + G_{hj,k}(x-y)\right\}dy =$$

$$= -\frac{1}{2}\int_\Omega D_{ijlm}\varepsilon_{lm}^r\left\{G_{kj,hi}(x-y) + G_{hj,ki}(x-y)\right\}dy \quad (2.55)$$

Finally, it can be proved (detailed proof one can find in the book of Mura [24]) that for the ellipsoidal inclusion the above integral is independent on the space coordinate x and the relation (2.55) can be presented as

$$\varepsilon_{ij}^d = T_{ijmn}^\Omega \varepsilon_{mn}^r \quad (2.56)$$

where T_{ijmn}^Ω is so-called Eshelby's tensor.

The most amazing fact of this result is that the induced strain field in the inclusion is uniform, and the Eshelby's tensor for any ellipsoidal inclusion is a constant tensor.

The Eshelby's tensor can be explicitly expressed by elliptic integrals through the following identity [24,25]:

$$8\pi(1-v)T_{ijkl}^\Omega = \delta_{ij}\delta_{kl}\left(2vI_I + J_{IK}\right) + \left(\delta_{ik}\delta_{jl} + \delta_{jk}\delta_{il}\right)\cdot$$

$$\cdot\left[(1-v)(I_K + I_L) + J_{IJ}\right] \quad (2.57)$$

where the upper case indices are not summed with lower case indices, the Poisson's ratio v is of the host material in which the inclusion is embedded and

$$I_I = 2\pi R_1 R_2 R_3 \int_0^\infty \frac{ds}{(R_I^2 + s)\sqrt{(R_1^2 + s)(R_2^2 + s)(R_3^2 + s)}} \quad (2.58)$$

$$I_{IJ} = 2\pi R_1 R_2 R_3 \int_0^\infty \frac{ds}{(R_I^2 + s)(R_J^2 + s)\sqrt{(R_1^2 + s)(R_2^2 + s)(R_3^2 + s)}} \quad (2.59)$$

$$J_{IJ} = R_J^2 I_{IJ} - I_I = R_I^2 I_{IJ} - I_J = \frac{R_I^2 + R_J^2}{2} I_{IJ} - \frac{I_J + I_I}{2} \tag{2.60}$$

Symbols R_1, R_2, and R_3 denote the semi-axes of the ellipsoidal inclusion.

In applications, the following invariant formulas are very useful [24]:

$$I_1 + I_2 + I_3 = 4\pi$$
$$3I_{11} + I_{12} + I_{13} = 4\pi / R_1^2$$
$$3R_1^2 I_{11} + R_2^2 I_{12} + R_3^2 I_{13} = 3I_1 \tag{2.61}$$
$$I_{12} = \frac{I_2 - I_1}{R_1^2 - R_2^2}$$

as well as a symmetry property of the Eshelby's tensor:

$$T_{ijkl}^\Omega = T_{jikl}^\Omega = T_{ijlk}^\Omega \tag{2.62}$$

All non-zero components of the Eshelby's tensor are presented, in terms of the elliptic integrals, below:

$$T_{1111}^\Omega = \frac{3R_1^2}{8\pi(1-\nu)} I_{11} + \frac{1-2\nu}{8\pi(1-\nu)} I_1, \quad T_{1122}^\Omega = \frac{R_2^2}{8\pi(1-\nu)} I_{12} - \frac{1-2\nu}{8\pi(1-\nu)} I_1,$$

$$T_{1133}^\Omega = \frac{R_3^2}{8\pi(1-\nu)} I_{13} - \frac{1-2\nu}{8\pi(1-\nu)} I_1, \quad T_{2211}^\Omega = \frac{R_1^2}{8\pi(1-\nu)} I_{12} - \frac{1-2\nu}{8\pi(1-\nu)} I_2,$$

$$T_{2222}^\Omega = \frac{3R_2^2}{8\pi(1-\nu)} I_{22} + \frac{1-2\nu}{8\pi(1-\nu)} I_2, \quad T_{2233}^\Omega = \frac{R_3^2}{8\pi(1-\nu)} I_{23} - \frac{1-2\nu}{8\pi(1-\nu)} I_2,$$

$$T_{3311}^\Omega = \frac{R_1^2}{8\pi(1-\nu)} I_{13} - \frac{1-2\nu}{8\pi(1-\nu)} I_3, \quad T_{3322}^\Omega = \frac{R_2^2}{8\pi(1-\nu)} I_{23} - \frac{1-2\nu}{8\pi(1-\nu)} I_3,$$

$$T_{3333}^\Omega = \frac{3R_3^2}{8\pi(1-\nu)} I_{33} + \frac{1-2\nu}{8\pi(1-\nu)} I_3,$$

$$T_{1212}^\Omega = T_{2112}^\Omega = T_{1221}^\Omega = T_{2121}^\Omega = \frac{R_1^2 + R_2^2}{16\pi(1-\nu)} I_{12} + \frac{1-2\nu}{16\pi(1-\nu)} (I_1 + I_2)$$

$$T_{1313}^\Omega = T_{3113}^\Omega = T_{1331}^\Omega = T_{3131}^\Omega = \frac{R_1^2 + R_3^2}{16\pi(1-\nu)} I_{13} + \frac{1-2\nu}{16\pi(1-\nu)} (I_1 + I_3)$$

$$T_{2323}^\Omega = T_{3223}^\Omega = T_{2332}^\Omega = T_{3232}^\Omega = \frac{R_2^2 + R_3^2}{16\pi(1-\nu)} I_{23} + \frac{1-2\nu}{16\pi(1-\nu)} (I_2 + I_3) \tag{2.63}$$

The eigenstrain ε_{ij}^r, as it has been pointed above, should verify the condition (2.49) in order to preserve the equivalence between the stresses and strains induced by the inclusion and that by the eigenstrain field. This condition can be rewritten as:

$$\left(D_{ijkh}^{\Omega} - D_{ijkh}\right)\left(\varepsilon_{kh}^o + \varepsilon_{kh}^d\right) + D_{ijkh}\varepsilon_{kh}^r = 0 \tag{2.64}$$

or

$$D_{mnij}^{-1}\left(D_{ijkh}^{\Omega} - D_{ijkh}\right)\left(\varepsilon_{kh}^o + \varepsilon_{kh}^d\right) + \varepsilon_{mn}^r = 0 \tag{2.65}$$

where D_{mnij}^{-1} is a compliance tensor, which is defined as the inverse of the elastic stiffness. Using the relation (2.56), the equation (2.65) can be transformed to:

$$T_{pqmn}^{\Omega} D_{mnij}^{-1}\left(D_{ijkh}^{\Omega} - D_{ijkh}\right)\left(\varepsilon_{kh}^o + \varepsilon_{kh}^d\right) + \left(\varepsilon_{pq}^o + \varepsilon_{pq}^d\right) = \varepsilon_{pq}^o \tag{2.66}$$

and finally

$$\varepsilon_{kh}^o + \varepsilon_{kh}^d = P_{khpq}^{\Omega} \varepsilon_{pq}^o$$
$$P_{pqkh}^{\Omega} = \left[I_{pqkh} + T_{pqmn}^{\Omega} D_{mnij}^{-1}\left(D_{ijkh}^{\Omega} - D_{ijkh}\right)\right]^{-1} \tag{2.67}$$

where $I_{pqkh} = 1/2(\delta_{pk}\delta_{qh} + \delta_{ph}\delta_{qk})$ is a fourth order unit tensor.

The constant-valued fourth order tensor P_{khpq}^{Ω} is the localization tensor that defines the strain within the ellipsoidal inclusion in term of the uniform strain applied at the infinity to homogeneous medium in which the inclusion is embedded.

Determination of the Eshelby's tensor corresponding to some special types of inclusions like spherical, needle-shaped or disk-shaped is provided in a following.

2.2.1.1. Spherical inclusion

For a spherical inclusion of radius R the integrals (2.58)-(2.60) are simply estimated:

$$I_I = 2\pi R^3 \int_0^{\infty} \frac{ds}{\left(R^2 + s\right)^{\frac{5}{2}}} = -\frac{4\pi}{3} R^3 \left(R^2 + s\right)^{-3/2}\Big|_0^{\infty} = \frac{4\pi}{3}$$

$$I_{IJ} = 2\pi R^3 \int_0^{\infty} \frac{ds}{\left(R^2 + s\right)^{\frac{7}{2}}} = -\frac{4\pi}{5} R^3 \left(R^2 + s\right)^{-5/2}\Big|_0^{\infty} = \frac{4\pi}{5R^2}$$

$$J_{IJ} = R_J^2 I_{IJ} - I_I = -\frac{8\pi}{15}$$

Substitution of the above results in the relation (2.57) leads to:

$$T_{ijkl}^{\Omega} = \frac{5\nu - 1}{15(1 - \nu)}\delta_{ij}\delta_{kl} + \frac{4 - 5\nu}{15(1 - \nu)}\left(\delta_{ik}\delta_{jl} + \delta_{jk}\delta_{il}\right) \qquad (2.68)$$

The relation obtained above can be equivalently presented as

$$T_{ijkl}^{\Omega} = \frac{1+\nu}{3(1-\nu)}\Lambda_{ijkl}^{H} + \frac{8-10\nu}{15(1-\nu)}\Lambda_{ijkl}^{S} \qquad (2.69)$$

where the fourth order tensors Λ_{ijkh}^{H} and Λ_{ijkh}^{S} are defined as

$$\Lambda_{ijkh}^{H} = \frac{1}{3}\delta_{ij}\delta_{kh} \qquad \Lambda_{ijkh}^{S} = \frac{1}{2}\left(\delta_{ik}\delta_{jh} + \delta_{ik}\delta_{jk}\right) - \frac{1}{3}\delta_{ij}\delta_{kh} = I_{ijkh} - \Lambda_{ijkh}^{H} \qquad (2.70)$$

It can be shown, by simple algebraic transformations, that these tensors are orthogonal:

$$\Lambda_{ijkh}^{H}\Lambda_{khlm}^{S} = 0 \qquad (2.71)$$

and fulfill the following equalities:

$$\begin{aligned}
\Lambda_{ijkh}^{H}\Lambda_{khlm}^{H} &= \Lambda_{ijlm}^{H} \\
\Lambda_{ijkh}^{S}\Lambda_{khlm}^{S} &= \Lambda_{ijlm}^{S} \\
\Lambda_{ijkh}^{H}\Lambda_{ijkh}^{H} &= 1 \\
\Lambda_{ijkh}^{S}\Lambda_{ijkh}^{S} &= 5
\end{aligned} \qquad (2.72)$$

Furthermore, any fourth order isotropic tensor S_{ijkh} can be presented as

$$S_{ijkh} = a\Lambda_{ijkh}^{H} + b\Lambda_{ijkh}^{S} \qquad (2.73)$$

where a and b are scalar-valued constants.
Comparing (2.69) and (2.73) one can conclude that the Eshelby's tensor for the spherical inclusion is the isotropic one. The result is obvious since a spherical inclusion does not posses any preferential orientation; any orientation is equivalent.

The inclusion and the matrix are considered to be isotropic materials. Thus, their stiffness tensors as well as the compliance tensors are the isotropic fourth order tensors and have representations

$$D_{ijkh}^{\Omega} = 3K^{\Omega}\Lambda_{ijkh}^{H} + 2G^{\Omega}\Lambda_{ijkh}^{S}, \quad \left(D_{ijkh}^{\Omega}\right)^{-1} = \frac{1}{3K^{\Omega}}\Lambda_{ijkh}^{H} + \frac{1}{2G^{\Omega}}\Lambda_{ijkh}^{S}$$

$$D_{ijkh} = 3K\Lambda_{ijkh}^{H} + 2G\Lambda_{ijkh}^{S}, \quad \left(D_{ijkh}\right)^{-1} = \frac{1}{3K}\Lambda_{ijkh}^{H} + \frac{1}{2G}\Lambda_{ijkh}^{S}$$

(2.74)

where K^{Ω}, G^{Ω} and K, G denote bulk and shear modulus for the inclusion and for the matrix, respectively.

The relations (2.74), (2.69) imply

$$I_{pqkh} + T_{pqmn}^{\Omega}D_{mnij}^{-1}\left(D_{ijkh}^{\Omega} - D_{ijkh}\right) = \left(1 + \frac{K^{\Omega} - K}{K}\frac{1+\nu}{3(1-\nu)}\right)\Lambda_{pqkh}^{H} +$$

$$+ \left(1 + \frac{G^{\Omega} - G}{G}\frac{8-10\nu}{15(1-\nu)}\right)\Lambda_{pqkh}^{S}$$

(2.75)

since:

$$D_{mnij}^{-1}\left(D_{ijkh}^{\Omega} - D_{ijkh}\right) = \frac{K^{\Omega} - K}{K}\Lambda_{mnkh}^{H} + \frac{G^{\Omega} - G}{G}\Lambda_{mnkh}^{S}$$

(2.76)

The localization tensor P_{khpq}^{Ω} is, according to the definition (2.67), an inverse of the tensor defined by (2.75), therefore

$$P_{pqkh}^{\Omega} = \frac{1}{\left(1 + \dfrac{K^{\Omega} - K}{K}\dfrac{1+\nu}{3(1-\nu)}\right)}\Lambda_{pqkh}^{H} + \frac{1}{\left(1 + \dfrac{G^{\Omega} - G}{G}\dfrac{8-10\nu}{15(1-\nu)}\right)}\Lambda_{pqkh}^{S}$$

(2.77)

The elasticity constants: ν, K and G are connected by

$$\nu = \frac{3K - 2G}{2(G + 3K)}$$

(2.78)

Substituting (2.78) in (2.77) leads, after some simple transformations, to a following final form of the strain localization tensor

$$P_{pqkh}^{\Omega} = \frac{K + \dfrac{4}{3}G}{K^{\Omega} + \dfrac{4}{3}G}\Lambda_{pqkh}^{H} + \frac{G + \zeta}{G^{\Omega} + \zeta}\Lambda_{pqkh}^{S}$$

(2.79)

where

$$\zeta = \frac{G(8G+9K)}{6(2G+K)} \tag{2.80}$$

Evidently, the strain localization tensor P_{khpq}^{Ω} for spherical inclusion, Eq. (2.79), is the fourth order isotropic tensor.

2.2.1.2. Eshelby's tensor for particular shapes of ellipsoidal inclusion

The Eshelby's tensor as well as the strain localization tensor is so simply determine only for a spherical inclusion. Other types of ellipsoidal inclusions need much more effort in order to calculate components of the Eshelby's tensor and the strain polarization tensor. This is brought about by a lack of isotropy of these tensors. If the Eshelby's tensor is not the isotropic tensor then determination of the strain localization tensor is not so straightforward as has been presented for the spherical inclusion. The procedure is quite complex and it is postponed up to the next section.

Different particulate shapes of ellipsoidal inclusion are considered only in the context of determination of the Eshelby's tensor components, in this section. The analytical form of this tensor is presented for a needle-shaped inclusion, a disk-shaped inclusion as well as for oblate and prolate spheroids.

Needle-shaped inclusion (R_1=R_2=R, R_3->∞)
For a needle-shaped inclusion with the semi-axes: R_1=R_2=R and R_3->∞ , the elliptic integrals (2.58)-(2.59) yield

$$I_1 = I_2 = 2\pi, \ I_3 = 0$$
$$I_{11} = I_{22} = I_{12} = \frac{\pi}{R^2}, \ I_{13} = I_{23} = I_{33} = 0 \tag{2.81}$$
$$R_3^2 I_{13} = I_1, R_3^2 I_{23} = I_2, R_3^2 I_{33} = I_3$$

Bearing in mind Eq. (2.63), the non-zero components of the Eshelby's tensor are as follows:

$$T_{1111}^{\Omega} = T_{2222}^{\Omega} = \frac{5-4\nu}{8(1-\nu)}, \ T_{1122}^{\Omega} = T_{2211}^{\Omega} = \frac{4\nu-1}{8(1-\nu)}$$
$$T_{1133}^{\Omega} = T_{2233}^{\Omega} = \frac{\nu}{2(1-\nu)}, \ T_{1212}^{\Omega} = T_{2112}^{\Omega} = T_{2121}^{\Omega} = T_{1221}^{\Omega} = \frac{3-4\nu}{8(1-\nu)} \tag{2.82}$$
$$T_{1313}^{\Omega} = T_{3113}^{\Omega} = T_{3131}^{\Omega} = T_{1331}^{\Omega} = T_{2323}^{\Omega} = T_{3223}^{\Omega} = T_{3232}^{\Omega} = T_{2332}^{\Omega} = \frac{1}{4}$$

Disk-shaped inclusion ($R_1=R_2=R$, $R_3->0$)
For a disk-shaped inclusion with semi-axes $R_1=R_2=R$ and $R_3->0$, the elliptic integrals (2.58)-(2.59) yield

$$
\begin{aligned}
&I_1 = I_2 = 0, \ I_3 = 4\pi \\
&I_{11} = I_{22} = I_{12} = 0 \\
&R_1^2 I_{13} = R_2^2 I_{23} = 4\pi, \ R_3^2 I_{33} = \frac{4\pi}{3}
\end{aligned}
\tag{2.83}
$$

The above values imply, according to the relations (2.63), the following values of non-vanishing components of the Eshelby's tensor:

$$
\begin{aligned}
&T_{3311}^{\Omega} = T_{3322}^{\Omega} = \frac{\nu}{1-\nu}, \ T_{3333}^{\Omega} = 1 \\
&T_{1313}^{\Omega} = T_{1331}^{\Omega} = T_{3131}^{\Omega} = T_{3113}^{\Omega} = T_{2323}^{\Omega} = T_{2332}^{\Omega} = T_{3232}^{\Omega} = T_{3223}^{\Omega} = \frac{1}{2}
\end{aligned}
\tag{2.84}
$$

Oblate spheroid ($R_1=R_2=R$, $R>R_3$)
An oblate spheroid is characterized by two geometrical parameters, i.e. $R=R_1=R_2$ being the length of two semi-axes and $\omega = R_3 / R < 1$ being an aspect ratio of the spheroid. For such inclusion the elliptic integrals (2.58)-(2.59) imply

$$
I_1 = I_2 = 2\pi \frac{\omega}{\left(1-\omega^2\right)^{3/2}} \left(\cos^{-1}\omega - \omega\left(1-\omega^2\right)^{1/2}\right), \ I_3 = 4\pi - 2I_1
$$

$$
I_{11} = I_{12} = I_{22} = \frac{\pi}{R^2} - \frac{1}{4}\frac{4\pi - 3I_1}{R^2\left(1-\omega^2\right)}
\tag{2.85}
$$

$$
I_{13} = I_{23} = \frac{4\pi - 3I_1}{R^2\left(1-\omega^2\right)}, \ I_{33} = \frac{1}{3}\left[\frac{4\pi}{\omega^2 R^2} - 2\frac{4\pi - 3I_1}{R^2\left(1-\omega^2\right)}\right]
$$

Introducing a parameter λ defined as

$$
\lambda = \frac{\omega}{\left(1-\omega^2\right)^{3/2}} \left(\cos^{-1}\omega - \omega\left(1-\omega^2\right)^{1/2}\right)
\tag{2.86}
$$

the relations (2.85) can be written in a more convenient form:

$$I_1 = I_2 = 2\pi\lambda, \ I_3 = 4\pi(1-\lambda),$$

$$R^2 I_{11} = R^2 I_{12} = R^2 I_{22} = \pi \frac{\dfrac{3}{2}\lambda - \omega^2}{\left(1-\omega^2\right)} \tag{2.87}$$

$$R^2 I_{13} = R^2 I_{23} = 4\pi \frac{1-\dfrac{3}{2}\lambda}{\left(1-\omega^2\right)}, \ \ \omega^2 R^2 I_{33} = \frac{4\pi}{3}\left[1-(2-3\lambda)\frac{\omega^2}{\left(1-\omega^2\right)}\right]$$

Implementing the relations (2.87) in the equations (2.63) enables to determine the Eshelby's tensor components. The non-zero components are as follows:

$$T_{1111}^{\Omega} = T_{2222}^{\Omega} = \frac{3}{8(1-v)}\frac{\omega^2}{\omega^2-1} + \frac{\lambda}{4(1-v)}\left[1-2v-\frac{9}{4(\omega^2-1)}\right]$$

$$T_{3333}^{\Omega} = \frac{1}{2(1-v)}\left\{2-2v+\frac{2\omega^2}{\omega^2-1}-\lambda\left[1-2v+\frac{3\omega^2}{\omega^2-1}\right]\right\}$$

$$T_{1122}^{\Omega} = T_{2211}^{\Omega} = \frac{1}{4(1-v)}\left\{\frac{\omega^2}{2(\omega^2-1)}-\lambda\left[1-2v+\frac{3}{4(\omega^2-1)}\right]\right\}$$

$$T_{1133}^{\Omega} = T_{2233}^{\Omega} = \frac{1}{2(1-v)}\left\{\frac{-\omega^2}{\omega^2-1}+\frac{\lambda}{2}\left[2v-1+\frac{3\omega^2}{\omega^2-1}\right]\right\}$$

$$T_{3311}^{\Omega} = T_{3322}^{\Omega} = \frac{1}{2(1-v)}\left\{2v-1-\frac{1}{\omega^2-1}-\lambda\left[2v-1-\frac{3}{2(\omega^2-1)}\right]\right\}$$

$$T_{1212}^{\Omega} = T_{1221}^{\Omega} = T_{2121}^{\Omega} = T_{2112}^{\Omega} = \frac{1}{4(1-v)}\left\{\frac{\omega^2}{2(\omega^2-1)}+\lambda\left[1-2v-\frac{3}{4(\omega^2-1)}\right]\right\}$$

$$T_{1313}^{\Omega} = T_{3113}^{\Omega} = T_{3131}^{\Omega} = T_{1331}^{\Omega} = \frac{1}{4(1-v)}\left\{1-2v-\frac{1+\omega^2}{\omega^2-1}-\frac{\lambda}{2}\left[1-2v-\frac{3(\omega^2+1)}{\omega^2-1}\right]\right\} \tag{2.88}$$

$$T_{2323}^{\Omega} = T_{3223}^{\Omega} = T_{3232}^{\Omega} = T_{2332}^{\Omega} = \frac{1}{4(1-v)}\left\{1-2v-\frac{1+\omega^2}{\omega^2-1}-\frac{\lambda}{2}\left[1-2v-\frac{3(\omega^2+1)}{\omega^2-1}\right]\right\}$$

Prolate spheroid ($R_1=R_2=R$, $R<R_3$)
A prolate spheroid is, geometrically, characterized by the same parameters as that of the oblate spheroid, i.e. by R and $\omega = R_3/R$. The spheroid is, however, classified as prolate if $\omega = R_3/R > 1$. For such geometry of inclusion, the elliptic integral (2.58) is analytically determined and can be presented as:

$$I_1 = I_2 = 2\pi \frac{\omega}{\left(\omega^2 - 1\right)^{3/2}} \left[\omega \left(\omega^2 - 1\right)^{1/2} - \cosh^{-1} \omega \right] \qquad (2.89)$$

Using a parameter λ defined as:

$$\lambda = \frac{\omega}{\left(\omega^2 - 1\right)^{3/2}} \left[\omega \left(\omega^2 - 1\right)^{1/2} - \cosh^{-1} \omega \right] \qquad (2.90)$$

the relation (2.89) can be rewritten as:

$$I_1 = I_2 = 2\pi\lambda \qquad (2.91)$$

The equation (2.91) together with the invariant formulas (2.61) imply

$$I_3 = 4\pi(1-\lambda)$$

$$R^2 I_{11} = R^2 I_{12} = R^2 I_{22} = \pi \frac{\frac{3}{2}\lambda - \omega^2}{\left(1-\omega^2\right)} \qquad (2.92)$$

$$R^2 I_{13} = R^2 I_{23} = 4\pi \frac{1 - \frac{3}{2}\lambda}{\left(1-\omega^2\right)}, \quad \omega^2 R^2 I_{33} = \frac{4\pi}{3}\left[1 - (2-3\lambda)\frac{\omega^2}{\left(1-\omega^2\right)} \right]$$

Obviously, the elliptic integrals corresponding to prolate spheroid fulfill exactly the same relations as the integrals corresponding to the oblate spheroid; compare the Eqs. (2.91)-(2.92) with the Eqs. (2.87). Since the Eshelby's tensor components are evaluated by the elliptic integrals (2.63) therefore the relations (2.88) are also valid for the Eshelby's tensor for prolate spheroid, except the parameter λ is defined by the equation (2.90).

2.2.1.3. The strain localization tensor for particular shapes of ellipsoidal inclusion

The strain localization tensor is defined by the relation (2.67). This relation is not so convenient for a determination of components of the strain localization tensor since to do that one need to invert a following fourth order tensor:

$$B_{pqkh} = I_{pqkh} + T^{\Omega}_{pqmn} D^{-1}_{mnij} \left(D^{\Omega}_{ijkh} - D_{ijkh} \right) \qquad (2.93)$$

Evaluation of the inverse of the tensor B_{pqkh} is quite simple task if the Eshelby's tensor and the stiffness tensors D^{Ω}_{ijkh} and D_{ijkh} are the isotropic ones, as in a case of a spherical inclusion. In a following the stiffness tensors are still considered as the isotropic ones but any constraints on a form of the Eshelby's tensor are not laid.

The stiffness tensors are isotropic, therefore:

$$D^\Omega_{ijkh} = 3K^\Omega \Lambda^H_{ijkh} + 2G^\Omega \Lambda^S_{ijkh}, \quad \left(D^\Omega_{ijkh}\right)^{-1} = \frac{1}{3K^\Omega}\Lambda^H_{ijkh} + \frac{1}{2G^\Omega}\Lambda^S_{ijkh}$$

$$D_{ijkh} = 3K \Lambda^H_{ijkh} + 2G \Lambda^S_{ijkh}, \quad \left(D_{ijkh}\right)^{-1} = \frac{1}{3K}\Lambda^H_{ijkh} + \frac{1}{2G}\Lambda^S_{ijkh}$$

(2.94)

where the tensors Λ^H_{ijkh} and Λ^S_{ijkh} are defined as:

$$\Lambda^H_{ijkh} = \frac{1}{3}\delta_{ij}\delta_{kh} \qquad \Lambda^S_{ijkh} = \frac{1}{2}\left(\delta_{ik}\delta_{jh} + \delta_{ik}\delta_{jk}\right) - \frac{1}{3}\delta_{ij}\delta_{kh} = I_{ijkh} - \Lambda^H_{ijkh}$$

(2.95)

Since the tensor Λ^H_{ijkh} and Λ^S_{ijkh} are orthogonal, therefore

$$D^{-1}_{mnij}\left(D^\Omega_{ijkh} - D_{ijkh}\right) = \frac{K^\Omega - K}{K}\Lambda^H_{mnkh} + \frac{G^\Omega - G}{G}\Lambda^S_{mnkh}$$

(2.96)

Bearing in mind the definitions (2.95) it is simply evaluated that:

$$T^\Omega_{pqmn}\Lambda^H_{mnkh} = \frac{1}{3}T^\Omega_{pqmm}\delta_{kh} = \frac{T^\Omega_{pq11} + T^\Omega_{pq22}T^\Omega_{pq33}}{3}\delta_{kh}$$

$$T^\Omega_{pqmn}\Lambda^S_{mnkh} = T^\Omega_{pqmn}\left(I_{mnkh} - \Lambda^H_{mnkh}\right) = T^\Omega_{pqkh} - \frac{1}{3}T^\Omega_{pqmm}\delta_{kh}$$

(2.97)

By virtue of Eqs. (2.96) and (2.97) one gets:

$$T^\Omega_{pqmn}D^{-1}_{mnij}\left(D^\Omega_{ijkh} - D_{ijkh}\right) = \frac{K^\Omega - K}{K}T^\Omega_{pqmn}\Lambda^H_{mnkh} + \frac{G^\Omega - G}{G}T^\Omega_{pqmn}\Lambda^S_{mnkh} =$$

$$= \frac{1}{3}\left(\frac{K^\Omega - K}{K} - \frac{G^\Omega - G}{G}\right)T^\Omega_{pqmm}\delta_{kh} + \frac{G^\Omega - G}{G}T^\Omega_{pqkh}$$

(2.98)

Finally, the tensor B_{pqkh}, defined by Eq.(2.93), can be presented as:

$$B_{pqkh} = I_{pqkh} + \frac{1}{3}\left(\frac{K^\Omega - K}{K} - \frac{G^\Omega - G}{G}\right)T^\Omega_{pqmm}\delta_{kh} + \frac{G^\Omega - G}{G}T^\Omega_{pqkh}$$

(2.99)

The strain localization tensor P^Ω_{pqkh} is the inverse of the tensor B_{pqkh}. In order to invert this tensor it is more convenient to operate with its representation IP, in a matrix form:

60

$$
\mathbf{IP} = \begin{bmatrix}
IP_{11} & IP_{12} & IP_{13} & 0 & 0 & 0 & 0 & 0 & 0 \\
IP_{21} & IP_{22} & IP_{23} & 0 & 0 & 0 & 0 & 0 & 0 \\
IP_{31} & IP_{32} & IP_{33} & 0 & 0 & 0 & 0 & 0 & 0 \\
0 & 0 & 0 & IP_{44} & IP_{45} & 0 & 0 & 0 & 0 \\
0 & 0 & 0 & IP_{54} & IP_{55} & 0 & 0 & 0 & 0 \\
0 & 0 & 0 & 0 & 0 & IP_{66} & IP_{67} & 0 & 0 \\
0 & 0 & 0 & 0 & 0 & IP_{76} & IP_{77} & 0 & 0 \\
0 & 0 & 0 & 0 & 0 & 0 & 0 & IP_{88} & IP_{89} \\
0 & 0 & 0 & 0 & 0 & 0 & 0 & IP_{98} & IP_{99}
\end{bmatrix}
\tag{2.100}
$$

where:

$$
IP_{11} = 1 + A_1 \left(\frac{K^\Omega - K}{K} - \frac{G^\Omega - G}{G} \right) + \frac{G^\Omega - G}{G} T_{1111}^\Omega
$$

$$
IP_{12} = A_1 \left(\frac{K^\Omega - K}{K} - \frac{G^\Omega - G}{G} \right) + \frac{G^\Omega - G}{G} T_{1122}^\Omega
$$

$$
IP_{13} = A_1 \left(\frac{K^\Omega - K}{K} - \frac{G^\Omega - G}{G} \right) + \frac{G^\Omega - G}{G} T_{1133}^\Omega
$$

$$
IP_{21} = A_2 \left(\frac{K^\Omega - K}{K} - \frac{G^\Omega - G}{G} \right) + \frac{G^\Omega - G}{G} T_{2211}^\Omega
$$

$$
IP_{22} = 1 + A_2 \left(\frac{K^\Omega - K}{K} - \frac{G^\Omega - G}{G} \right) + \frac{G^\Omega - G}{G} T_{2222}^\Omega
$$

$$
IP_{23} = A_2 \left(\frac{K^\Omega - K}{K} - \frac{G^\Omega - G}{G} \right) + \frac{G^\Omega - G}{G} T_{2233}^\Omega
$$

$$
IP_{31} = A_3 \left(\frac{K^\Omega - K}{K} - \frac{G^\Omega - G}{G} \right) + \frac{G^\Omega - G}{G} T_{3311}^\Omega
$$

$$
IP_{32} = A_3 \left(\frac{K^\Omega - K}{K} - \frac{G^\Omega - G}{G} \right) + \frac{G^\Omega - G}{G} T_{3322}^\Omega
$$

$$
IP_{33} = 1 + A_3 \left(\frac{K^\Omega - K}{K} - \frac{G^\Omega - G}{G} \right) + \frac{G^\Omega - G}{G} T_{3333}^\Omega
$$

$$
IP_{44} = IP_{45} = IP_{54} = IP_{55} = \frac{1}{2} + \frac{G^\Omega - G}{G} T_{1212}^\Omega
$$

$$
IP_{66} = IP_{67} = IP_{76} = IP_{77} = \frac{1}{2} + \frac{G^\Omega - G}{G} T_{1313}^\Omega
$$

$$
IP_{88} = IP_{89} = IP_{98} = IP_{99} = \frac{1}{2} + \frac{G^\Omega - G}{G} T_{2323}^\Omega
$$

$$
\tag{2.101}
$$

The structure (2.100) of the matrix, a few of non-zero components, is a consequence of the equation (2.99) and the general form (2.63) of the Eshelby's tensor for the ellipsoidal inclusion. The equivalence:

$$
\begin{aligned}
IP_{44} &= IP_{45} = IP_{54} = IP_{55} \\
IP_{66} &= IP_{67} = IP_{76} = IP_{77} \\
IP_{88} &= IP_{89} = IP_{98} = IP_{99}
\end{aligned}
\tag{2.102}
$$

is a direct consequence of the symmetry the Eshelby's tensor, i.e.: $T_{ijkh}^{\Omega} = T_{jikh}^{\Omega} = T_{jihk}^{\Omega} = T_{ijhk}^{\Omega}$.
Furthermore:

$$
\begin{aligned}
A_1 &= \frac{T_{1111}^{\Omega} + T_{1122}^{\Omega} + T_{1133}^{\Omega}}{3} \\
A_2 &= \frac{T_{2211}^{\Omega} + T_{2222}^{\Omega} + T_{2233}^{\Omega}}{3} \\
A_3 &= \frac{T_{3311}^{\Omega} + T_{3322}^{\Omega} + T_{3333}^{\Omega}}{3}
\end{aligned}
\tag{2.103}
$$

Since the strain localization tensor P_{pqkh}^{Ω} is the inverse of the tensor B_{pqkh}, or equivalently it is the inverse of the matrix IP, the form (2.100) implies a similar format of the tensor P_{pqkh}^{Ω}, i.e.:

$$
P_{ijkh}^{\Omega} =
\begin{bmatrix}
P_{1111}^{\Omega} & P_{1122}^{\Omega} & P_{1133}^{\Omega} & 0 & 0 & 0 & 0 & 0 & 0 \\
P_{2211}^{\Omega} & P_{2222}^{\Omega} & P_{2233}^{\Omega} & 0 & 0 & 0 & 0 & 0 & 0 \\
P_{3311}^{\Omega} & P_{3322}^{\Omega} & P_{3333}^{\Omega} & 0 & 0 & 0 & 0 & 0 & 0 \\
0 & 0 & 0 & P_{1212}^{\Omega} & P_{1221}^{\Omega} & 0 & 0 & 0 & 0 \\
0 & 0 & 0 & P_{2112}^{\Omega} & P_{2121}^{\Omega} & 0 & 0 & 0 & 0 \\
0 & 0 & 0 & 0 & 0 & P_{1313}^{\Omega} & P_{1331}^{\Omega} & 0 & 0 \\
0 & 0 & 0 & 0 & 0 & P_{3113}^{\Omega} & P_{3131}^{\Omega} & 0 & 0 \\
0 & 0 & 0 & 0 & 0 & 0 & 0 & P_{2323}^{\Omega} & P_{2332}^{\Omega} \\
0 & 0 & 0 & 0 & 0 & 0 & 0 & P_{3223}^{\Omega} & P_{3232}^{\Omega}
\end{bmatrix}
\tag{2.104}
$$

with following symmetries:

$$
\begin{aligned}
P_{1212}^{\Omega} &= P_{1221}^{\Omega} = P_{2121}^{\Omega} = P_{2112}^{\Omega} \\
P_{1313}^{\Omega} &= P_{1331}^{\Omega} = P_{3131}^{\Omega} = P_{3113}^{\Omega} \\
P_{2323}^{\Omega} &= P_{2332}^{\Omega} = P_{3232}^{\Omega} = P_{3223}^{\Omega}
\end{aligned}
\tag{2.105}
$$

The tensors P_{pqkh}^{Ω} and B_{pqkh} have to verify the identity equation, i.e.:

$$P_{ijkh}^{\Omega} B_{khlm} = I_{ijlm} = \begin{bmatrix} 1 & 0 & 0 & 0 & 0 & 0 & 0 & 0 & 0 \\ 0 & 1 & 0 & 0 & 0 & 0 & 0 & 0 & 0 \\ 0 & 0 & 1 & 0 & 0 & 0 & 0 & 0 & 0 \\ 0 & 0 & 0 & 1/2 & 1/2 & 0 & 0 & 0 & 0 \\ 0 & 0 & 0 & 1/2 & 1/2 & 0 & 0 & 0 & 0 \\ 0 & 0 & 0 & 0 & 0 & 1/2 & 1/2 & 0 & 0 \\ 0 & 0 & 0 & 0 & 0 & 1/2 & 1/2 & 0 & 0 \\ 0 & 0 & 0 & 0 & 0 & 0 & 0 & 1/2 & 1/2 \\ 0 & 0 & 0 & 0 & 0 & 0 & 0 & 1/2 & 1/2 \end{bmatrix} \qquad (2.106)$$

From properties of the matrix calculus one gets that:

$$\begin{bmatrix} P_{1111}^{\Omega} & P_{1122}^{\Omega} & P_{1133}^{\Omega} \\ P_{2211}^{\Omega} & P_{2222}^{\Omega} & P_{2233}^{\Omega} \\ P_{3311}^{\Omega} & P_{3322}^{\Omega} & P_{3333}^{\Omega} \end{bmatrix} = \begin{bmatrix} IP_{11} & IP_{12} & IP_{13} \\ IP_{21} & IP_{22} & IP_{23} \\ IP_{31} & IP_{32} & IP_{33} \end{bmatrix}^{-1} \qquad (2.107)$$

which finally results in:

$$P_{1111}^{\Omega} = \frac{IP_{22}IP_{33} - IP_{23}IP_{32}}{\det IP}, P_{1122}^{\Omega} = \frac{IP_{13}IP_{32} - IP_{12}IP_{33}}{\det IP},$$

$$P_{1133}^{\Omega} = \frac{IP_{12}IP_{23} - IP_{13}IP_{22}}{\det IP}, P_{2211}^{\Omega} = \frac{IP_{23}IP_{31} - IP_{21}IP_{33}}{\det IP},$$

$$P_{2222}^{\Omega} = \frac{IP_{11}IP_{33} - IP_{13}IP_{31}}{\det IP}, P_{2233}^{\Omega} = \frac{IP_{13}IP_{21} - IP_{11}IP_{23}}{\det IP},$$

$$P_{3311}^{\Omega} = \frac{IP_{21}IP_{32} - IP_{22}IP_{31}}{\det IP}, P_{3322}^{\Omega} = \frac{IP_{12}IP_{31} - IP_{11}IP_{32}}{\det IP}, \qquad (2.108)$$

$$P_{3333}^{\Omega} = \frac{IP_{11}IP_{22} - IP_{12}IP_{21}}{\det IP},$$

$$\det IP = -IP_{13}IP_{22}IP_{31} + IP_{12}IP_{23}IP_{31} + IP_{13}IP_{21}IP_{32} -$$
$$- IP_{11}IP_{23}IP_{32} - IP_{12}IP_{21}IP_{33} + IP_{11}IP_{22}IP_{33}$$

Furthermore, due to the symmetry properties (2.102), (2.105), the identity equation (2.106) implies also:

$$\begin{bmatrix} P^\Omega_{1212} & P^\Omega_{1221} \\ P^\Omega_{2112} & P^\Omega_{2121} \end{bmatrix} = \frac{1}{4}\begin{bmatrix} \dfrac{1}{IP_{44}} & \dfrac{1}{IP_{44}} \\ \dfrac{1}{IP_{44}} & \dfrac{1}{IP_{44}} \end{bmatrix}, \quad \begin{bmatrix} P^\Omega_{1313} & P^\Omega_{1331} \\ P^\Omega_{3113} & P^\Omega_{3131} \end{bmatrix} = \frac{1}{4}\begin{bmatrix} \dfrac{1}{IP_{66}} & \dfrac{1}{IP_{66}} \\ \dfrac{1}{IP_{66}} & \dfrac{1}{IP_{66}} \end{bmatrix}, \quad \begin{bmatrix} P^\Omega_{2323} & P^\Omega_{2332} \\ P^\Omega_{3223} & P^\Omega_{3232} \end{bmatrix} = \frac{1}{4}\begin{bmatrix} \dfrac{1}{IP_{88}} & \dfrac{1}{IP_{88}} \\ \dfrac{1}{IP_{88}} & \dfrac{1}{IP_{88}} \end{bmatrix}$$

which, using the relations (2.101), leads to:

$$P^\Omega_{1212} = \frac{1}{4IP_{44}} = \frac{1}{2 + 4\dfrac{G^\Omega - G}{G}T^\Omega_{1212}}$$

$$P^\Omega_{1313} = \frac{1}{4IP_{66}} = \frac{1}{2 + 4\dfrac{G^\Omega - G}{G}T^\Omega_{1313}} \tag{2.109}$$

$$P^\Omega_{2323} = \frac{1}{4IP_{88}} = \frac{1}{2 + 4\dfrac{G^\Omega - G}{G}T^\Omega_{2323}}$$

Summing up, determination of the strain localization tensor consists in two following steps: determination of the components of the matrix IP according to the relations (2.101) and (2.103) and then direct use of the equations (2.108) and (2.109). The procedure is, from a mathematics point of view, quite simple but simultaneously, from a practical point of view, it is very tedious since it involves a lot of algebraic transformations.

The final form of the strain localization tensor is presented for the particular shapes of ellipsoidal inclusions, i.e. for a needle shaped inclusion and for a disk shaped inclusion.

Needle-shaped inclusion ($R_1=R_2=R$, R_3->∞)
For a needle-shaped inclusion with the semi-axes: $R_1=R_2=R$ and R_3->∞ , the non-vanishing components of the strain localization tensor are as follows:

$$P^\Omega_{1111} = P^\Omega_{2222} = \frac{1}{2}(4G+3K)\left[\frac{2G}{G(G+7G^\Omega)+3(G+G^\Omega)K} + \frac{1}{3G+3K^\Omega+G^\Omega}\right],$$

$$P^\Omega_{1122} = P^\Omega_{2211} = \frac{1}{2}(4G+3K)\left[\frac{-2G}{G(G+7G^\Omega)+3(G+G^\Omega)K} + \frac{1}{3G+3K^\Omega+G^\Omega}\right], \tag{2.110a}$$

$$P^\Omega_{1133} = P^\Omega_{2233} = \frac{1}{2}\left[\frac{G+3(G^\Omega+K)}{3G+3K^\Omega+G^\Omega} - 1\right], \quad P^\Omega_{3333} = 1,$$

$$P^\Omega_{1212} = P^\Omega_{1221} = P^\Omega_{2112} = P^\Omega_{2121} = \frac{G(4G+3K)}{G(G+7G^\Omega)+3(G+G^\Omega)K},$$

$$P^\Omega_{1313} = P^\Omega_{1331} = P^\Omega_{3113} = P^\Omega_{3131} = \frac{G}{G+G^\Omega} \qquad (2.110\text{b})$$

$$P^\Omega_{2323} = P^\Omega_{2332} = P^\Omega_{3223} = P^\Omega_{3232} = \frac{G}{G+G^\Omega}$$

Disk-shaped inclusion ($R_1=R_2=R$, $R_3->0$)
For a disk-shaped inclusion with semi-axes $R_1=R_2=R$ and $R_3->0$, the non-vanishing components of the strain localization tensor read:

$$P^\Omega_{1111} = P^\Omega_{2222} = 1,$$

$$P^\Omega_{3333} = \frac{4G+3K}{4G^\Omega+3K^\Omega}, \qquad (2.111\text{a})$$

$$P^\Omega_{3311} = P^\Omega_{3322} = -1 + \frac{-2G+6G^\Omega+3K}{4G^\Omega+3K^\Omega}$$

$$P^\Omega_{1212} = P^\Omega_{1221} = P^\Omega_{2112} = P^\Omega_{2121} = \frac{1}{2},$$

$$P^\Omega_{1313} = P^\Omega_{1331} = P^\Omega_{3113} = P^\Omega_{3131} = \frac{G}{2G^\Omega} \qquad (2.111\text{b})$$

$$P^\Omega_{2323} = P^\Omega_{2332} = P^\Omega_{3223} = P^\Omega_{3232} = \frac{G}{2G^\Omega}$$

It is obvious, comparing the tensorial representation (2.73) of a fourth order isotropic tensor, that both the strain localization tensors for a needle shaped inclusion and for a disk shaped inclusion are not the isotropic tensors. This is a consequence of a lack of the isotropy of the Eshelby's tensor corresponding to these shapes of inclusions. The same goes for an oblate and a prolate spheroids.

Oblate/Prolate spheroid
For the oblate or prolate spheroid the analytical form of the strain localization tensor, expressed by the geometrical parameters of the spheroid as well as the bulk and shear moduli of the matrix and the inclusion, involves a lot of algebraic terms and it is not of a practical use. A more convenient way to work with the oblate/prolate spheroid is, at each time when is needed, a determination of the strain localization tensor for given values of the geometrical parameters and that of the elasticity moduli. As an example, a final result of such calculation, i.e. the strain localization tensor for the oblate spheroid is presented below (Eq.(2.112)). The components were determined assuming the aspect ration of semi-axes to be ω=0.5 and $G^\Omega/K^\Omega = G/K = 3/5$ and $K/K^\Omega = 10$.

$$
\begin{bmatrix} P^\Omega_{1111} & P^\Omega_{1122} & P^\Omega_{1133} \\ P^\Omega_{2211} & P^\Omega_{2222} & P^\Omega_{2233} \\ P^\Omega_{3311} & P^\Omega_{3322} & P^\Omega_{3333} \end{bmatrix} = \begin{bmatrix} 1.525 & 0.042 & -0.056 \\ 0.042 & 1.525 & -0.056 \\ 0.326 & 0.326 & 2.769 \end{bmatrix}
$$

$$
\begin{bmatrix} P^\Omega_{1212} & P^\Omega_{1221} \\ P^\Omega_{2112} & P^\Omega_{2121} \\ P^\Omega_{1313} & P^\Omega_{1331} \\ P^\Omega_{3113} & P^\Omega_{3131} \\ P^\Omega_{2323} & P^\Omega_{2332} \\ P^\Omega_{3223} & P^\Omega_{3232} \end{bmatrix} = \begin{bmatrix} 0.741 & 0.741 \\ 0.741 & 0.741 \\ 1.041 & 1.041 \\ 1.041 & 1.041 \\ 1.041 & 1.041 \\ 1.041 & 1.041 \end{bmatrix}
\tag{2.112}
$$

The same values of the elasticity moduli were used to determine the strain localization tensor for a prolate spheroid. The aspect ratio of semi-axes were assumed to be $\omega=2.0$.

$$
\begin{bmatrix} P^\Omega_{1111} & P^\Omega_{1122} & P^\Omega_{1133} \\ P^\Omega_{2211} & P^\Omega_{2222} & P^\Omega_{2233} \\ P^\Omega_{3311} & P^\Omega_{3322} & P^\Omega_{3333} \end{bmatrix} = \begin{bmatrix} 1.284 & -0.097 & 0.531 \\ -0.097 & 1.284 & 0.531 \\ 0.317 & 0.317 & 0.015 \end{bmatrix}
$$

$$
\begin{bmatrix} P^\Omega_{1212} & P^\Omega_{1221} \\ P^\Omega_{2112} & P^\Omega_{2121} \\ P^\Omega_{1313} & P^\Omega_{1331} \\ P^\Omega_{3113} & P^\Omega_{3131} \\ P^\Omega_{2323} & P^\Omega_{2332} \\ P^\Omega_{3223} & P^\Omega_{3232} \end{bmatrix} = \begin{bmatrix} 0.691 & 0.691 \\ 0.691 & 0.691 \\ 0.178 & 0.178 \\ 0.178 & 0.178 \\ 0.178 & 0.178 \\ 0.178 & 0.178 \end{bmatrix}
\tag{2.113}
$$

2.2.1.4. Isotropization of the strain localization tensor

The strain localization tensor for a single ellipsoidal inclusion embedded in an infinite homogenous medium depends on the orientation of the ellipsoid relative to the direction of the applied strain. In a composite medium the inclusions are, however, distributed over all orientations. If the distribution of inclusions is perfectly random, i.e. any preferential direction can be distinguished, then the distribution is isotropic. This implies, in a practical application, a necessity of averaging of the strain localization tensor over all orientations of the ellipsoid. The averaging process over all orientations, in case of the isotropic distribution, is equivalent to a so-called isotropization operation.

Consider an isotropic fourth order tensor. Its tensorial representation can be presented as:

$$
P^\Omega_{ijkh} = P^\Omega_H \Lambda^H_{ijkh} + P^\Omega_S \Lambda^S_{ijkh}
\tag{2.114}
$$

where the tensors Λ_{ijkh}^{H}, Λ_{ijkh}^{S} are defined by Eqs. (2.70), P_{H}^{Ω} and P_{S}^{Ω} represent a hydrostatic and a shearing part of the tensor P_{ijkh}^{Ω}.

The above relation implies

$$P_{ijkh}^{\Omega}\Lambda_{ijkh}^{H} = P_{H}^{\Omega}\Lambda_{ijkh}^{H}\Lambda_{ijkh}^{H} + P_{S}^{\Omega}\Lambda_{ijkh}^{S}\Lambda_{ijkh}^{H} = P_{H}^{\Omega} \tag{2.115}$$

since the tensors Λ_{ijkh}^{H}, Λ_{ijkh}^{S} are orthogonal and $\Lambda_{ijkh}^{H}\Lambda_{ijkh}^{H} = 1$.

Furthermore, it can be shown that

$$P_{ijkh}^{\Omega}\Lambda_{ijkh}^{H} = \frac{1}{3}P_{iikk}^{\Omega} = \frac{P_{1111}^{\Omega} + P_{1122}^{\Omega} + P_{1133}^{\Omega} + P_{2211}^{\Omega} + P_{2222}^{\Omega} + P_{2233}^{\Omega} + P_{3311}^{\Omega} + P_{3322}^{\Omega} + P_{3333}^{\Omega}}{3} \tag{2.116}$$

Comparing Eq.(2.115) and Eq.(2.116) one can immediately conclude that:

$$P_{H}^{\Omega} = \frac{1}{3}P_{iikk}^{\Omega} = \frac{P_{1111}^{\Omega} + P_{1122}^{\Omega} + P_{1133}^{\Omega} + P_{2211}^{\Omega} + P_{2222}^{\Omega} + P_{2233}^{\Omega} + P_{3311}^{\Omega} + P_{3322}^{\Omega} + P_{3333}^{\Omega}}{3} \tag{2.117}$$

The equation (2.114) implies also

$$P_{ijkh}^{\Omega}\Lambda_{ijkh}^{S} = P_{H}^{\Omega}\Lambda_{ijkh}^{H}\Lambda_{ijkh}^{S} + P_{S}^{\Omega}\Lambda_{ijkh}^{S}\Lambda_{ijkh}^{S} = 5P_{S}^{\Omega} \tag{2.118}$$

since $\Lambda_{ijkh}^{S}\Lambda_{ijkh}^{S} = 5$.

Simple algebraic transformations yield:

$$P_{ijkh}^{\Omega}\Lambda_{ijkh}^{S} = P_{ijij}^{\Omega} - P_{H}^{\Omega} \tag{2.119}$$

where:

$$P_{ijij}^{\Omega} = P_{1111}^{\Omega} + P_{1212}^{\Omega} + P_{1313}^{\Omega} + P_{2121}^{\Omega} + P_{2222}^{\Omega} + P_{2323}^{\Omega} + P_{3131}^{\Omega} + P_{3232}^{\Omega} + P_{3333}^{\Omega} \tag{2.120}$$

By virtue of Eq.(2.118) and Eq.(2.119), one can finally obtain that:

$$P_{S}^{\Omega} = \frac{P_{ijij}^{\Omega} - P_{H}^{\Omega}}{5} \tag{2.121}$$

Consider now any fourth order tensor P_{ijkh}^{Ω} being not isotropic one, in general. The isotropization operation consists in a determination of the hydrostatic and the shearing part of the tensor P_{ijkh}^{Ω}, i.e. P_{H}^{Ω} and P_{S}^{Ω}. These parts are defined by the relations (2.117) and (2.121), respectively. Values of P_{H}^{Ω} and P_{S}^{Ω} for the cases of spheres, needles and disks are given in a table below in terms of the moduli K and G. Symbols with superscript

Ω correspond to the parameters of the inclusion whereas that without superscript correspond to the matrix.

Inclusion shape	P_H^Ω	$P_S^{\Omega\,\alpha}$
Spheres	$\dfrac{K + \frac{4}{3}G}{K^\Omega + \frac{4}{3}G}$	$\dfrac{G + \zeta}{G^\Omega + \zeta}$
Needles	$\dfrac{K + G + \frac{1}{3}G^\Omega}{K^\Omega + G + \frac{1}{3}G^\Omega}$	$\dfrac{1}{5}\left(\dfrac{4G}{G+G^\Omega} + 2\dfrac{G+\gamma}{G^\Omega+\gamma} + \dfrac{K^\Omega + \frac{4}{3}G}{K^\Omega + G + \frac{1}{3}G^\Omega} \right)$
Disks	$\dfrac{K+\frac{4}{3}G^\Omega}{K^\Omega+\frac{4}{3}G^\Omega}$	$\dfrac{G + \upsilon^\Omega}{G^\Omega + \upsilon^\Omega}$

The variables γ, ζ, υ are defined as:

$$\gamma = G\,\frac{3K + G}{3K + 4G}, \quad \zeta = \frac{G\left(9K + 8G\right)}{6\left(K + 2G\right)}, \quad \upsilon = \frac{G\left(3K/2 + 4G/3\right)}{K + 2G} \tag{2.122}$$

2.2.2. Mori-Tanaka approximation scheme

The main idea and principles of the Mori-Tanaka approximation have been presented in section 2.1.2 where its formulation with respect to the diffusion problem has been discussed. The Mori-Tanaka scheme is typically applied to composites in which one of the constituents forms the matrix, while the remaining ones represent the inclusions.

Consider a composite material composed of M different constituents. One of the constituents forms the matrix and the remaining ones are the inclusions. Assume that the composite is embedded in an infinite homogeneous medium with elastic properties of the matrix of the composite. The distribution of inclusions is dilute, so that the strain tensor in constituent α can be approximated based on the solution for a single inclusion in an infinite matrix. Furthermore, the strain localization tensor for the matrix is assumed to be a unit tensor. The effective elasticity tensor is estimated based on the analysis of the stress tensor within the composite.

The strain tensor within the constituent α can be expressed in terms of the strain localization tensor P_{ijkh}^α and the strain tensor e_{kh}^o applied at infinity to the homogeneous medium in which the composite is embedded. Therefore:

$$\langle e_{ij} \rangle^{\alpha} = P^{\alpha}_{ijkh} e^{o}_{kh} \qquad \alpha = 1,2,...,M, \qquad\qquad (2.123)$$

where $\langle e_{ij} \rangle^{\alpha}$ is an averaged strain tensor within the constituent α.
The averaged strain tensor in the composite can be expressed as:

$$\langle e_{ij} \rangle = \sum_{\alpha=1}^{M} c^{\alpha} \langle e_{ij} \rangle^{\alpha} \qquad\qquad (2.124)$$

where c^{α} represents a volume fraction of the constituent α within the composite.
The relations (2.124) and (2.123) imply

$$\langle e_{ij} \rangle = \sum_{\alpha=1}^{M} c^{\alpha} P^{\alpha}_{ijkh} e^{o}_{kh} \qquad\qquad (2.125)$$

Volume averaging of the constitutive equations of the elasticity results in:

$$\langle \sigma_{ij} \rangle^{\alpha} = C^{\alpha}_{ijkh} \langle e_{kh} \rangle^{\alpha} \qquad\qquad (2.126)$$

or, using the strain localization tensor

$$\langle \sigma_{ij} \rangle^{\alpha} = C^{\alpha}_{ijkh} P^{\alpha}_{khlm} e^{o}_{lm} \qquad\qquad (2.127)$$

Since the averaged stress tensor within the composite is defined as

$$\langle \sigma_{ij} \rangle = \sum_{\alpha=1}^{M} c^{\alpha} \langle \sigma_{ij} \rangle^{\alpha} \qquad\qquad (2.128)$$

therefore

$$\langle \sigma_{ij} \rangle = \sum_{\alpha=1}^{M} c^{\alpha} C^{\alpha}_{ijkh} P^{\alpha}_{khlm} e^{o}_{lm} \qquad\qquad (2.129)$$

The effective elasticity tensor for the composite fulfills the elasticity constitutive equation

$$\langle \sigma_{ij} \rangle = C^{\text{hom}}_{ijkh} \langle e_{kh} \rangle \qquad\qquad (2.130)$$

thus, combining the relations (2.125),(2.129) and (2.130), one immediately gets:

$$\left\langle \sigma_{ij} \right\rangle = \sum_{\alpha=1}^{M} c^{\alpha} C_{ijkh}^{\text{hom}} P_{khlm}^{\alpha} e_{lm}^{o} = \sum_{\alpha=1}^{M} c^{\alpha} C_{ijkh}^{\alpha} P_{khlm}^{\alpha} e_{lm}^{o} \tag{2.131}$$

The above relation has to be satisfied for any values of components of the strain tensor e_{lm}^{o}, therefore

$$\sum_{\alpha=1}^{M} c^{\alpha} \left(C_{ijkh}^{\text{hom}} - C_{ijkh}^{\alpha} \right) P_{khlm}^{\alpha} = 0 \tag{2.132}$$

Furthermore, if the distribution of constituents within the composite is random, then both tensors C_{ijkh}^{hom} and P_{khlm}^{α} are isotropic, i.e.

$$
\begin{aligned}
C_{ijkh}^{\text{eff}} &= 3K^{\text{hom}} \Lambda_{ijkh}^{H} + 2G^{\text{hom}} \Lambda_{ijkh}^{S} \\
P_{khlm}^{\alpha} &= P_{H}^{\alpha} \Lambda_{khlm}^{H} + P_{S}^{\alpha} \Lambda_{khlm}^{S}
\end{aligned}
\tag{2.133}
$$

In view of this, Eq. (2.132) can be simplified to:

$$K^{\text{hom}} = \frac{\displaystyle\sum_{\alpha=1}^{N} c^{\alpha} K^{\alpha} P_{H}^{\alpha}}{\displaystyle\sum_{\alpha=1}^{N} c^{\alpha} P_{H}^{\alpha}} \tag{2.134}$$

$$G^{\text{hom}} = \frac{\displaystyle\sum_{\alpha=1}^{N} c^{\alpha} G^{\alpha} P_{S}^{\alpha}}{\displaystyle\sum_{\alpha=1}^{N} c^{\alpha} P_{S}^{\alpha}} \tag{2.135}$$

Mori-Tanaka approximation scheme is an explicit approach, in the sense that the effective elasticity constants are obtained directly from parameters that define the properties of constituents.

For the composite with spherical inclusions the estimates (2.134) and (2.135) are identical to Hashin-Shtrikman bounds. Namely, for the spherical inclusions the estimate (2.134) implies

$$K^{\text{hom}} = \frac{\displaystyle\sum_{\alpha=1}^{N} c^{\alpha} K^{\alpha} \frac{K + \frac{4}{3}G}{K^{\alpha} + \frac{4}{3}G}}{\displaystyle\sum_{\alpha=1}^{N} c^{\alpha} \frac{K + \frac{4}{3}G}{K^{\alpha} + \frac{4}{3}G}} = \frac{\displaystyle\sum_{\alpha=1}^{N} c^{\alpha} K^{\alpha} \frac{1}{K^{\alpha} + \frac{4}{3}G}}{\displaystyle\sum_{\alpha=1}^{N} c^{\alpha} \frac{1}{K^{\alpha} + \frac{4}{3}G}} = \frac{1}{\displaystyle\sum_{\alpha=1}^{N} c^{\alpha} \frac{1}{K^{\alpha} + \frac{4}{3}G}} - \frac{4}{3}G \tag{2.136}$$

Comparing the Hashin-Shtrikman inequalities (2.3) one can note that if the elasticity moduli of inclusions are smaller/larger than the values corresponding to the matrix, then the Mori-Tanaka estimates are identical to upper/lower bounds of Hashin-Shtrikman.
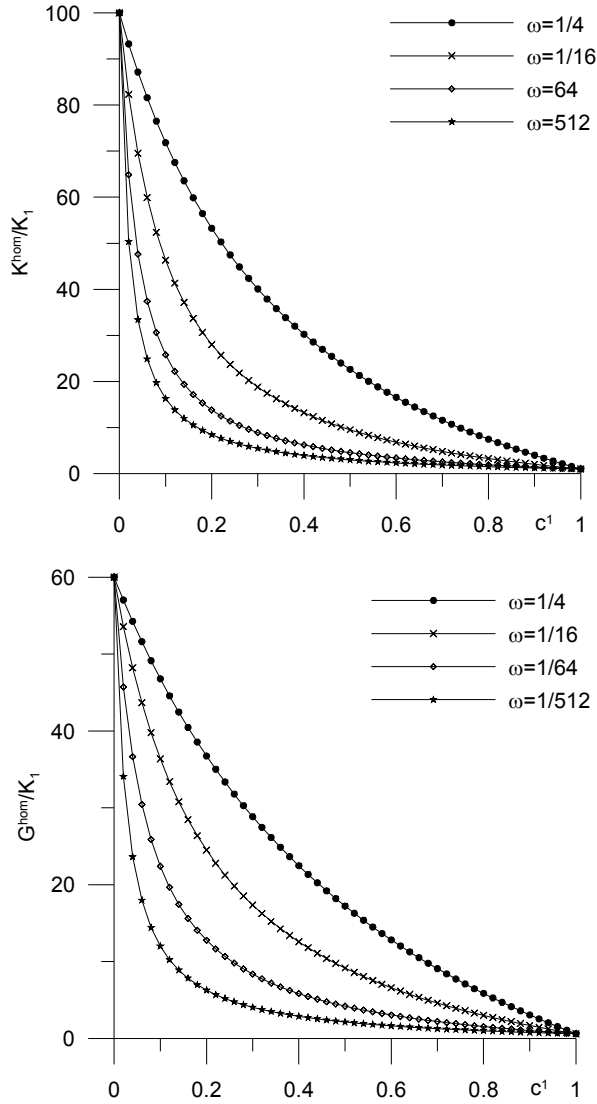

Fig.2.13. Mori-Tanaka approximation –oblate spheroids α=1 immersed in a matrix α=2

Figures 2.13-2.14 present estimates of the effective bulk modulus and effective shear modulus predicted by Mori-Tanaka approximation scheme. The estimates have been obtained as functions of volume fraction of inclusions $\alpha=1$ embedded in the matrix $\alpha=2$. The inclusions are assumed to be of a spheroid type with semi-axes $R_1=R_2$ and $R_3=\omega R_1$. The elastic constants are assumed as $G_1/K_1=3/5$, $G_2/K_2=3/5$ and $K_1/K_2=1/100$.
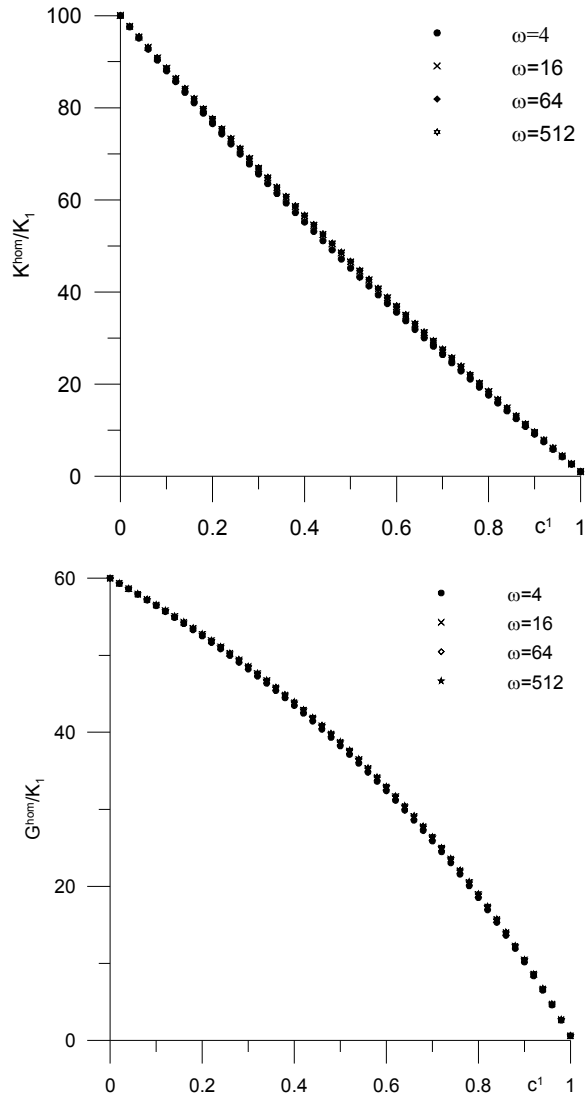

Fig.2.14. Mori-Tanaka approximation –prolate spheroids $\alpha=1$ immersed in a matrix $\alpha=2$

Figures 2.15-2.16 present also estimates of the effective bulk modulus and effective shear modulus predicted by Mori-Tanaka approximation scheme. This time the inclusions are made of stiffer material $\alpha=2$ and are embedded in the matrix $\alpha=1$.
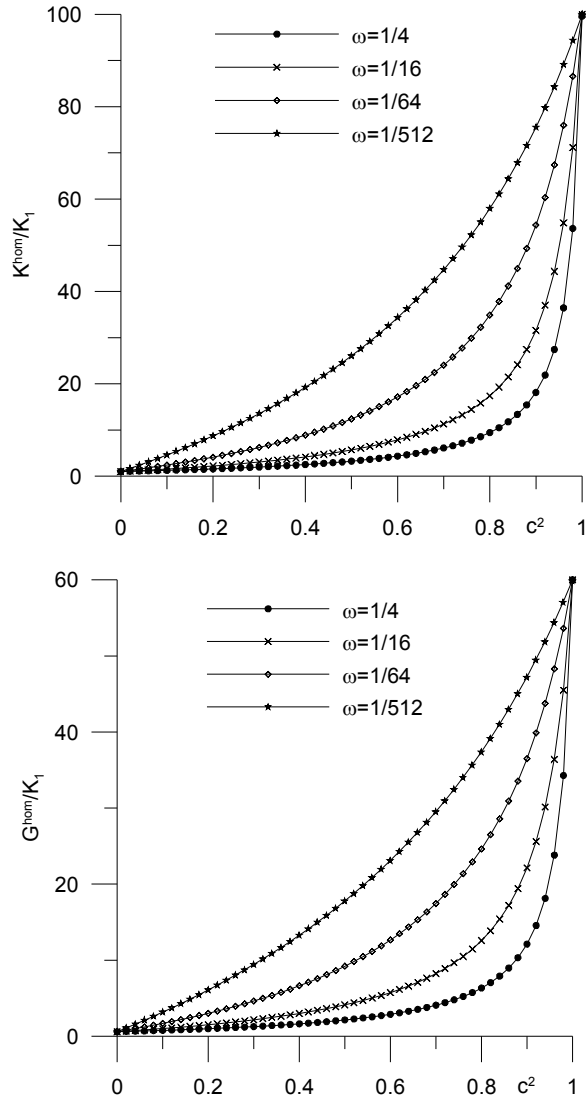

Fig.2.15. Mori-Tanaka approximation –oblate spheroids $\alpha=2$ immersed in a matrix $\alpha=1$
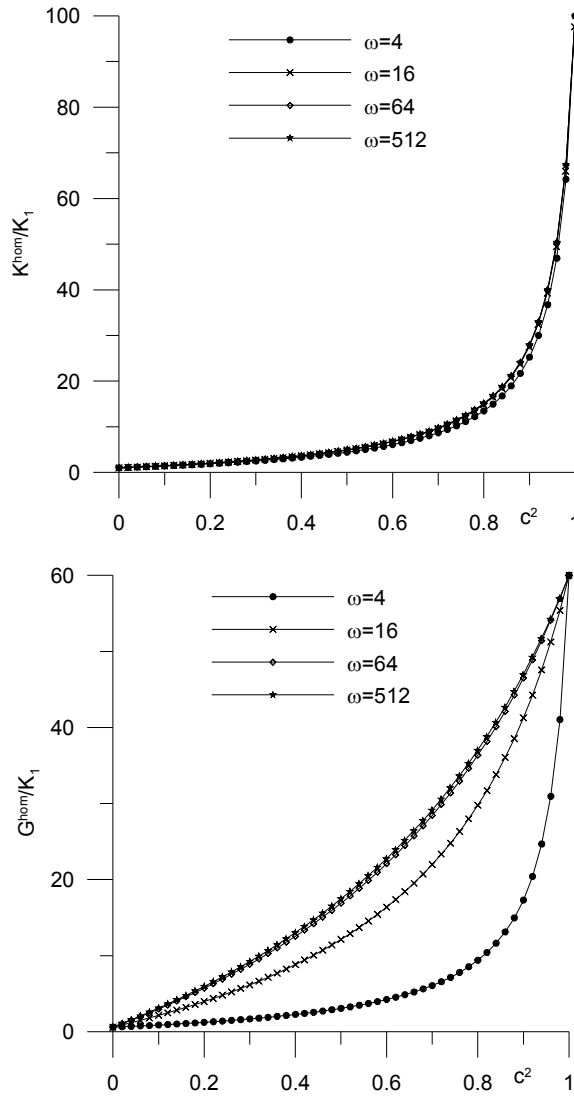
Fig.2.16. Mori-Tanaka approximation –prolate spheroids α=2 immersed in a matrix α=1

Using the well-known relation defining a value E of Young modulus:

$$E = \frac{9KG}{3K+G} \qquad (2.137)$$

74

Mori-Tanaka approximation scheme allows also for a prediction of an effective Young modulus of a composite medium.

Figures (2.17) and (2.18) present the prediction of the Young modulus corresponding to the bulk and shear moduli presented in figures (2.15) and (2.16), respectively.
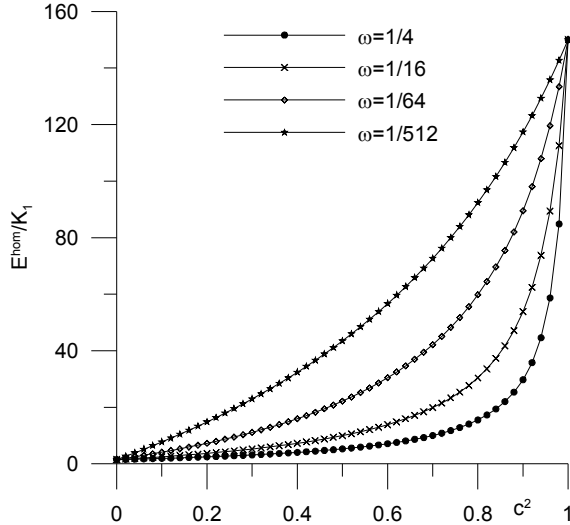

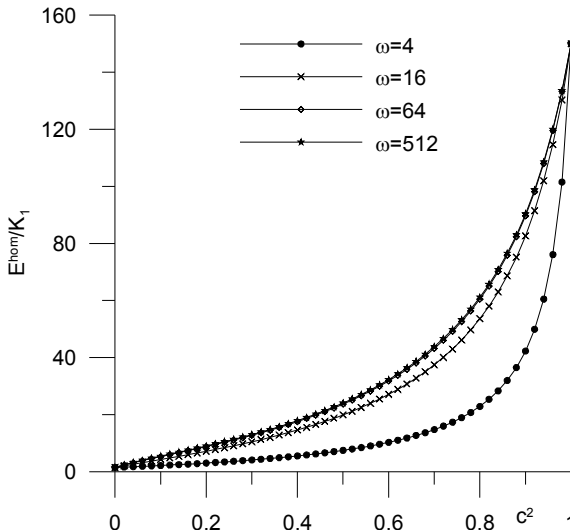Fig.2.17. Mori-Tanaka approximation –oblate spheroids $\alpha=2$ immersed in a matrix $\alpha=1$

Fig.2.18. Mori-Tanaka approximation –prolate spheroids $\alpha=2$ immersed in a matrix $\alpha=1$

2.2.3. Self-consistent approximation scheme

In the Self-consistent scheme, the effective properties are assessed by approximating complex interactions among constituents by those between constituent and the homogenized composite. In other words, the effect of all of the material outside a type α inclusion is to produce a homogeneous matrix whose effective elastic constants are the unknowns to be calculated. The strain localization tensor for the inclusion α is therefore determined based on a single inclusion solution assuming that the inclusion is embedded in the matrix with the unknowns effective elastic constants. For instance, in case of a spherical inclusion α, a hydrostatic part P_H^α of the strain localization tensor is approximated within the self-consistent scheme as:

$$P_H^{\alpha,\text{hom}} = \frac{K^{\text{hom}} + \frac{4}{3}G^{\text{hom}}}{K^\alpha + \frac{4}{3}G^{\text{hom}}} \tag{2.138}$$

Following the procedure analogous to that employed earlier in Mori-Tanaka scheme, one can write:

$$\sum_{\alpha=1}^{M} c^\alpha \left(C_{ijkh}^{\text{hom}} - C_{ijkh}^\alpha \right) P_{khlm}^{\alpha,\text{hom}} = 0 \tag{2.139}$$

which for a macroscopically isotropic medium simplifies to:

$$\sum_{\alpha=1}^{M} c^\alpha \left(K^{\text{hom}} - K^\alpha \right) P_H^{\alpha,\text{hom}} = 0$$
$$\sum_{\alpha=1}^{M} c^\alpha \left(G^{\text{hom}} - G^\alpha \right) P_S^{\alpha,\text{hom}} = 0 \tag{2.140}$$

The above system represents a set of two conjugate nonlinear equations. Solution to this system is, typically, searched using an iteration procedure. The self-consistent scheme is therefore an implicit scheme, i.e. the assessment of effective properties requires a solution to an implicit system of equations.

As an example, consider a composite composed of M different types of spherical inclusions. Bearing in mind the form of a strain localization tensor for spherical inclusions (see table), the system (2.140) can be transformed to:

$$\sum_{\alpha=1}^{M} c^\alpha \frac{\left(K^{\text{hom}} - K^\alpha \right)}{K^\alpha + \frac{4}{3}G^{\text{hom}}} = 0, \quad \sum_{\alpha=1}^{M} c^\alpha \frac{\left(G^{\text{hom}} - G^\alpha \right)}{G^\alpha + \frac{G^{\text{hom}}\left(9K^{\text{hom}} + 8G^{\text{hom}} \right)}{6\left(K^{\text{hom}} + 2G^{\text{hom}} \right)}} = 0 \tag{2.141}$$

Estimations of the effective bulk and shear moduli predicted by the self-consistent scheme are presented in figures 2.19 and 2.20. The composite is modeled as two-component medium with spherical inclusions. Elastic parameters of the components are assumed as $G_1/K_1=3/5$, $G_2/K_2=3/5$ and $K_1/K_2=1/100$.
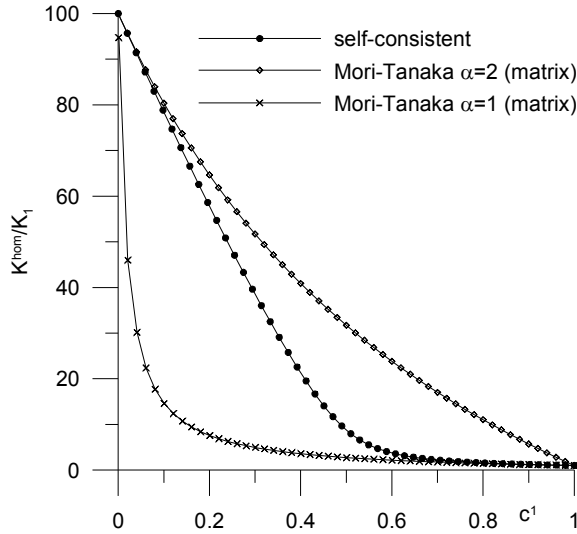

Fig.2.19. Bulk modulus: comparison of the self-consistent and Mori-Tanaka estimates
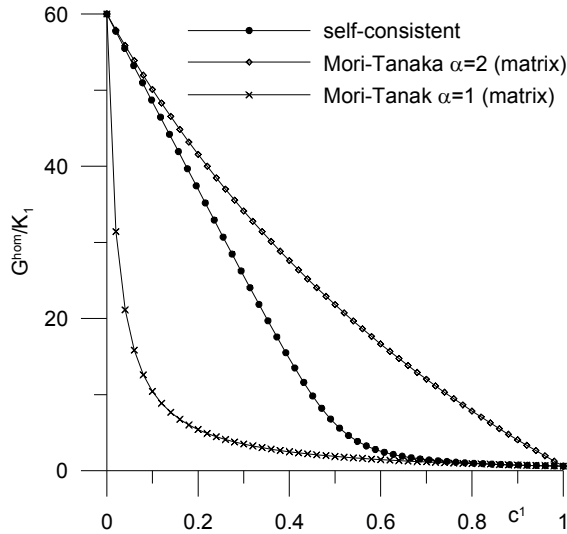

Fig.2.20. Shear modulus: comparison of the self-consistent and Mori-Tanaka estimates

The equations (2.141) show that the self-consistent scheme treats all the composite constituents as equivalent, in the sense that an exchange of constituents $\left(K^{\alpha}, G^{\alpha}\right) \leftrightarrow \left(K^{\beta}, G^{\beta}\right)$ and $c^{\alpha} \leftrightarrow c^{\beta}$ has no impact on the macroscopic response of the composite. The self-consistent approximation scheme is, therefore, particularly suited for assessing the effective properties of composites with polycrystalline morphology.

CHAPTER 3

Numerical Determination Of The Effective Properties From Digital Images Of Microstructure

A sample of random heterogeneous material is assumed to be a realization of a specific random or stochastic process. More precisely, a realization is an event, ω, that belongs to a sample space, Ω. Furthermore, a collection of all the possible realization of a random medium generated by a specific random/stochastic process is an ensemble. Since composite media are assumed to be a statistically homogeneous thus these realizations are different in the view of microscopic scale, while within the point of view of macroscopic details the realizations are identical (for more information see: [26]-[28]).

Consider a sample space Ω over which a probability density function $p(\omega)$ is defined, $\omega \in \Omega$. Then any particular random medium property $\eta(\mathbf{x}; \omega)$, called also as a structure function [20], is a function of a space position and a realization ω. An ensemble average of $\eta(\mathbf{x}; \omega)$ is defined as:

$$\overline{\langle \eta(\mathbf{x}) \rangle} = \int_{\Omega} \eta(\mathbf{x}; \omega) p(\omega) d\omega \qquad (3.1)$$

One can remark that the ensemble average is equivalent to an expectation of the function $\eta(\mathbf{x}; \omega)$. Furthermore, since the composite media are statistically homogeneous therefore the ensemble average of the structure function does not depend on the space variable x, for such the media.

The definition (3.1) implies a necessity of generation of all the realizations forming ensemble in order to determine the ensemble average. This exceptionally complex procedure is usually overcome using an ergodic hypothesis which allows replacing the ensemble average with a volume average, providing that a volume of the medium considered tends to infinity, i.e.:

$$\overline{\langle \eta \rangle} = \langle \eta \rangle = \lim_{V \to \infty} \frac{1}{V} \int_V \eta(\mathbf{x} + \mathbf{y}) d\mathbf{y} \qquad (3.2)$$

The relation (3.2) gives the possibility of considering only one arbitrary realization providing that the sample volume is infinite. The term *a sample with infinite volume* means, in an engineering application, a *sufficiently large sample*. This *sufficiently large sample* is called as *Representative Volume Element* (RVE).

In the wide literature a large number of specific RVE definitions can be found ([29]-[32]). These definitions are usually mathematically strict, however, none of them provides precise information on the RVE size - in other words, the definitions do not quantify the size of RVE.

A lot of attempt has been made in order to quantify the RVE size on the basis of statistical and numerical analysis. Within all the methods proposed (e.g.[29], [33]-[34]) the RVE size is usually determined by investigating the convergence of apparent property, with increasing the size of RVE. It causes that the process of RVE size evaluation requires a very large number of numerical calculations, e.g. the finite element method analysis.

In this book a methodology developed and presented in a series of papers [35]-[39] is adopted for an estimation of the ensemble average (3.1) or (3.2). The sample is here considered as a set of a finite number n of RVE elements (Fig.3.1), each having the same finite size, N_{RVE}, being a number of pixels in a row of RVE digital image. The ensemble average is then estimated as:

$$\overline{\langle \eta \rangle} \approx n^{-1} \sum_{j=1}^{n} \langle \eta_j \rangle = n^{-1} \sum_{j=1}^{n} \frac{1}{V_{RVE}} \int_{V_{RVE}} \eta_j(\mathbf{y}) d\mathbf{y} \qquad (3.3)$$

where η_j is a structural function corresponding to the j-realization of RVE and n is the size of the sample.
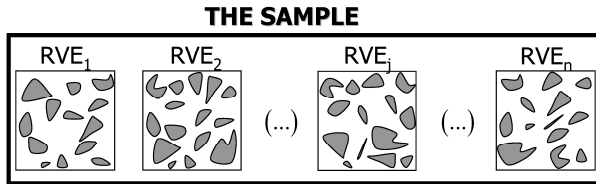
THE SAMPLE

Fig. 3.1. The graphical illustration of the notion of a sample

The crucial role in this approach plays a proper determination of the RVE size, N_{RVE}, as well as the size, n, of the sample. The both values are related to each other, i.e. larger size of RVE then a smaller sample size n can be used or inversely smaller size of RVE requires necessity of larger size of the sample use. It has to be, however, underlined that the RVE size can not be as small as one may wish. There exist some critical value, a

minimum size of RVE, which can not be decreased if a proper estimation of the ensemble average has to be assured. In other words, use of the RVE size smaller than the critical one will improperly estimate the ensemble average (3.1), usually will result in an overestimation of this value. It appears also that the minimum size of RVE strongly depends on a type of a structural function, $\eta(\mathbf{x}; \omega)$, considered.

The condition for the minimum size of RVE used in this book is such that it preserves a satisfactory replica of so-called 2-point correlation function ([20], [39]). Różanski, in his PhD thesis [38], has shown that this minimum size of RVE can be also successfully used for determination of effective mechanical properties of random composites. In fact, his result is much stronger: there exists a one to one mapping between the minimum RVE size preserving a satisfactory replica of 2-point probability function and the minimum RVE size corresponding to the effective transport properties, i.e.:

$$N_K(\varepsilon) = N_{2-\text{point}}(\varepsilon b(\theta)) \tag{3.4}$$

where: $N_K(\varepsilon)$ and $N_{2-\text{point}}(\varepsilon)$ are the minimum RVE sizes corresponding to the effective transport property and the 2-point correlation function, respectively. Symbol ε denotes an assumed value of an error tolerance whereas $\theta = k_2/k_1$ is a measure of a contrast in transport properties of composite constituents. Function $b(\theta)$ is defined as:

$$b(\theta) = \frac{(c_1 + a(\theta)c_2)^2}{(1 - a(\theta))^2 c_1^2} \quad \text{with} \quad a(\theta) = \min\left\{\theta, \frac{1}{\theta}\right\} \tag{3.5}$$

where c_1 and c_2 are the volume fractions of constituents in a composite.

The relation (3.4) indicates that the RVE size corresponding to the effective transport property, estimated with the error tolerance ε, is equated to the RVE size corresponding to the 2-point probability function, estimated with the error tolerance $\varepsilon b(\theta)$. Since $b(\theta) \geq 1$ and $N_{2-\text{point}}(\varepsilon)$ is a decreasing function of ε, therefore:

$$N_K(\varepsilon) \leq N_{2-\text{point}}(\varepsilon) \tag{3.6}$$

The inequality (3.6) indicates that the RVE size resulting from the 2-point probability function can be always used for determination of the effective mechanical properties of composite media since it is never smaller than the minimum RVE size corresponding to the effective mechanical properties.

This innovative procedure of RVE size determination (Eq.(3.4) utilizes only the microstructure morphology that is contained within the 2-point correlation function, and therefore, it gives the possibility of RVE size determination with no large number of numerical calculations - the numerical analysis like those of Finite Element Method or other methods as Generalized Method of Cells [40] are not necessary.

3.1. Microstructure descriptors

Consider an M-phase random medium. The total volume of ς is partitioned into M-disjoint random sets or phases. Let $\varsigma_i(\omega)$ denotes region occupied by a phase i. Introduce now a structure function $\eta(\mathbf{x}; \omega)$, for phase i, such that:

$$\eta(\mathbf{x};\omega) = I^{(i)}(\mathbf{x};\omega) = \begin{cases} 1, & \text{if } \mathbf{x} \in V_i(\omega) \\ 0, & \text{otherwise} \end{cases} \tag{3.7}$$

The function introduced above is just the indicator function, i.e. for fixed $\mathbf{x}$ it has only two possible values: 0 or 1, depending on the realization ω.

For an M-phase random medium a following relation holds true:

$$\sum_{i=1}^{M} I^{(i)}(\mathbf{x}) = 1 \tag{3.8}$$

The expectation or probability of finding phase i at a chosen point, x, is then evaluated as:

$$S_1^i(x) = \overline{\langle I^{(i)}(x,\omega) \rangle} = \int_\Omega I^{(i)}(x,\omega) p(\omega) d\omega = P\{I^{(i)}(x) = 1\} \tag{3.9}$$

The above function is referred to as a 1-point probability function for phase, i, since it gives the probability to find phase i at position x. It is also referred to as 1-point correlation function for the phase indicator function, $I^{(i)}(x)$.

We focus now on the n-point probability function, also called the n-point correlation function. This function denotes the probability that n points at positions $\mathbf{x}_1$, $\mathbf{x}_2$, ..., $\mathbf{x}_n$ are simultaneously found in phase i. According to its definition $S_n^{(i)}$ can be expressed in term of probability that the indicator function is 1 for all points $\mathbf{x}_1$, $\mathbf{x}_2$, ..., $\mathbf{x}_n$, i.e.

$$S_n^{(i)}(\mathbf{x}_1, \mathbf{x}_2, ..., \mathbf{x}_n) = P\left(I^{(i)}(\mathbf{x}_1) = 1, I^{(i)}(\mathbf{x}_2) = 1, ..., I^{(i)}(\mathbf{x}_n) = 1\right) \tag{3.10}$$

or equivalently

$$S_n^{(i)}(\mathbf{x}_1, \mathbf{x}_2, ..., \mathbf{x}_n) = \int_\Omega I^{(i)}(\mathbf{x}_1, \omega) I^{(i)}(\mathbf{x}_2, \omega) ... I^{(i)}(\mathbf{x}_n, \omega) p(\omega) d\omega \tag{3.11}$$

Above and in what follows, ω is omitted from the notation, for brevity of a description.

For composite media which are statistically homogeneous and, in addition, isotropic ones, the probability given by relation (3.11) is invariant under any translation and rotation of the space origin [20], thus

$$S_n^{(i)}(\mathbf{x}_1, \mathbf{x}_2, ..., \mathbf{x}_n) = S_n^{(i)}(x_{12}, ..., x_{1n}) \tag{3.12}$$

where

$$x_{ij} = \left\| \mathbf{x}_i - \mathbf{x}_j \right\| = \sqrt{\left(x_1^i - x_1^j\right)^2 + \left(x_2^i - x_2^j\right)^2 + \left(x_3^i - x_3^j\right)^2} \qquad (3.13)$$

Geometrical interpretation of 2-point and 3-point probability functions are sketched in figure 3.2. The 2-point probability for phase i, $S_2^{(i)}$, is the probability that two ends of a line segment of length r lie in ς_i when randomly placed in the sample (Fig. 3.2). In the same manner the geometrical meaning of 3-point probability, $S_3^{(i)}$, for phase i can be easily formulated: it is the probability that all three vertices of a triangle are found in ς_i when randomly placed in the volume ς (Fig. 3.2).

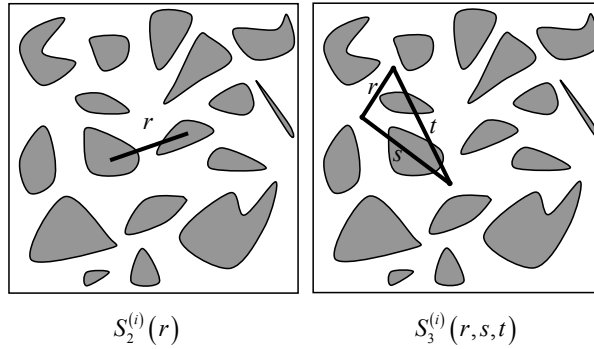$$S_2^{(i)}(r) \qquad\qquad S_3^{(i)}(r,s,t)$$

Fig.3.2. Geometrical interpretation of 2-point and 3-point probability.

Hereafter, the primary attention is limited to the 2-point probability function, since a determination of the minimum RVE size used in this book is based only on this microstructure descriptor. One can interpret the 2-point probability function as a measure of morphology of phase distribution within composite medium, i.e. the information of how the end points of line segment of length r are correlated within the microstructure. The limit of $S_2^{(i)}(r)$, for $r \to \infty$, is equal to the square of the volume fraction of phase i. If this limit is reached before $r \to \infty$, say for certain value $r = r*$, then the points within the microstructure with a distance larger than $r*$ are not correlated.

The two-point probability provides, in addition, the information on specific surface s of the system which is defined as the interface area per unit volume of composite. The slope of $S_2(r)$, at $r=0$, is related to the specific surface s by a following relation [20,45]:

$$s = -4 \left. \frac{d}{dr} S_2^{(i)}(r) \right|_{r=0} \qquad (3.14)$$

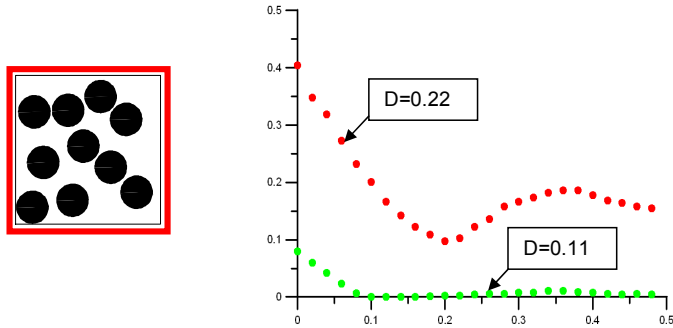An example of the 2-point probability function is plotted in figure 3.3.

Fig.3.3 The 2-point probability function for system of non-overlapping spheres; one function corresponds to composite with spherical inclusions of diameter D=0.22 pixels whereas the second one - D=0.11 pixels.

3.1.1. Numerical estimation of 2-point probability function from digital image of microstructure

In general, evaluation of the 2-point correlation function can be successfully performed by simple Monte Carlo simulations [20] i.e. by randomly tossing the line segment of length r and counting the fraction of times the end points are found in the phase for which the correlation function is evaluated. If one works, however, with a digital image of microstructure, this procedure can lead to a large computational cost. For an isotropic digitised systems, more accurate procedure is that one proposed in [43].

Consider a binary - $M \times M$ pixels – an image of random microstructure. We attribute to each pixel only one of two possible values: 0 or 1. Therefore, the digital image can be expressed by a square matrix $\mathbf{A}_{[M \times M]}$, in such a way, that each element of matrix A is equal to 0 or 1, i.e.: $A[i, j] = 1$ if pixel "contains" the phase for which the 2-point correlation function is going to be evaluated. Indices i and j correspond to the localization of the pixel within the image and denote the number of a row and a column, respectively. Then, the 2-point correlation function for phase 1 can be expressed as:

$$S_2^{(1)}(r) = \frac{1}{M^2} \sum_{j=1}^{M} \sum_{i=1}^{M} \frac{A[i,j](A[i,j+r] + A[i+r,j])}{2}, \qquad r = 1, 2, \ldots \qquad (3.14)$$

Geometrical interpretation of this procedure is as follows (Fig.3.4). The 2-point correlation function is evaluated by translating a line segment of length r (in pixels) at a distance of one pixel at a time and spanning the whole image. Each time the end points of r are located at the pixel centers. The number of successful events, such that two end points of line segment of length r are found in phase 1, are counted and divided by the

84

total number of trials. Note that by the assumption of system isotropy sampling is performed only along two orthogonal directions: rows and columns.
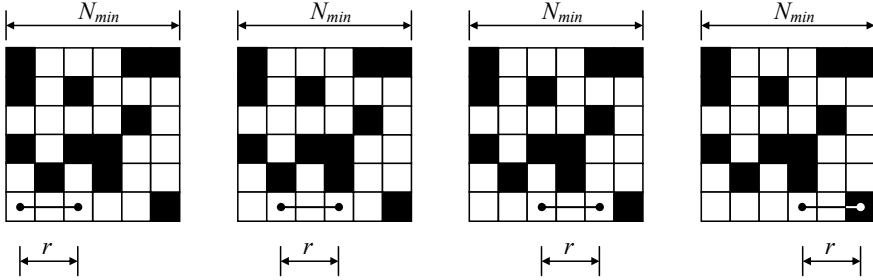

Fig.3.4. Geometrical interpretation of numerical evaluation of the 2-point probability function

3.1.2. Microstructure reconstruction based on 2-point probability function

A reconstruction process of a microstructure consists in finding such realization for which the calculated 2-point correlation function, $S_2^{(i)}$, best matches the "target" 2-point correlation function $S_2^{(i)}$ (note that $S_2^{(i)}$ is the phase i 2-point correlation function). Starting from some initial realization, preserving volume fractions of phases, the microstructure is evolved towards $S_2^{(i)}$ by minimizing an fictitious energy E, which at any time step, is defined as:

$$E = \sum_r \left[S_2^{(i)}(r) - S_2^{(i)}(r) \right]^2 \tag{3.15}$$

The minimization of E (at any time step) is performed by simulated annealing algorithm [44]. Namely, the states of two randomly chosen pixels of different phases are interchanged - white pixel is changed into black one, while black pixel is changed into white one. Interchanging the states of two pixels causes the change in energy, such that $E \to \bar{E}$. The phase interchange is accepted with the following probability

$$P_{\Delta E} = \begin{cases} 1, & \Delta E \le 0 \\ \exp(-\Delta E/T), & \Delta E > 0 \end{cases} \tag{3.16}$$

where:

$$\Delta E = \overline{E} - E \qquad (3.17)$$

and T is a fictitious temperature which its actual value is defined by the cooling schedule procedure applied. Starting with a high value of T the cooling procedure is performed. The cooling process which governs the value and the rate of T should be chosen to be sufficiently slow to allow the system to evolve to the desired state as quickly as possible without getting any meta-stable local energy minima [20]. Usually, the cooling algorithm is adopted in the form of geometrical series, i.e.

$$T(k) = T_o q^k \quad \text{with} \quad q \leq 1 \qquad (3.18)$$

A value of q is taken as 0.8 or 0.9. At each cooling step, say at actual value of T, the system is allowed to evolve long enough to thermalize, about 10000-20000 iteration, i.e. 10000-20000 interchanges of pixels are performed. The solution is obtained as $T \to 0$.

At the starting point of the reconstruction algorithm outlined above a checkerboard microstructure is typically used. Such a microstructure is shown in figure 3.5, for different resolutions.

Fig.3.5. Checkerboard microstructures corresponding to different number of pixels per row in a digital image

Examples of microstructures reconstructed by the author's own algorithm are presented in figures 3.6-3.8. The final picture of the microstructure reconstructed are presented together with pictures corresponding to some intermediate steps of the process.

The microstructure shown in the figure 3.6 is characterized by a following target 2-point probability function:

$$S_2^{(i)} = c_i (1 - c_i) \left(1 - \frac{r}{d}\right) H \left(1 - \frac{r}{d}\right) + c_i^2 \qquad (3.19)$$

where d is a parameter characterizing a size of rectangular inclusions embedded in a matrix and c_i represents a volume fraction of the composite constituent for which the target function is given. It has been assumed d=6 pixels, in the example studied in figure

3.6. The plot presented in the figure 3.6 shows a target 2-point probability function (continuous line in the plot) and that of the microstructure reconstructed (dots in the plot).
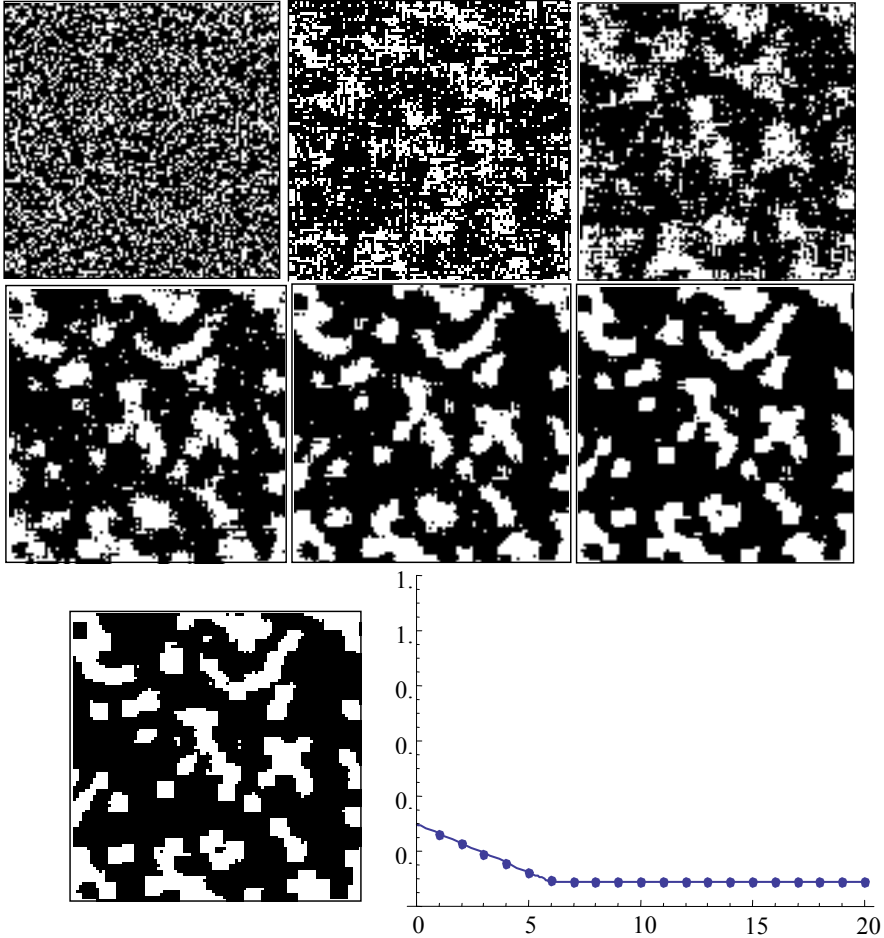
Fig.3.6. Snapshots of the microstructure corresponding to some steps of reconstruction process. The target 2-point probability function defined by Eq. (3.19).

The target 2-point correlation function corresponding to the microstructure shown in the figure 3.7 is:

$$S_2^{(i)} = c_i(1 - c_i)e^{-\frac{r}{d}} + c_i^2 \tag{3.20}$$

whereas

$$S_2^{(i)} = c_i(1 - c_i)e^{-\frac{r}{d}}\frac{\sin(qd)}{qd} + c_i^2 \tag{3.21}$$

corresponds to the microstructure presented in the figure 3.8.
The equation (3.20) and (3.21) characterize so-called Debye and modified Debye microstructure, respectively [20].

Fig.3.7. Reconstruction of Debye microstructure.

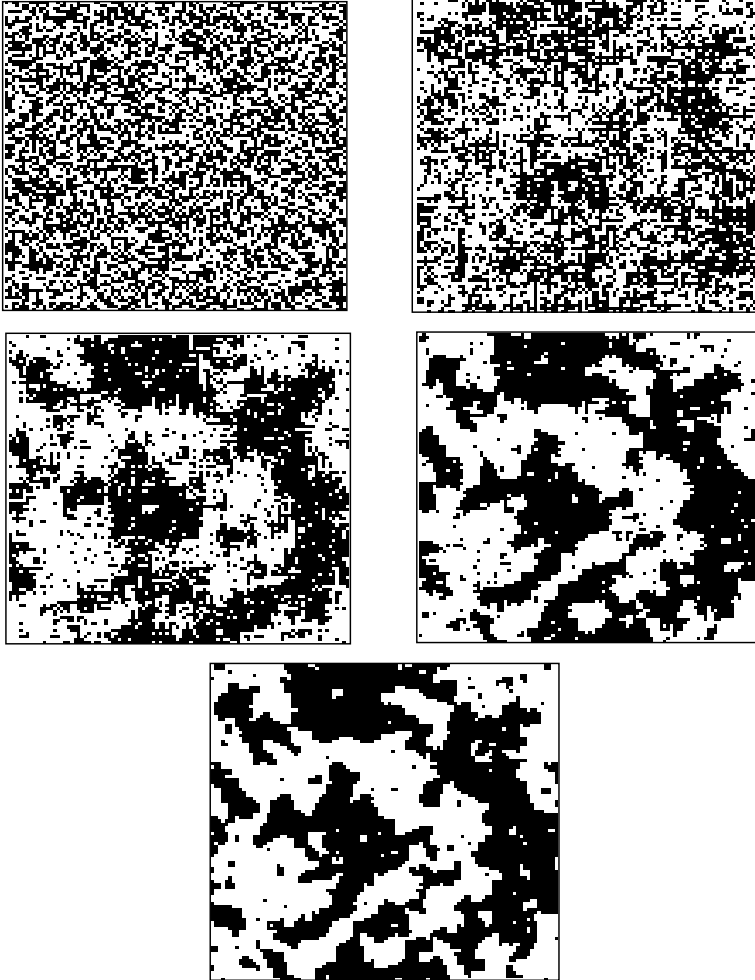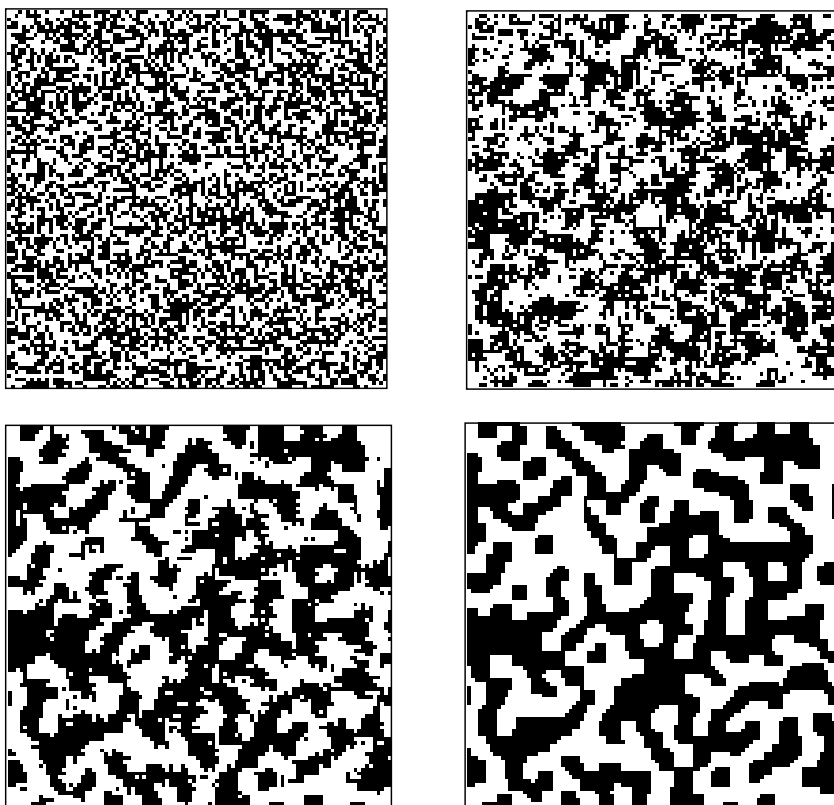Fig.3.8. Reconstruction of modified Debye microstructure.

The reconstruction process shown in the figures presented above has been done in 2D. The algorithm outlined above can, however, be successively applied to 3D reconstruction of the microstructure.

It can be seen that the 2-point probability function contains enough morphological information to reconstruct the microstructure of random composites. Furthermore, from 2D digital image of the microstructure one can always determine, using the method outlined in section 3.1.1, the 2-point probability function. Then a 3D reconstruction of the microstructure can be done using the reconstruction algorithm presented above. The 3D microstructure, reconstructed from 2D digital image of the microstructure, can then be used for an estimation of the effective properties of the composite medium. The crucial role, as has been discussed previously, plays a determination of an appropriate size of RVE. Solution to this problem is presented in the next section.

It has to be marked that the 2-point correlation function provides only some partial information on the microstructure, so the reconstruction process is not unique. In other

words, the infinite number of microstructure corresponds to a given 2-point probability function.

3.2. Minimum RVE size

The condition for minimum size of RVE, adopted in this book, is that one proposed in [42] and [38]. It is presented, in a slightly modified form, below:

$$N_{2\text{-point}} = \max\left\{N_1(\varepsilon), N_2(\varepsilon), 2l_c(\varepsilon)\right\} \tag{3.22}$$

where ε is an assumed error tolerance, l_c is so-called correlation length defined as:

$$\forall r \geq l_c(\varepsilon) \Rightarrow \left|\frac{S_2(r) - c_1^2}{c_1^2}\right| \leq \varepsilon \tag{3.23}$$

The numbers $N_1(\varepsilon)$ and $N_2(\varepsilon)$ are such that the following inequalities hold true, i.e.:

$$\forall N \geq N_i(\varepsilon) \Rightarrow \frac{\text{var}(c_i)}{c_i^2} \leq \varepsilon \quad i = 1, 2 \tag{3.24}$$

The variance of volume fraction, $\text{var}(c_i)$, is related to the 2-point probability function and the size of RVE used by a following relation [38],[45]:

2D case

$$\text{var}(c_i)\big|_{N_{RVE}} = \frac{4}{N_{RVE}^4} \int_0^{N_{RVE}} \int_0^{N_{RVE}} \left(S_2^{(1)}\left(\sqrt{x_1^2 + x_2^2}\right) - c_i^2\right)\left(N_{RVE} - x_1\right)\left(N_{RVE} - x_2\right)dx_1 dx_2$$

3D case

$$\text{var}(c_i)\big|_{N_{RVE}} =$$

$$= \frac{8}{N_{RVE}^6} \int_0^{N_{RVE}} \int_0^{N_{RVE}} \int_0^{N_{RVE}} \left(S_2^{(1)}\left(\sqrt{x_1^2 + x_2^2 + x_3^2}\right) - c_i^2\right)\left(N_{RVE} - x_1\right)\left(N_{RVE} - x_2\right)\left(N_{RVE} - x_3\right)dx_1 dx_2 dx_3$$

The above relations together with the condition (3.24) lead to the following implicit equations for the numbers $N_1(\varepsilon)$ and $N_2(\varepsilon)$, i.e.:

2D case

$$N_1(\varepsilon) = \sqrt[4]{\frac{4\int\limits_0^{N_1}\int\limits_0^{N_1}\left(S_2^{(1)}\left(\sqrt{x_1^2+x_2^2}\right)-c_1^2\right)\left(N_1(\varepsilon)-x_1\right)\left(N_1(\varepsilon)-x_2\right)dx_1dx_2}{c_1^2\varepsilon}}$$

$$N_2(\varepsilon) = \sqrt[4]{\frac{4\int\limits_0^{N_2}\int\limits_0^{N_2}\left(S_2^{(1)}\left(\sqrt{x_1^2+x_2^2}\right)-c_1^2\right)\left(N_2(\varepsilon)-x_1\right)\left(N_2(\varepsilon)-x_2\right)dx_1dx_2}{c_2^2\varepsilon}}$$

(3.25)

3D case

$$N_1(\varepsilon) =$$

$$= \sqrt[6]{\frac{8\int\limits_0^{N_1}\int\limits_0^{N_1}\int\limits_o^{N_1}\left(S_2^{(1)}\left(\sqrt{x_1^2+x_2^2+x_3^2}\right)-c_1^2\right)\left(N_1(\varepsilon)-x_1\right)\left(N_1(\varepsilon)-x_2\right)\left(N_1(\varepsilon)-x_3\right)dx_1dx_2dx_3}{c_1^2\varepsilon}}$$

(3.26)

$$N_2(\varepsilon) =$$

$$= \sqrt[6]{\frac{8\int\limits_0^{N_2}\int\limits_0^{N_2}\int\limits_o^{N_2}\left(S_2^{(1)}\left(\sqrt{x_1^2+x_2^2+x_3^2}\right)-c_1^2\right)\left(N_2(\varepsilon)-x_1\right)\left(N_2(\varepsilon)-x_2\right)\left(N_2(\varepsilon)-x_3\right)dx_1dx_2dx_3}{c_2^2\varepsilon}}$$

The relations (3.22), (3.23) and (3.25) (or (3.26)) allow for determination of the minimum size, $N_{2\text{-point}}$, of RVE. It requires, however, numerical calculations. This problem is carefully discussed in the next paragraph.

3.2.1. Numerical determination of minimum RVE size

In order to evaluate the integral of the 2-point correlation function involved in the definition of the minimum size of RVE (Eqs. (3.25) or (3.26)), the Monte Carlo integration approach is convenient to use [38, 50]. Interested reader of the Monte Carlo method is referred to [47,48,49] for fundamentals and methodology of the approach. Hereafter, we assume that RVE is a square/cube consisted of N^2/N^3 pixels (square for 2D whereas cube for 3D).

Consider the function g given by the following formula:

2D case

$$g_2(N) = \frac{4}{N^4} \int_0^N \int_0^N \left(S_2^{(i)} \left(\sqrt{x_1^2 + x_2^2} \right) - c_i^2 \right) (N - x_1)(N - x_2) dx_1 dx_2 \qquad (3.27)$$

3D case

$$g_3(N) = \frac{8}{N^6} \int_0^N \int_0^N \int_0^N \left(S_2^{(i)} \left(\sqrt{x_1^2 + x_2^2 + x_3^2} \right) - c_i^2 \right) (N - x_1)(N - x_2)(N - x_3) dx_1 dx_2 dx_3 \qquad (3.28)$$

Note that a following equivalence holds true, i.e.:

$$\frac{2}{N^2} \int_0^N (N - t) dt = 1 \qquad (3.29)$$

which allows, in turn, to define a probability function:

$$p(t) = \frac{2}{N^2} (N - t) \qquad (3.30)$$

Furthermore

$$p_2(x_1, x_2) = p(x_1) p(x_2) \text{ or } p_2(x_1, x_2, x_3) = p(x_1) p(x_2) p(x_3) \qquad (3.31)$$

can be treated as the probability density functions in Ω for 2D and 3D case, respectively. Introducing functions defined as:

$$h_2(x_1, x_2) = \left(S_2^{(i)} \left(\sqrt{x_1^2 + x_2^2} \right) - c_i^2 \right)$$

(3.32)

$$h_3(x_1, x_2, x_3) = \left(S_2^{(i)} \left(\sqrt{x_1^2 + x_2^2 + x_3^2} \right) - c_i^2 \right)$$

the integrals (3.27) and (3.28) can be interpreted, within the probability theory, as an expectation of functions h_2 and h_3, respectively:

$$g_2(N) = \int_0^N \int_0^N h_2(x_1, x_2) p(x_1, x_2) dx_1 dx_2 = E\{h_2(X_1, X_2)\}$$

(3.33)

$$g_3(N) = \int_0^N \int_0^N \int_0^N h_3(x_1, x_2, x_3) p(x_1, x_2, x_3) dx_1 dx_2 dx_3 = E\{h_2(X_1, X_2, X_2)\}$$

where $E\{\ \}$ stands for the expectation operator.

According the Monte Carlo (MC) technique, evaluation of the expectation consists in generating random numbers $\left(X_1^\alpha, X_2^\alpha \right)$ from the density function $p(t)$ and then computing the mean of $h_2(x_1, x_2)$, (respectively $\left(X_1^\alpha, X_2^\alpha, X_3^\alpha \right)$ and $h_3(x_1, x_2, x_3)$) i.e.:

$$g_2(N) \approx \frac{1}{M} \sum_{\alpha=1}^{M} h_2\left(X_1^\alpha, X_2^\alpha \right) \text{ and } g_3(N) \approx \frac{1}{M} \sum_{\alpha=1}^{M} h_3\left(X_1^\alpha, X_2^\alpha, X_3^\alpha \right) \tag{3.34}$$

where M stands for number of MC realization.

In order to evaluate the MC estimator (3.34), pseudo random numbers from a non-uniform distribution have to be drawn. Following [51] this problem is divided into two parts. First, a simple generator is used to generate uniformly distributed random numbers, which in a second step are transformed to follow the required distribution. This generation process is referred to as the inverse method.

Note, the non-decreasing cumulative distribution function (CDF) of $p(t)$ reads:

$$Q(X) = \int_0^X \frac{2}{N^2}(N-x)dx = 1 - \frac{(N-X)^2}{N^2} \tag{3.35}$$

Note that the CDF always grows monotonically from 0 to 1, such that Q values are uniformly distributed. Therefore, the problem of generating the numbers of any distribution consists in drawing a uniformly distributed random number, say RN, such that $RN = Q(X)$ and, if the inverse function exists, setting $X = Q^{-1}(RN)$. It is evident that in the case of relation (3.35) the inverse function exists and has the following form:

$$X(Q) = N\left(1 - \sqrt{1 - Q(X)}\right) \tag{3.36}$$

The estimator of the integral (3.34) is therefore evaluated as:

$$g_2(N) \cong \frac{1}{M} \sum_{\alpha=1}^{M} \left(S_2^{(i)} \left(\sqrt{\sum_{j=1}^{2} X(Q_j)^2} \right) - c_i^2 \right)$$

$$g_3(N) \cong \frac{1}{M} \sum_{\alpha=1}^{M} \left(S_2^{(i)} \left(\sqrt{\sum_{j=1}^{3} X(Q_j)^2} \right) - c_i^2 \right) \tag{3.37}$$

The values of Qj are obtained from the uniform distribution on the interval [0,1], while $X(Q_i)$ are the non-uniformly distributed random numbers determined via relation (3.36).

The process of the minimum size of RVE determination, from the digital image of microstructure, can be summarized in the following steps:

- having a digital image of microstructure, evaluate the 2-point correlation function of one of the phases, say phase i, using relation (3.14),

- assume the value of error tolerance ε and determine the correlation length $l_c(\varepsilon)$ defined by the inequality (3.23),

- using MC approach (Eq.(3.37)), outlined above, determine numerically $g_2(N)$ (respectively $g_3(N)$) as a function of variable N,

- evaluate values of $N_1(\varepsilon)$ and $N_2(\varepsilon)$ from the following equations (for 3D case use the function $g_3(N)$, respectively):

$$\frac{g_2\big(N_1(\varepsilon)\big)}{c_1^2} = \varepsilon \text{ and } \frac{g_2\big(N_2(\varepsilon)\big)}{c_2^2} = \varepsilon \qquad (3.38)$$

- determine the minimum RVE size as (Eq.(3.22)):

$$N_{2-\text{point}} = \max\big\{N_1(\varepsilon), N_2(\varepsilon), 2l_c(\varepsilon)\big\} \qquad (3.39)$$

3.2.2. Evaluation of sample size

The proper estimation of the effective properties of composite media, as has been marked before, needs evaluation of the sample size, n, in addition to determination the minimum RVE size.

To begin with, let us recall some useful theorems:

Theorem 1 (Weak Law of Large Numbers): Let $X_1, X_2, \ldots$ be a sequence of independent and identically distributed random variables, each with mean μ and variance σ^2. Then for every $\varepsilon > 0$,

$$\lim_{n\to\infty} P\left(\left|\frac{1}{n}\sum_{i=1}^{n} X_i - \mu\right| > \varepsilon\right) = 0 \qquad (3.40)$$

If X_i is a structure function $\eta(\text{x}; \omega)$ then the Weak Law of Large Numbers assures that the estimator (3.3) converges in probability to the expectation value (3.1) being the ensemble average of a structure function. The next theorem enables to determine the sample size, n.

Theorem 2 (Central Limit Theorem): Let $X_1, X_2, \ldots$ be a sequence of independent and identically distributed random variables, each with mean μ and variance σ^2. Let

$$Z_n = \frac{n^{-1}\sum_{i=1}^{n} X_i - \mu}{\sigma/\sqrt{n}} \qquad (3.41)$$

then Z_n converges in distribution to Z, where Z is a standard normal random variable.

In other words, the Central Limit Theorem says that mean of independent identically distributed random variables can be approximated by a standard normal distribution, for a large number n.

The estimator of the ensemble average of the structure function $\eta(x; \omega)$, according to the equation (3.3), is defined as:

$$\langle \eta \rangle^{app} = n^{-1} \sum_{j=1}^{n} \frac{1}{V_{RVE}} \int_{V_{RVE}} \eta_j(\mathbf{y}) d\mathbf{y} \tag{3.42}$$

This estimator should satisfy the following condition

$$P\left(\left| \overline{\langle \eta \rangle} - \langle \eta \rangle^{app} \right| \leq \varepsilon_{abs} \right) \geq 1 - \alpha \tag{3.43}$$

where $\varepsilon_{abs} > 0$ and $0 < \alpha$ are the absolute error and the significance level, respectively. The values of ε_{abs} as well as α are a priori known.

The relation (3.43) can be transform to a following equivalent form, i.e.:

$$P\left(\left| \frac{\overline{\langle \eta \rangle} - \langle \eta \rangle^{app}}{\sqrt{\operatorname{var}(\eta)}/\sqrt{n}} \right| \leq \frac{\varepsilon_{abs}}{\sqrt{\operatorname{var}(\eta)}/\sqrt{n}} \right) \geq 1 - \alpha \tag{3.44}$$

Now, according to the Central Limit Theorem, the distribution of random variable $\dfrac{\overline{\langle \eta \rangle} - \langle \eta \rangle^{app}}{\sqrt{\operatorname{var}(\eta)}/\sqrt{n}}$ can be approximated by the standard normal distribution, for large values of n, therefore the inequalities (3.44) implies:

$$\Phi\left(\frac{\varepsilon_{abs}}{\sqrt{\operatorname{var}(\eta)}/\sqrt{n}} \right) \geq 1 - \frac{\alpha}{2} \tag{3.45}$$

or equivalently:

$$n \geq \frac{\operatorname{var}(\eta)}{\varepsilon_{abs}^2} \left(\Phi^{-1}\left(1 - \frac{\alpha}{2} \right) \right)^2 \tag{3.46}$$

where $\Phi(*)$ is the cumulative distribution function of standard normal random variable.

In the descriptions (3.22) and (3.23) the error tolerance ε represents the relative error, therefore the inequality (3.46) is rewritten as:

$$n \geq \frac{\text{var}(\eta)}{\langle \eta \rangle^2 \varepsilon^2} \left(\Phi^{-1} \left(1 - \frac{\alpha}{2} \right) \right)^2 \qquad (3.47)$$

where

$$\varepsilon = \frac{\varepsilon_{abs}}{\langle \eta \rangle} \qquad (3.48)$$

The inequality (3.47) defines the sample size, n, in term of the effective property, $\overline{\langle \eta \rangle}$, to be determined, still unknown. It appears, however, that the size of the sample required for assuring a satisfactory replica of the 2-point probability function is larger than that one required for evaluation of the effective mechanical properties of composite media. To preserve a satisfactory replica of the 2-point correlation function a following approximation can be applied [38]:

$$\frac{\text{var}(\eta)}{\langle \eta \rangle^2} \leq 4 \frac{\text{var}(c_i)}{c_i^2} \qquad (3.49)$$

Since the RVE size satisfies the inequality (3.24), i.e:

$$\frac{\text{var}(c_i)}{c_i^2} \leq \varepsilon \qquad i = 1,2 \qquad (3.50)$$

therefore the sample size determined such that

$$n \geq \frac{4}{\varepsilon} \left(\Phi^{-1} \left(1 - \frac{\alpha}{2} \right) \right)^2 \qquad (3.51)$$

assures a proper estimation of the ensemble average (3.1) of the effective mechanical properties of composite media.

The significance level is typically assumed as: 5%, 3% or 1% , which corresponds to: $\alpha=0.05$, $\alpha=0.03$ and $\alpha=0.01$, respectively. These values, according to the table of standard normal distribution, imply: $\Phi^{-1} \left(1 - \frac{0.05}{2} \right) = 1.96$, $\Phi^{-1} \left(1 - \frac{0.03}{2} \right) = 2.17$ and $\Phi^{-1} \left(1 - \frac{0.01}{2} \right) = 2.575$. Substituting these values to the inequality (3.51) leads to:

$$n \geq \begin{cases} n_{5\%} = \dfrac{15.37}{\varepsilon} \\[2ex] n_{3\%} = \dfrac{18.84}{\varepsilon} \\[2ex] n_{1\%} = \dfrac{26.52}{\varepsilon} \end{cases} \qquad (3.52)$$

The sample size, n, given by the above inequalities corresponds to the minimum RVE size. If the RVE size would be used larger than the critical one then the sample size can be decreased. In such a case, determine numerically, as has been presented in the previous section, the value:

$$\frac{\operatorname{var}(c_i)}{c_i^2} = \frac{g_2(N(\varepsilon))}{c_i^2} \quad \text{or} \quad \frac{\operatorname{var}(c_i)}{c_i^2} = \frac{g_3(N(\varepsilon))}{c_2^2}$$

and use inequalities (3.47) and (3.49) for evaluation of the proper sample size.
According to the inequality (3.44), the correctness of the ensemble average estimator is assured only with some probability value. The significance levels assumed above imply:

$$P\left(\left| \frac{\overline{\langle \eta \rangle} - \langle \eta \rangle^{app}}{\overline{\langle \eta \rangle}} \right| \leq \varepsilon \right) \geq \begin{cases} 0.95 & \text{for } n \geq n_{5\%} \\ 0.97 & \text{for } n \geq n_{3\%} \\ 0.99 & \text{for } n \geq n_{1\%} \end{cases} \qquad (3.53)$$

Of course, with increasing the sample size this probability will also increase.

3.3. Procedure of numerical estimation of effective properties

The determination of effective mechanical properties of random composites from digital image of microstructure consists of the following main steps:
1. determine the minimum size of RVE according to the method presented in the section 3.2.1
   - ✓ having a digital image of microstructure evaluate the two-point probability function using the relation (3.14),
   - ✓ determine the variance of local volume fraction, var(c_i), use the Monte Carlo approach,
   - ✓ set the wanted precision, ε, and evaluate the minimum size of RVE- use condition (3.22),
   - ✓ choose RVE size, N_{RVE}, larger than or equal to the minimum one,
2. evaluate, according to the methodology presented in the section 3.2.2, the sample size, n, for a chosen RVE size,

✓ set the significance level, α, and determine the sample size, n, according the relations (3.52),

3. choose randomly n windows, $N_{RVE} \times N_{RVE}$, from the digital image of microstructure,
4. solve, for any chosen window, an appropriate boundary value problem using Finite Element or Finite Volume numerical procedure,
   ✓ the appropriate boundary value problem for determination of transport properties reads:

$$\frac{\partial}{\partial x_i}\left[k(\mathbf{x})\left\{\delta_{ij} + \frac{\partial \xi_j(\mathbf{x})}{\partial x_i}\right\}\right] = 0 \quad \text{in } V_{RVE} \tag{3.54}$$

$$\xi_j(\mathbf{x}) = \xi_j(\mathbf{x} + N_{RVE}) \quad \text{on } \partial V_{RVE} \tag{3.55}$$

   ✓ the appropriate boundary value problem for determination of elasticity constants reads:

$$\frac{\partial}{\partial y_i}\left[\frac{1}{2}D_{ijlm}\left(\delta_{lk}\delta_{mh} + \delta_{lh}\delta_{mk}\right) + D_{ijlm}\varepsilon_{lm}\left(\xi^{kh}\right)\right] = 0 \quad \text{in } V_{RVE} \tag{3.56}$$

$$\xi^{kh}(\mathbf{x}) = \xi^{kh}(\mathbf{x} + N_{RVE}) \quad \text{on } \partial V_{RVE} \tag{3.57}$$

5. evaluate the volume averaged value of the solution of the boundary value problem for each window
   ✓ for transport properties

$$K_j = \frac{1}{V_{RVE}} \int_{V_{RVE}} k(\mathbf{x})\left\{1 + \frac{1}{3}\frac{\partial \xi_j}{\partial x_j}\right\} d\mathbf{x} \tag{3.58}$$

   ✓ for elasticity constants

$$K_j = \frac{1}{3}\frac{1}{V_{RVE}} \int_{V_{RVE}} \left\{D_{ijkh}\delta_{kh} + D_{ijlm}e_{lm}\left(\xi^{kh}\right)\delta_{kh}\right\} d\mathbf{x} \tag{3.59}$$

$$G_j = \frac{1}{V_{RVE}} \int_{V_{RVE}} \left\{D_{ij12} + D_{ijlm}e_{lm}\left(\xi^{12}\right)\delta_{kh}\right\} d\mathbf{x} \tag{3.60}$$

6. determine the effective property using the Monte Carlo estimator, i.e:

$$\overline{K} = \frac{1}{n}\sum_{j=1}^{n} K_j$$

$$\overline{G} = \frac{1}{n}\sum_{j=1}^{n} G_j$$

CHAPTER 4

_____

Final Remarks

The chapter devoted to a micro-macro passage presents only a general methodology of upscalling of mathematical description of the processes taking place in composite media. The presentation is limited to the heuristic/engineering methods as volume averaging or micromechanics. Special attention is paid for a practical use of this procedure, so the transport processes as diffusion or heat conduction as well as the elasticity problem are discussed in details.

The mathematical theory of homogenization is omitted in this book. The interested reader for the asymptotic homogenization method, two-scale convergence method, G- or H- or Γ- convergence method is referred to the exhaustive literature on the subject as, for instance, [1], [18], [20], [41].

The analytical methods of effective properties estimation are mainly based on, so called, single inclusion solution. The final results presented in the book are valid only for ellipsoidal inclusions embedded in an isotropic matrix. The inclusion as well as the matrix considered in the book are assumed to be governed by the linear constitutive equations. Typically, such composite are called in the literature as the "linear composites".

The matrix anisotropy is still an open and challenging problem. The non-linear composites need a special treatment even analytical methods of estimation of effective behavior of such composites use a methodology and results stated for linear composites [3],[14],[19].

Strong development of powerful computers has been triggered in the last two decades a strong development of numerical procedures of composites' effective properties determination. These techniques need mainly precise definitions of the Representative Volume Element and the Sample. This problem has been studied in details in the chapter 3 of this book. The results presented in this chapter are really recent and original. The methodology proposed uses a 2-point probability function for determination of the size of Representative Volume Element and the size of the sample. The method is very fast, simple and efficient. Usefulness and correctness of this methodology has been proved by my PhD student, Adrian Różański, in his dissertation [38] in which a lot of different complex microstructures of random composites is investigated.

REFERENCES

[1] Hornung U. (ed), *Homogenization and Porous Media*, Interdisciplinary Applied Mathematics, Vol. 6, Springer-Verlag, Berlin 1997.

[2] Bielski R.W., Telega J.J., *Effective properties of geomaterials: rocks and porous media*, Publ. Inst. Geophys. Pol. Acad. Sci., A-26 (285), 1997.

[3] de Buhan P., Taliercio A., *A homogenization approach to the yield strength of composite material*, Eur. J. Mech. A/Solids, 10, 1991, 129–154.

[4] Drugan W.J., Willis J.R., *A micromechanics-based nonlocal constitutive equation and estimates of representative volume element size for elastic composities*, J. Mech. Phys. Solids, 44, 1996, 497–524.

[5] Cushmann J.H., *The physics of fluids in hierarchical porous media: angstroms to miles*, Kluwer Academic Publishers, 1990.

[6] Ene H.I., Polisewski D., *Thermal flow in porous media*, D. Reidel Publishing Company, Boston 1987.

[7] Gilbert F., *Change of scale in multiphase media: the case of saturated soils*, in: *Geomaterials: Constitutive equations and modelling*, F. Darve (ed.), 1990, 329–347.

[8] Nigmatulin R.I., *Three-Dimensional Averaging in the Mechanics of Heteregoneous Media*, Fluids Mechanics-Soviet Research, 10 (4), 1981, 72–105.

[9] Fung Y.C., *Podstawy mechaniki ciała stałego*, PWN, Warszawa 1969.

[10] Slattery J.C., *Single phase flow through porous media*, AIChE J., 15, 1969, 866–872.

[11] Suquet P., *Elements of homogenization for inelastic solid mechanics*, in: *Homogenization Techniques for Composite Media*, Lecture Notes in Physics, 272, Springer-Verlag, Berlin 1987.

[12] Bouchitte G., Suquet P., *Homogemization, plasticity and yield design*, in: *Composite Media and Homogenization Theory*, Dal Maso G. and Dell'Antonio G. (eds), 1991, 107-133.

[13] Suquet P., *Analyse limite et homogeneisation*, C.R. Acad. Sc. Paris, Serie II, t. 296, 1983, 1355–1358.

[14] Suquet P., *Overall potentials and extremal surfaces of power law or ideally plastic composites*,
J. Mech. Phys. Solids, **41**, 1993, 981–1002.

[15] Berryman J.G., *Single-scattering approximations for coefficients in Biot's equations of poro-elasticity*, J. Acoust. Soc. Am., **91** (2), 1992, 551–571.

[16] Dvorak G.J., *Transformation field analysis of inelastic composite materials*, Proc. R. Soc. Lond. A, **437**, 1992, 311–327.

[17] Ponte Castañeda P., Willis J.R., *The effect of spatial distribution on the effective behaviour of composite materials and cracked media*, J. Mech. Phys. Solids, **43**, 1995, 1919–1951.

[18] Milton G.W., *The theory of composites*, Cambridge University Press, 2002.

[19] Ponte Castañeda P., Suquet P., *Nonlinear composites*, Advances in Applied Mechanics, Vol. **34**, 1998, 172–295.

[20] Torquato S., *Random Heterogeneous Materials. Microstructure and Macroscopic Properties*, Springer-Verlag, New York, 2002.

[21] Mori T., Tanaka K., *Average stress in matrix and average elastic energy of materials with misfitting inclusions*, Acta Metall., **21**, 1973, 571-574.

[22] Norris A.N., *An examination of the Mori-Tanaka effective medium approximation for multiphase composites*, J. Appl. Mech., **56**, 1989, 83-88.

[23] Milton G.W., *The coherent potential approximation is a realizable effective medium scheme*, Comm.Math.Phys., **99**,1985, 463-500.

[24] Mura T., *Micromechanics of defects in solids*, Martinus Nijhoff Publishers, 1987

[25] Shaofan Li, *Introduction to micromechanics and nanomechanics*, Lecture Notes, University of California, 2006

[26] Beran M.J.: *Statistical Continuum Theories*, Monographs in Statistical Physics, Interscience Publishers, 1968.

[27] Drugan W.J., Willis J.R.: *A micromechanics-based nonlocal constitutive equation and estimates of representative volume element size ofr elastic composites*, J. Mech. Phys., Vol. 44, 1996, pp.497-524.

[28] Sejnoha M., Zeman J.: *Micromechanical Analysis of Random Composites*, Czech Technical University, 2000.

[29] Kanit T., Forest S., Galliet I., Mounoury V., Jeulin D.: *Determination of the size of the representative volume element for random composites: statistical and numerical approach*, Int J Solids Struct, Vol. 40, 2003, pp.3647.

[30] Kanit T., N'Guyen F., Forest S., Jeulin D., Reed M., Singleton S.: *Apparent and effective physical properties of heterogeneous materials: Representativity of samples of two materials form food industry*, Comput. Methods Appl. Mech. Engrg, 195 (33-36), 2006, pp.3960-3982.

[31] Stroeven M., Askes H., Sluys L.J.: *Numerical determination of representative volumes for granular materials*, Comput Meth Appl Mech Engng, Vol. 193, 2004, pp.3221.

[32] Gitman I.M., Askes H., Sluys L.J.: *Representative volume: existence and size determination*, Eng Fract Mech, Vol. 74, 2007, pp.2518.

[33] Gusev A.A.: *Representative volume element size for elastic composites: a numerical study*, J. Mech. Phys. Solids, Vol. 45, 1997, pp.1449–1459.

[34] Povirk G.L.: *Incorporation of microstructural information into model of two-phase materials*, Acta Metall. Mater., 43 (8), 1995, pp. 3199-3206.

[35] Różański A., Łydżba D.: *Some remarks on the size of representative volume element (RVE) in case of 2D lattice model*, Górnictwo i Geoinżynieria, 2009, Vol. 33 (1), pp.507-517 (in polish).

[36] Różański A., Łydżba D., Shao J.F.: *Numerical evaluation of effective transport properties of random cell models: two-point probability approach*, Proceedings of the 3rd International Symposium GeoProc 2008, Lille, 1st-5th June, 2008, pp.345.

[37] Różański A., Łydżba D., Shao J.F.: *Numerical determination of minimum size of RVE for random composite materials: two-point probability approach*, Proceedings of the First International Symposium on Computational Geomechanics, COMGEO I, Juan les Pins, France, 29 April - 1 May, 2009 / eds S. Pietruszczak *et al.*, Rhodes : IC2E International Centre for Computational Engineering, 2009, pp.26-37.

[38] Różański A. (2010), *Random composites: representativity, minimum RVE size, effective transport properties*, PhD dissertation, Universite Lille 1, LML (UMR CNRS 8107), No.: 40444.

[39] Łydżba D., Różański A.: *Statistical characterization of geometrical measures of random microstructures: definitions, properties and applications*, Górnictwo i Geoinżynieria, 2009, Vol. 33 (1), pp.399-410 (in polish).

[40] Łydżba D., Różański A., Kawa M.: *Generalized Method of Cells – computationally more efficient formulation*, Scientific Papers of the Wroclaw University of Technology 2007, pp. 154-164 (in polish).

[41] Łydżba D.: *Applications of asymptotic homogenization method in soil and rock mechanics*, Scientific Papers of the Institute of Geotechnics and Hydrotechnics of the Wroclaw University of Technology, 2002 (in polish).

[42] Łydżba D., Różański A.; *Wielkość próbki a reprezentatywność geometryczna mikrostruktury kompozytów losowych*, Górnictwo i Geoinżynieria, R. 34, z. 2, 443-450, 2010

[43] Yeong, C.L.Y. and Torquato, S., *Reconstructing random media II. Three dimensional media from two-dimensional cuts*. Phys. Rev. E, Vol. 58, 224, 1998

[44] Kirkpatrick, S. & Gelatt, C.D. & Vecchi M.P.; *Optimization by simulated annealing*. Science, Vol. 220, 671-680. ,1983.

[45] Berryman J.G., Milton G.W.: *Microgeometry of random composites and porous media*, J. Phys. D: Appl. Phys., Vol. 21, 1988, pp.87-94.

[46] Lu B., Torquato S.: *Local volume fraction fluctuations in heterogeneous media*, J. Chem. Phys. 93 (5), 1990, pp. 3452-3459.

[47] Fehske H., Schneider R., Weiße A. (Eds.): *Computational Many-Particle Physics*, Lect. Notes Phys. 739, Springer Berlin Heidelberg, 2008.

[48] Fishman G.S.: *Monte Carlo: Concepts, Algorithms, and Applications*, Springer-Verlag, New York, 1996.

[49] Kalos M.H., Whitlock P.A.: *Monte Carlo Methods. Second Edition*, Wiley-VCH Verlag, Weinheim, 2008.

[50] Różański A., Łydżba D., *RVE determination from a digital image of microstructure*, Proceedings of the Second International Symposium on Computational Geomechanics, COMGEO II, eds S. Pietruszczak *et al.*, Rhodes: IC2E International Centre for Computational Engineering, 2011.

[51] Janke, W.; *Pseudo random number: generation and quality checks*. Lecture Notes John von Neumann Institute for Computing, Vol. 10, 447, 2002.